Preparation of Well-defined Alkaline Earth Metal Complexes and their Applications in Molecular Catalysis

Thesis Submitted to AcSIR

For the Award of the Degree of

DOCTOR OF PHILOSOPHY

in

CHEMICAL SCIENCES

by

Sandeep

AcSIR No. 10CC14A26025

Under the guidance of

Dr. Sakya Singha Sen

Catalysis and Inorganic Chemistry Division

CSIR-National Chemical Laboratory (CSIR-NCL)

Pune-411008, INDIA.

February-2019

CERTIFICATE

This is to certify that the work incorporated in this Ph.D. thesis entitled **"Preparation of Well-defind Alkaline Earth Metal Complexes and their Applications in Molecular Catalysis"** submitted by **Mr. Sandeep** (AcSIR Registration Number 10CC14A26025) to Academy of Scientific and Innovative Research (AcSIR) in fulfillment of the requirements for the award of the Degree of the Doctor of Philosophy, embodies original research work under my supervision at Catalysis and Inorganic Chemistry Division, CSIR-National Chemical Laboratory (CSIR-NCL), Pune, India. I further certify that this work has not been submitted to any other University or Institution in part or full for the award of any degree or diploma. Research material obtained from other sources has been duly acknowledged in the thesis. Any text, illustration, table etc., used in the thesis from other sources, have been duly cited and acknowledged.

It is also certified that this work done by the student, under my supervision, is plagiarism free.

Sandeep

(Research Student)

(Reg. No. 10CC14A26025)

Dr. Sakya Singha Sen

(Research Supervisor)

Date: 24th February, 2019

Place: CSIR-NCL, Pune.

DECLARATION

I hereby declare that the original research work embodied in this thesis entitled **"Preparation of Well-defined Alkaline Earth Metal Complexes and their Applications in Molecular Catalysis"** submitted to the Academy of Scientific and Innovative Research (AcSIR), New Delhi, for the award of degree of **Doctor of Philosophy** in **Chemical Sciences** is the outcome of experimental investigations carried out by me under the supervision of **Dr. Sakya Singha Sen**, Senior Scientist, CSIR-National Chemical Laboratory (CSIR-NCL), Pune. I affirm that the work incorporated is original and has not been submitted to any other academy, university or institution in part or full for the award of any degree or diploma.

Sandeep

Date: 28th February, 2019

This dissertation is dedicated to

my grandfather

Late Rao RamjiLal Yadav

Acknowledgment

Table of Contents

Chapter 3: Beyond Hydrofunctionalisation: A Well-Defined Calcium Compound Catalysed Mild and Efficient Carbonyl Cyanosilylation

Chapter 4: Alkaline Earth Metal Compounds of Methylpyridinato β-Diketiminate Ligands and their Catalytic Application in Hydroboration of Aldehydes and Ketones

4.7: Conclusions

Chapter 5: Investigation of Silylene/Germylene and Zinc bonding

5.1: Introduction

5.2: Synthesis and characterization of complex **14** and **15**

5.3: DFT studies to understand dimerization process

5.4: Synthesis and characterization of complex **16** and **17**

5.5: Conclusions

5.6: References

Appendix: Experimental details, NMR and crystal data

Abbreviations

Units and standard terms

BDE   Bond Dissociation Energy

°C   Degree Centigrade

DFT   Density Functional Theory

mg   Milligram

h   Hour

Hz   Hertz

mL   Millilitre

min.   Minute

mmol   Millimole

NPA   Natural Population Analysis

ppm   Parts per million

%   Percentage

Chemical Notations

Ar   Aryl

MeCN   Acetonitrile

$CDCl_3$ Deuterated chloroform

DMF   N, N'-Dimethylformamide

DMSO   Dimethyl sulfoxide

EtOH	Ethanol
Et	Ethyl
EtOAc	Ethyl Acetate
HBpin	Pinacolborane
MeOH	Methanol
Me	Methyl
py	Pyridine
THF	Tetrahydrofuran
TMSCN	Trimethylsilyl cyanide

Other Notations

δ	Chemical shift
J	Coupling constant in NMR
Equiv.	Equivalents
HRMS	High Resolution Mass Spectrometry
NMR	Nuclear Magnetic Resonance
rt	Room temperature
UV	Ultraviolet
XRD	X-Ray Diffraction

General remarks

➢ All chemicals were purchased from commercial sources and used as received.

➢ All reactions were carried out under inert atmosphere following standard procedures using Schlenk techniques and glovebox.

➢ Deuterated solvents for NMR spectroscopic analyses were used as received. All ^{1}H NMR and ^{13}C NMR analysis were obtained using a Bruker or JEOL 200 MHz, 400 MHz or 500 MHz spectrometers. Coupling constants were measured in Hertz. All chemical shifts are quoted in ppm, relative to TMS, using the residual solvent peak as a reference standard.

➢ HRMS spectra were recorded at UHPLC-MS (Q-exactive-Orbitrap Mass Spectrometer) using electron spray ionization [(ESI^{+}, +/− 5kV), solvent medium: acetonitrile and methanol] technique and mass values are expressed as *m/z*. GC-HRMS (EI) was recorded in Agilent 7200 Accurate-mass-Q-TOF.

➢ The solvent used were purified by an MBRAUN solvent purification system MBSPS-800.

➢ Column chromatography was performed on silica gel (100-200 mesh size).

➢ Chemical nomenclature (IUPAC) and structures were generated using ChemDraw Professional 15.1.

Synopsis

This thesis deals with the synthesis of alkaline earth metal based complexes and their application in homogenous catalysis. The present thesis comprises of five chapters. The first chapter is the introduction wherein the evolution and importance of alkaline earth metal chemistry with recent literature precedence are described in details. Second to fifth chapter are working chapters narrating our approach to the synthesis and catalytic activity of novel alkaline earth metal complexes. The second chapter describes synthesis of amidinate stablized organocalcium complexes and their application in hydroboration of aldehydes and ketones. The third chapter explores the utilization of amidinato calcium iodide complex for the cyanosilyation of carbonyl compounds and the catalytic cycle has been investigated by experiment and DFT calculations. The synthesis of catalytically active homoleptic magnesium and calcium complexes and their utilization in carbonyl hydroboration has been explained in fourth chapter. The fifth chapter describes the bonding between a silylene and a germylene with the d^0 metal complexes.

Chapter I: **Introduction**

The synthesis of organomagnesium halides by Grignard proved to be a milestone in organometallic chemistry. The organomagnesium halides have been utilized as strong bases, nucleophiles as well as alkyl and aryl transfer reagents. But as we move down the group 2, the higher analogues of Mg have not been studied extensively. The electropositivity increases as moving down the group, which lead to increase the metal-carbon bond polarity. This increase in the ionicity of the metal-carbon bond leading to decrease in the bond strength as well as significant increase in the reactivity. Therefore, the Grignard-like synthetic routes face the ether cleavage reactions and also lead to the side reactions like Würtz-coupling; (2RI + Ca → R-R + CaI_2). The bigger challenge, however, is the Schlenk equilibrium, where the homoleptic complexes are more favored as compared to the heteroleptic complexes. Over the last decade, an array of heavy organocalcium metal compounds has been synthesized utilizing various sterically demanding monoanionic ligand systems such as amidinate, guanidinate, and β-diketiminate. The chemistry of calcium is marked by its stable +2 oxidation state with d^0 electronic configuration and their property resembles with the trivalent and redox inactive lanthanides having d^0 electronic configuration, especially the chemistry of Ca is extremely similar to that of Yb^{2+}. The alkaline earth metals behave similar to the lanthanides in terms of Lewis acidity. The reactivity of calcium metal can be correlated with the lanthanide chemistry in which σ bond metathesis and polarised insertion are the two prototypical mechanistic steps.
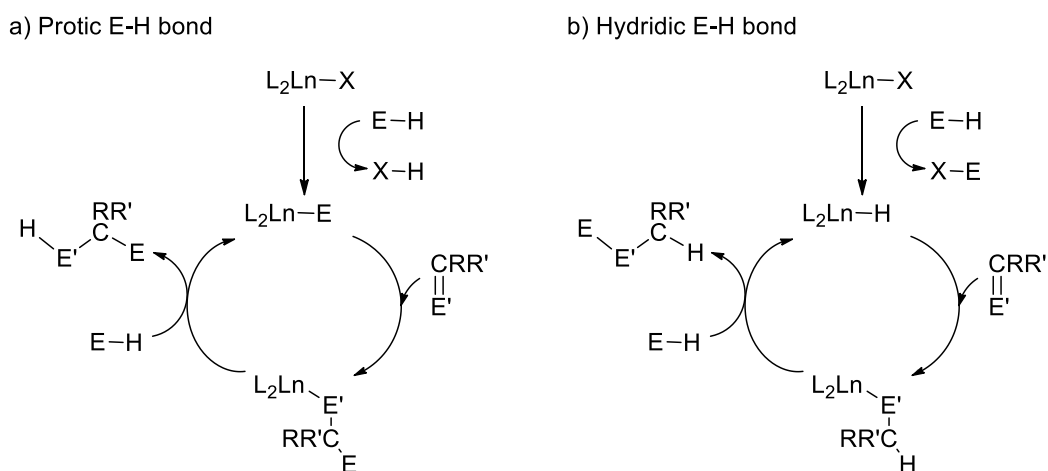
Scheme 1: Catalytic cycles predicated in lanthanide-mediated heterofunctionalization of unsaturated compounds.

The catalytic pathway mainly depends on the substrate polarity. The protic E-H bond leads to protonolysis to give an Ln-E fragment, while the hydridic E-H bond undergoes σ bond metathesis to give lanthanide hydride; Ln-H fragment. Inspired by the success of lanthanides in molecular chemistry, a variety of organocalcium complexes have been synthesized and used in catalysis such as hydrophosphination, hydrosilylation, hydrogenation reactions. The calcium based catalyst may be a key player in organometallic chemistry due to its cost effectiveness, large abundance and biocompatibility. Despite of these impressive headway, there is a scope to develop easy synthesizable calcium based catalysts with more stability and catalytic reactivity.

Chapter II: **Synthesis of Amidinate Stablized Organocalcium Complexes and Their Application in Hydroboration of Aldehydes and Ketones**

Soluble calcium halides reported so far are mostly dimeric in nature. The halides occupy the bridging position and thus provide additional coordination to the metal. We obtained a monomeric calcium iodide $[\{PhC(NiPr)_2\}CaI(thf)_3]$ from the reaction of $[PhC(NiPr)_2]Li$ with CaI_2 in THF. The compound has been stabilized by electronic donation and steric shielding from the amidinate ligand as well as coordination of three THF molecules. $[\{PhC(NiPr)_2\}CaI(thf)_3]$ does not show any propensity towards ligand exchange reaction. When the same reaction is carried out in diethyl ether instead of THF, it led to the formation of a Li calciate(II) cluster of composition $L_2Ca_4I_8Li_4O$ (L=PhC(NiPr)$_2$) with an encapsulated O^{2-} in the middle of a tetrahedron spanned by four Ca^{2+} ions. It represents a metal-rich halide comprising of both alkali and alkaline earth metals which is quite unprecedented. Subsequently, $[\{PhC(NiPr)_2\}CaI(thf)_3]$ has been utilized as a catalyst for hydroboration of a wide range of aldehydes and ketones using pinacolborane (HBpin) at room temperature. The catalyst shows functional group tolerance even towards OH and NH groups. The strategy has been further extended to imines.
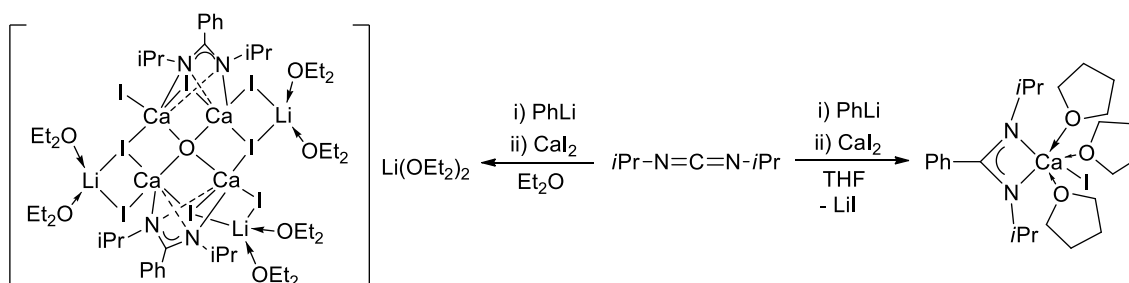
Scheme 2: Synthesis of monomeric calcium iodide complex and calcium iodide cluster.
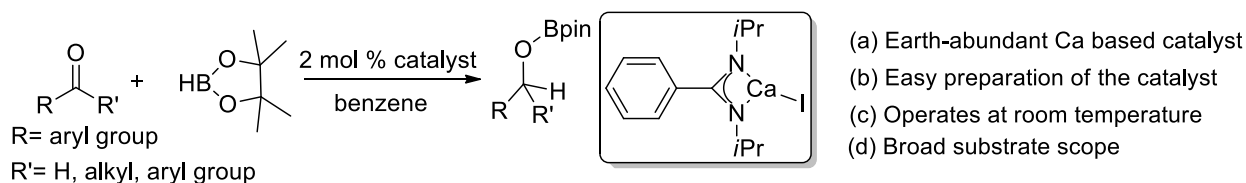
Scheme 3: Amidinato calcium (II) compound catalyzed hydroboration of aldehydes and ketones.

Chapter III: **Beyond Hydrofunctionalisation: A Well-Defined Calcium Compound Catalysed Mild and Efficient Carbonyl Cyanosilylation**

Organocalcium compounds have been reported as efficient catalysts for various transformations, for cases in which one of the substrates contained an E-H (E=B, N, Si, P) bond. Here, we look at the possibility of employing an organocalcium compound for a transformation in which none of the precursors has a polar E-H bond. This study demonstrates the utilization of a well-defined amidinatocalcium iodide, [PhC(NiPr)$_2$CaI] for cyanosilylation of a variety of aldehydes and ketones with Me$_3$SiCN under ambient conditions without the need of any co-catalyst. The reaction mechanism involves a weak adduct formation between [PhC(NiPr)$_2$CaI] and Me$_3$SiCN leading to the activation of the Si-C bond, which subsequently undergoes σ bond metathesis with a C=O moiety. The reaction intermediate has been characterized by multinuclear NMR spectroscopy and IR spectroscopy. Such a mechanistic pathway is unprecedented in alkaline earth metal chemistry. Experimental and computational studies support the mechanism.
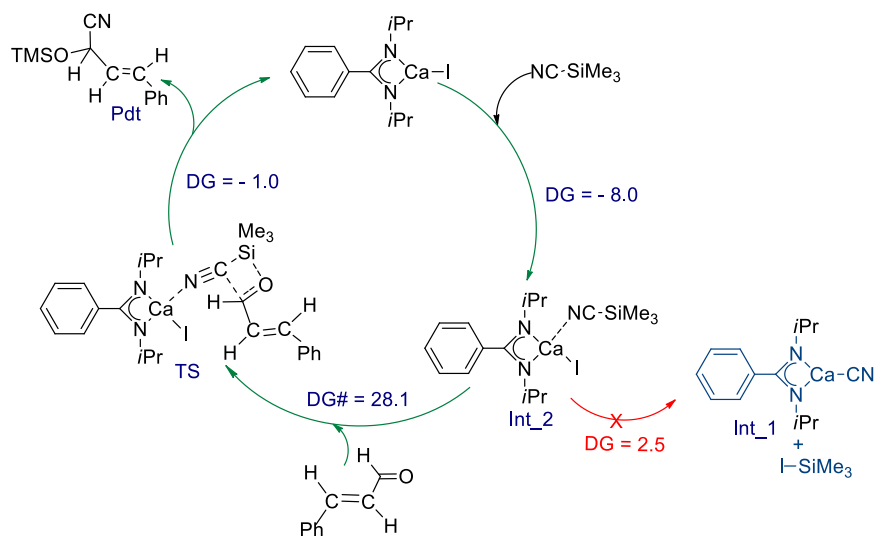
Scheme 4: The catalytic cycle and reaction mechanism for the cinnamaldehyde cyanosilylation reaction by catalyst.

Chapter IV: **Alkaline Earth Metal Compounds of Methylpyridinato β-diketiminate Ligands and their Catalytic Application in Hydroboration of Aldehydes and Ketones**

Ever increasing demand for green and sustainable chemical processes has set up a drive to replace transition metals with earth-abundant, non-toxic, and environmentally benign alternatives. Here, we have used a *β*-diketiminato ligand with methyl-pyridine side arm [(2, 6-*i*Pr-C$_6$H$_3$NC(Me)CHC(Me)NH(CH$_2$py)] to isolate homoleptic complex of magnesium and calcium. The introduction of a methyl-pyridine side arm in the *β*-diketiminato framework leads to a ligand that is tridentate in its nacnac imino-pyridine state. The pendant pyridine group on one of the nitrogen centres provides steric as well as an addition electronic stabilization to the metal center. Both the compounds were structurally characterized. Subsequently, we have used them as catalysts (1 mol%) for hydroboration of a wide range of aldehydes using pinacolborane (HBpin) at room temperature. The strategy was further extended to ketone with 2 mol% catalyst loading. The quantum mechanical calculations have been performed to understand the reaction mechanism.
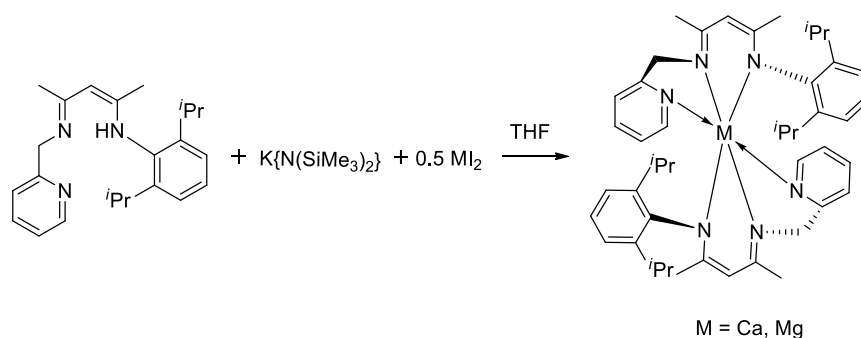
Scheme 5: Synthesis of magnesium and calcium compounds of methylpyridinato β-diketiminate ligand

Chapter V: **Investigation of Silylene/Germylene and Zinc bonding**

Usually when a silylene reacts with a transition metal Lewis acid, it forms either an adduct which could be either monomer or dimer. However, we observed that a silylene [PhC(NtBu)$_2$SiN(SiMe$_3$)$_2$] can form both monomeric [PhC(NtBu)$_2$Si{N(SiMe$_3$)$_2$}→ZnI$_2$]·THF and dimeric [{PhC(NtBu)$_2$}(N(SiMe$_3$)$_2$)SiZnI(μ-I)]$_2$ adducts upon reaction with a transition metal Lewis acid. The formation of these complexes depends upon the solvent used for the reaction or crystallization. Both the complexes were structurally authenticated and the nature of the Si–Zn bond in these complexes rationalized by quantum chemical calculations. In addition, an inter-conversion between these complexes by changing the solvents have also been observed. Analogous chemistry has been extended with germylene, [PhC(NtBu)$_2$GeN(SiMe$_3$)$_2$], with ZnX$_2$ (X=Br, I) although no monomeric adduct formation was observed exemplifying the lesser Lewis basicity of germylene that that of silylene.
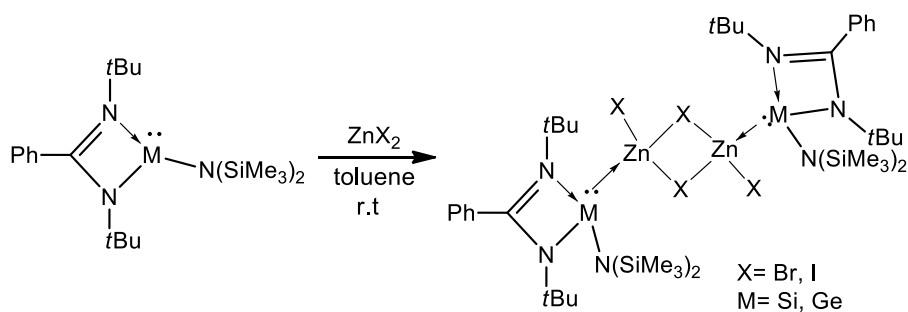
Scheme 6: Synthesis of silylene/germylene-ZnX$_2$ adducts

Chapter 1

General Introduction

Abstract

The first chapter provides an overview about the fundamental interest and formidable synthetic challenge regarding the synthesis of compounds with alkaline earth metals and a general introduction covering a brief description of important compounds in this research area is provided. The aim and the results presented in this contribution are outlined.

1: Introduction:

1.1: A brief history of organocalcium complexes

The synthesis of organomagnesium halides from the direct reaction of organic halides with magnesium metal by Grignard proved to be a milestone in organometallic chemistry.[1] The organomagnesium halides have been utilized as strong bases, nucleophiles as well as alkyl and aryl transfer reagents. [2-3] Moving down the group, the higher analogues of Mg have not been studied extensively. The general thought that the higher alkaline earth metals behave similar to magnesium chemistry is not only ambiguous but also impeded their development. The electropositivity increases as one moves down the group, which leads to an increase in the metal–carbon bond polarity.[4] This increase in the ionicity of the metal-carbon bond leads to decrease in the bond strength as well as significant increase in the reactivity down the group. Therefore, the Grignard-like synthetic routes face the ether cleavage reactions and also lead to the side reactions like Wurtz-coupling; (2RI + Ca → R-R + CaI$_2$).[5-6] Therefore, the maintenance of low-temperature is a must in order to avoid these degradation reactions. Also, the synthesis and characterization of organoalkaline complexes were often faced with many difficulties and challenges. One of the major challenges is the Schlenk equilibrium, where the homoleptic complexes are more favored as compared to the heteroleptic complexes.[7] As described by Schlenk, the ligand scrambling take place in organomagnesium complexes due to the substantially ionic bonding between ligand and magnesium leading to an equilibrium between homoleptic and heteroleptic species (Scheme 1.1). The ethereal solvents such as Et$_2$O and THF favour the heteroleptic complexes due to their coordinating property.[8]
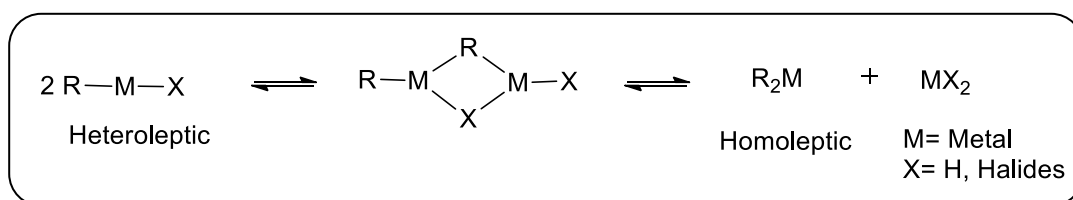
Scheme 1.1: The continuous scrambling of alkyl group and halide in Schlenk equilibrium.

Unfortunately, for the synthesis of heavier alkaline-earth metal complexes the Schlenk equilibrium is an impediment. The ligand scrambling leads to a shift in the equilibrium toward the homoleptic complexes with the formation of high lattice energy and insoluble MX$_2$ complex

precipitate. Solubility in organic solvents is also a serious issue with the heavier alkaline earth metals. As on moving down the group the ionic radii (Ca^{2+}, 1.00 Å; Sr^{2+}, 1.18 Å; and Ba^{2+}, 1.35 Å) increase significantly, which makes the coordination saturation difficult.[9] The use of steric demanding and multidentate ligand system can circumvent these issues. Despite the enormous challenges associated with this chemistry, many attempts were undertaken to synthesize the heavier alkaline earth metal compounds.

The chemistry of organocalcium complex began to emerge in 1950, when calcocene, $Ca(C_5H_5)_2$ (**1.1**) and $Ca(C_5H_5)_2.(THF)_2$(**1.2**) (Scheme 1.2) were synthesized and characterized by Stucky and co-workers from the reaction of activated calcium metal and cyclopentadiene.[10] The cyclopentadiene ring, due to its unique coordinating capability helped in the isolation and characterization of first well-defined organocalcium complex. In contrast to the metallocenes, the chemistry of Ca–C σ bond remained unexplored till Lappart and co-workers synthesized $[Ca\{CH(SiMe_3)_2\}_2(1,4-dioxane)_2]$(**1.3**).[11] This first Ca–C σ bonded complex was synthesized by the co-condensation of calcium vapors and $[(SiMe_3)_2CHBr]$ in THF and later in dioxane at 77 K. The Ca–C bond length was found to be 2.483(5) Å. It was presumed to form $RCaBr(THF)n$, but subsequently formed $[Ca\{CH(SiMe_3)_2\}_2(1,4-dioxane)_2]$ via a Schlenk-type equilibrium.
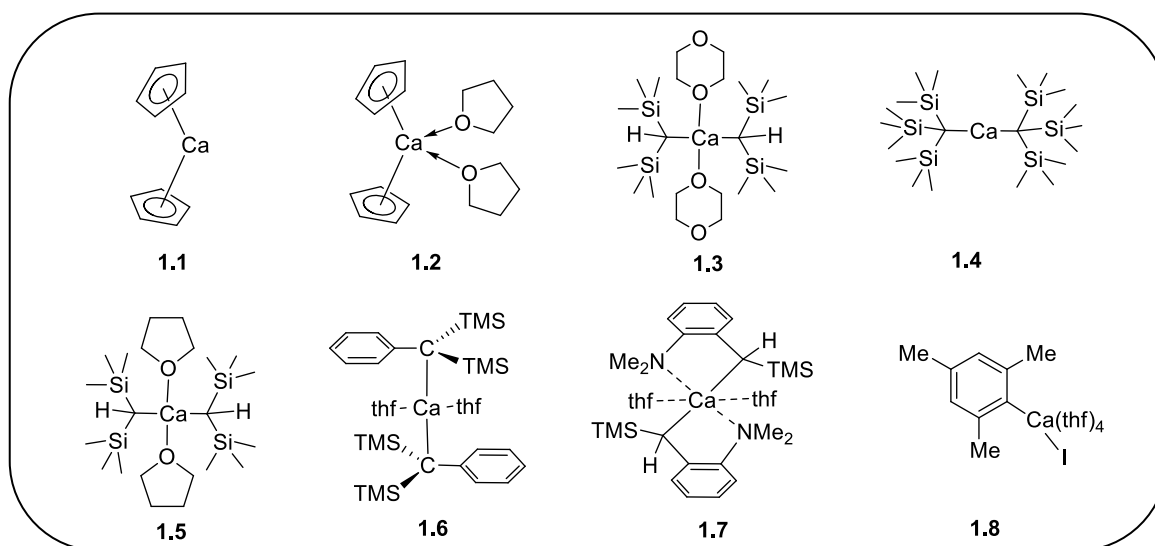
Scheme 1.2: The overview of journey of development of organocalcium complexes.

The first unsolvated calcium complex, calcium bis{tris(trimethylsilyl)methanide} [Ca{C$(SiMe_3)_3\}_2$](**1.4**) was prepared by the reaction of $KC(SiMe_3)_3$ and CaI_2 in benzene.[12a] The single

crystal XRD structure displays several Ca–H agostic interactions, providing additional steric saturation to the metal center. The Ca–C bond distance was reported to 2.459(9) Å and C–Ca–C bond angle was shown to be 149.7(6)°. Further treatment with excess of Et$_2$O resulted in the formation of parent hydrocarbon and Ca(OEt)$_2$, illustrating the high reactivity of organocalcium complexes. Hill and co-workers described the synthesis of THF coordinated [Ca{CH(SiMe$_3$)$_2$}$_2$](THF)$_2$ (**1.5**) by the reaction of CaI$_2$ and two equivalents of [K{CH(SiMe$_3$)$_3$}.(THF)] in THF as reaction solvent.[12b] In 2000, Harder and coworkers were able to synthesize the first benzyl organocalcium complex [{PhC(SiMe$_3$)$_2$Ca}$_2$](**1.6**) from the metathesis reaction between CaI$_2$ and α,α-bis(trimethylsilyl)benzylpotassium in THF.[12c] Following on this work, the same group reported bis(2-NMe$_2$-α-Me$_3$Si-benzyl)calcium(THF)$_2$(**1.7**) by replacing one TMS moiety by hydrogen and putting dimethylamino group on the benzene moiety.[12d]

However, the synthesis of alkyl and aryl calcium halides remained a challenge to the scientific community. In 1905, Beckmann claimed to synthesize the first aryl calcium iodide complex; PhCaI by the reaction of calcium metal and aryl halide in diethyl ether.[13] These compounds remained uncharacterized and repetition reactions showed the formation of diethyl ether coordinated calcium iodide complex.[14] Over the years, several research groups attempted to synthesize these elusive compounds leading to widely contradictory reports on their preparation and reactivity. Harder attempted to synthesize (2,6-dimethoxyphenyl)calcium iodide complex by the reaction of (2,6-dimethoxyphenyl)potassium and CaI$_2$ in THF, which yielded tetranuclear cluster of composition [2,6-(MeO)$_2$C$_6$H$_3$]$_6$Ca$_4$O].[15] In 2006, Westerhausen and his team reported a series of organocalcium iodide complexes; [MesCaI(THF)$_4$](**1.8**), [(*p*-tolyl)CaI(THF)$_4$], [PhCaI(THF)$_4$] and [PhCaBr(THF)$_4$] by the direct reaction of aryl iodide with activated calcium in THF at –78 °C.[16] In all these aryl calcium iodide complexes, the anion is in trans arrangement and the metal center is hexacoordinated.

Over the last decade, an array of heavy organocalcium metal compounds have been synthesized utilizing various steric demanding monoanionic ligand systems.[17] Despite the enormous synthetic challenges, the organocalcium complexes show very interesting reactivity leading to a new area of using these complexes in homogenous catalysis. Some selected examples of calcium based catalysts used in various heterofunctionalization reactions are shown in scheme 1.3.
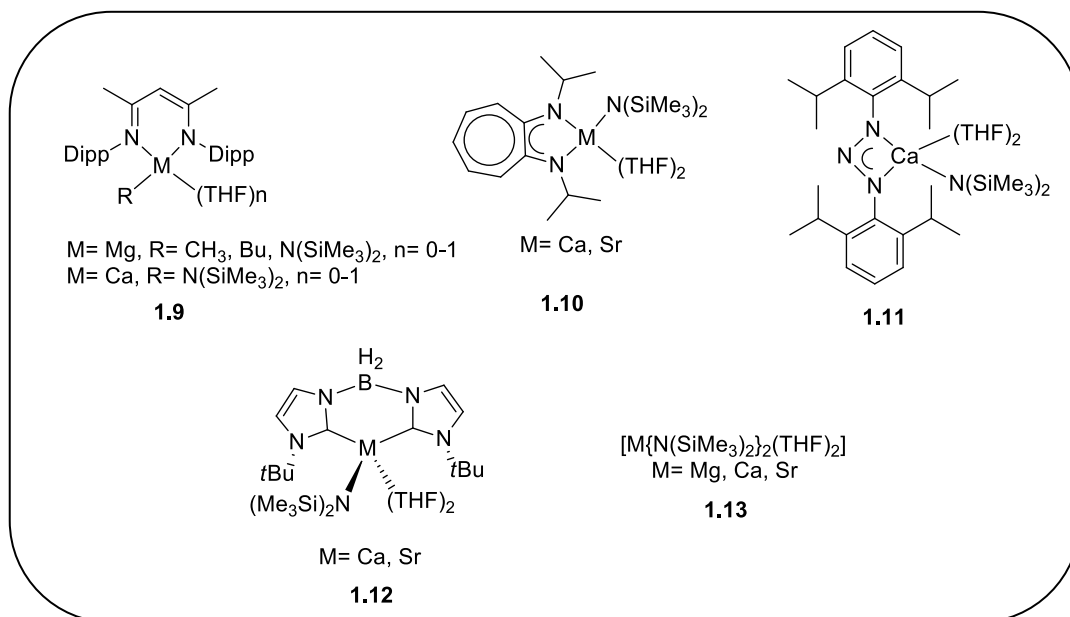
Scheme 1.3: Examples of precatalysts utilized in alkaline earth metal mediated catalysis, of relevance to this work.

The chemistry of calcium metal is marked by its stable +2 oxidation state with d^0 electronic configuration and its property resembles with the trivalent and redox inactive lanthanides having d^0 electronic configuration, especially the chemistry of Ca is extremely similar to that of Yb^{2+}.[18] The alkaline earth metals behave similar to the lanthanides in terms of Lewis acidity. The reactivity of calcium metal can be correlated with the lanthanide chemistry in which σ bond metathesis and polarized insertion are the two principal mechanistic steps. The catalytic pathway mainly depends on the substrate polarity. The protic E–H bond leads to protonolysis to give an Ln–E fragment, while the hydridic E–H bond undergoes σ bond metathesis to give lanthanide hydride, Ln–H fragment. In a complete catalytic cycle, the first fragment, Ln–E undergoes insertion to the unsaturated bond and after the subsequent protonolysis with one more equivalent of E–H gives the anti-Markovnikov product and regeneration of the Ln–E moiety (Scheme 1.4). On the other hand, the hydridic E–H bond leads to the formation of a metal hydride L_2LnH which acts as an active catalyst. This lanthanide hydride L_2LnH undergoes insertion with the unsaturated substrate and the further σ bond metathesis with the E–H moiety to yield the Markonikov product and regeneration of the active catalyst (Scheme 1.4).[19,20] These catalytic cycles support the various organolanthanide catalyzed reactions such as hydrogenation,

hydrosilylation, hydroamination, hydrophosphination, hydroalkoxylation of alkenes and olefin polymerization.[21-50.]

a) Protic E-H bond

b) Hydridic E-H bond
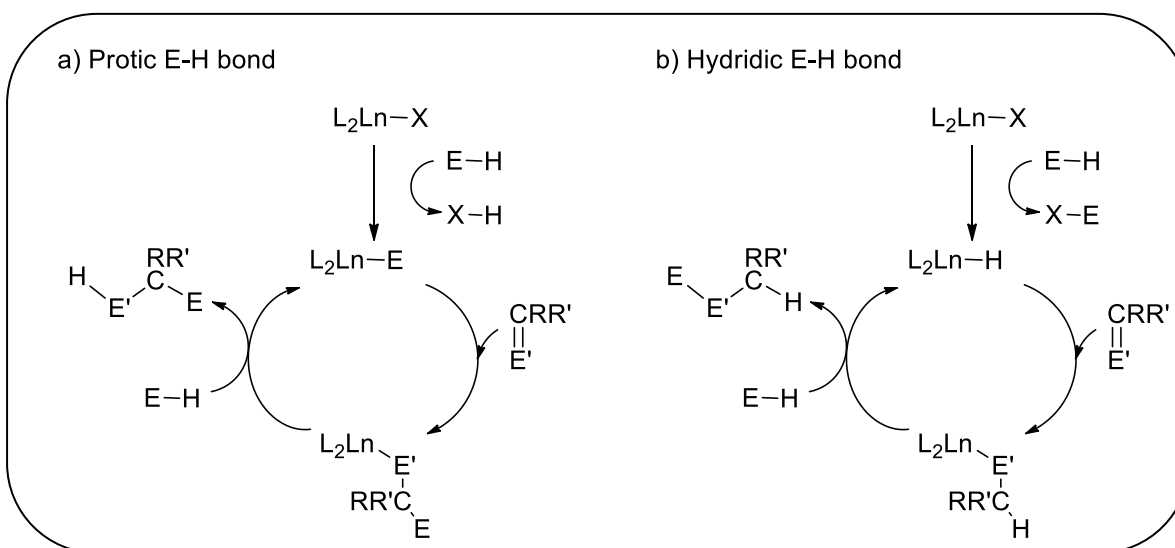
Scheme 1.4: Catalytic cycles predicated in lanthanide-mediated heterofunctionalisation of unsaturated compounds.

In terms of nucleophilicity and electrophilicity, organocalcium reagents behave as intermediate between group 1 and group 3 reagents. The calcium metal exhibits nucleophilic reactivity similar to group 1 reagent, and has significant Lewis acidity, typical to group 3 reagents (Scheme 1.5).
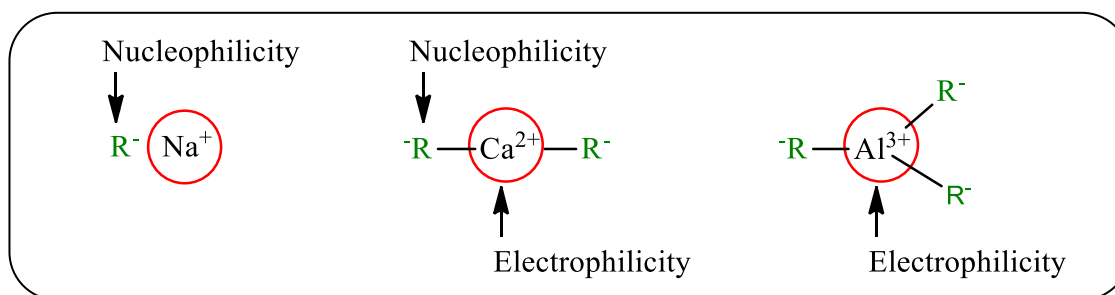
Scheme 1.5: Comparison of organocalcium reagents with group 1 and 3 reagents.

Using organocalcium complexes in catalysis has many advantages: i) Most of the industrial catalysts are based on the transition metals such as Ru, Os, Rh, Ir, Pd and Pt. To fulfill the goal of "cheap metals for noble tasks", calcium metal may be a promising candidate because calcium is the fifth most earth abundant (3.4 wt %) element [51] ii) It is biocompatible metal (consumption of 1g/day is considered safe in human body) having advantageous in the development of

polymers suitable for medical application and biodegradable materials. Also it is environment friendly as it can be converted to $CaCO_3$ and $Ca(OH)_2$, so fits perfectly in the current trend of making catalyst based on less poisonous metal.[52] iii) The field of organocalcium in catalysis has started to develop only a decade before, so it is very important and interesting field from the academic point of view.

1.2: Catalysis with organocalcium complexes

1.2.1: Calcium catalyzed hydroamination reactions

Hydroamination is an atom-efficient reaction involving the addition of N–H bond across an unsaturated bond such as C=C, C≡C, C=N and C≡N.[53] Although the hydroamination reaction is thermodynamically favorable but the repulsion between nitrogen lone pair and election density of unsaturated bond makes the reaction kinetically unfavorable. Due to the high Lewis acidity of organocalcium complexes, they may be used as catalysts in hydroamination reactions. Hill and co-workers introduced β-diketiminate calcium amide [{HC-(C(Me)$_2$N-2,6-iPr$_2$C$_6$H$_3$)$_2$}Ca-{N(SiMe$_3$)$_2$}(THF)](**1.9**) for the intramolecular hydroamination of α, ω-aminoalkene.[54] Subsequently, Roesky and co-workers reported aminotroponate and aminotropniminate calcium amide complex [{(iPr)$_2$ATI}Ca{N(SiMe$_3$)$_2$}(THF)$_2$] ((iPr)$_2$ATI = N-isopropyl-2-(isopropylamino)troponiminate) (**1.10**) for the intramolecular hydroamination of nonactivated terminal amino alkenes under mild reaction conditions.[55] Later, the group of Hill used triazenide calcium complex [{Ar$_2$N$_3$}Ca{N(SiMe$_3$)$_2$}(THF)n] (**1.11**), Bis(imidazolin-2-ylidene-1-yl)borate calcium amide [{H$_2$B(ImtBu)$_2$}M{N(SiMe$_3$)$_2$}(THF)n] (M=Ca, n=1; M=Sr, n=2)(**1.12**) for the intramolecular hydoamination.[56] These reactions were found to follow the Baldwin's rule of ring formation, i.e. heterocycles including 5- and 6-membered ring are more accessible compared to 7-membered ring.[57] The conversion rate of 5-membered ring is faster than 6-membered rings which, in turn have faster conversion than the problematic 7-membered rings. Substitution on aminoalkens has a drastic effect on the conversion rate. Generally, the terminal substitution decreases the reaction rate to a great extent, while the large geminal substitution increase the reaction rate by the Thorpe–Ingold effect.[58] Harder and co-workers attempted the enantioselective catalytic hydrosilylation and intramolecular hydroamination of alkene using a chiral β-diketimine calcium complex.[59] However, very less enantiomeric excess was obtained

during the reaction, as the heteroleptic calcium complex could be in equilibrium with the homolpetic complex due to the Schlenk equilibrium. This achiral homoleptic calcium complex might be the active catalyst during the reaction. Subsequently, Hill and co-workers theoretically as well as experimentally proved that the homoleptic alkaline earth metal complex $[M\{N(SiMe_3)_2\}_2]_2$ [M =Ca, Sr](**1.13**) can act as the pre-catalyst for the intermolecular hydroamination of vinyl arene and dienes under ambient reaction conditions (Scheme 1.6).[60]
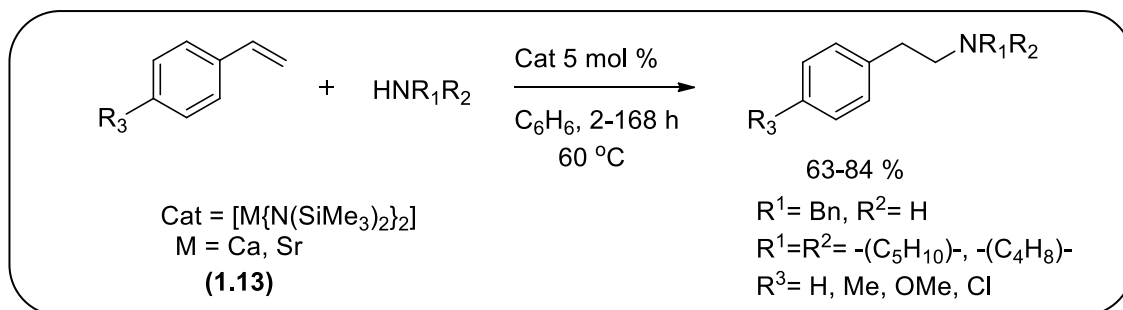
Scheme 1.6: Alkaline earth metal catalyzed Intermolecular hydroamination of activated alkenes.

The reaction kinetics showed that the conversion rate is first order with respect to amine and alkene, whereas it is second order with respect to catalyst.

$$\text{Rate} = k \, [\text{amine}]^1 [\text{alkene}]^1 [\text{catalyst}]^2$$

With the addition of excess alkene keeping the catalyst concentration constant, the overall reaction becomes a pseudo first-order reaction.
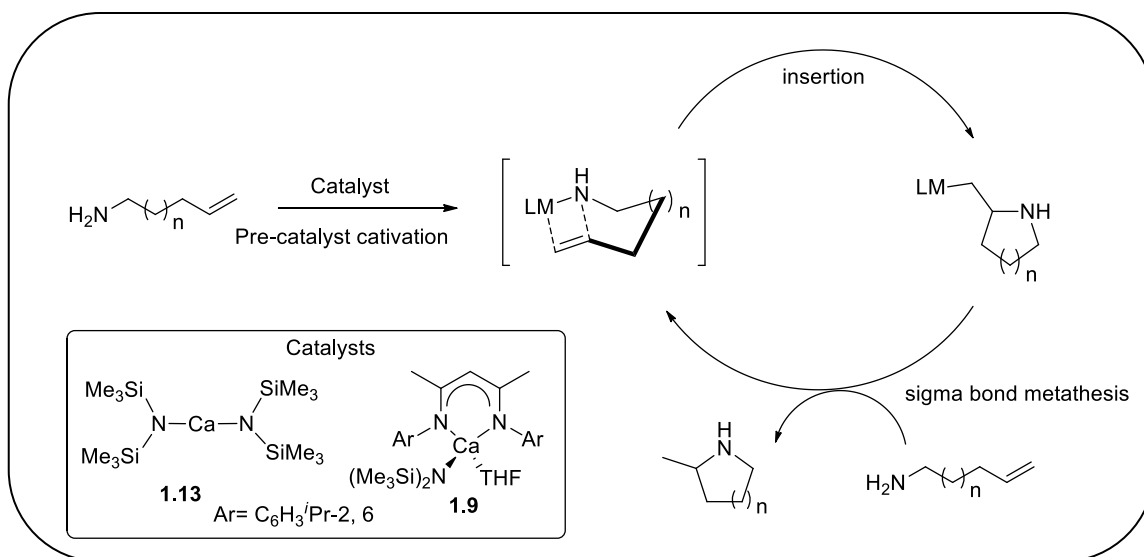
Scheme 1.7: Proposed catalytic cycle for the calcium catalyzed intramolecular hydroamination of aminoalkenes.

Similar to the organolanthanides mechanism, the first step in alkaline earth metal catalyzed hydroamination reaction is the σ bond metathesis between catalyst and amine to form metal amide as precatalystspecies. In the second step,the intramolecularnucleophilic attack leadsto insertion of the alkene into the Ca–N bond. Finally, the σ-bond metathesis between calcium alkyl and second equivalent of amine to give hydroamination product and active catalyst (Scheme 1.7).[61]In 2008, alkaline earth metal catalyzed hydroamination was further extended to the synthesis of ureas and guanidines from the isocyanates and carbodiimides, respectively using heteroleptic calcium complex [{HC-(C(Me)$_2$N-2,6-iPr$_2$C$_6$H$_3$)$_2$}Ca-{N(SiMe$_3$)$_2$}(THF)](**1.9**)and the homolepticalkaline earth metal series [M{N(SiMe$_3$)$_2$}$_2$(THF)$_n$] (M = Ca, Sr, Ba; n = 0, 2)(**1.13**) as precatalysts (Scheme 1.8).[62]The turnover frequency was found to be the highest for strontium compared to calcium and barium complexes.
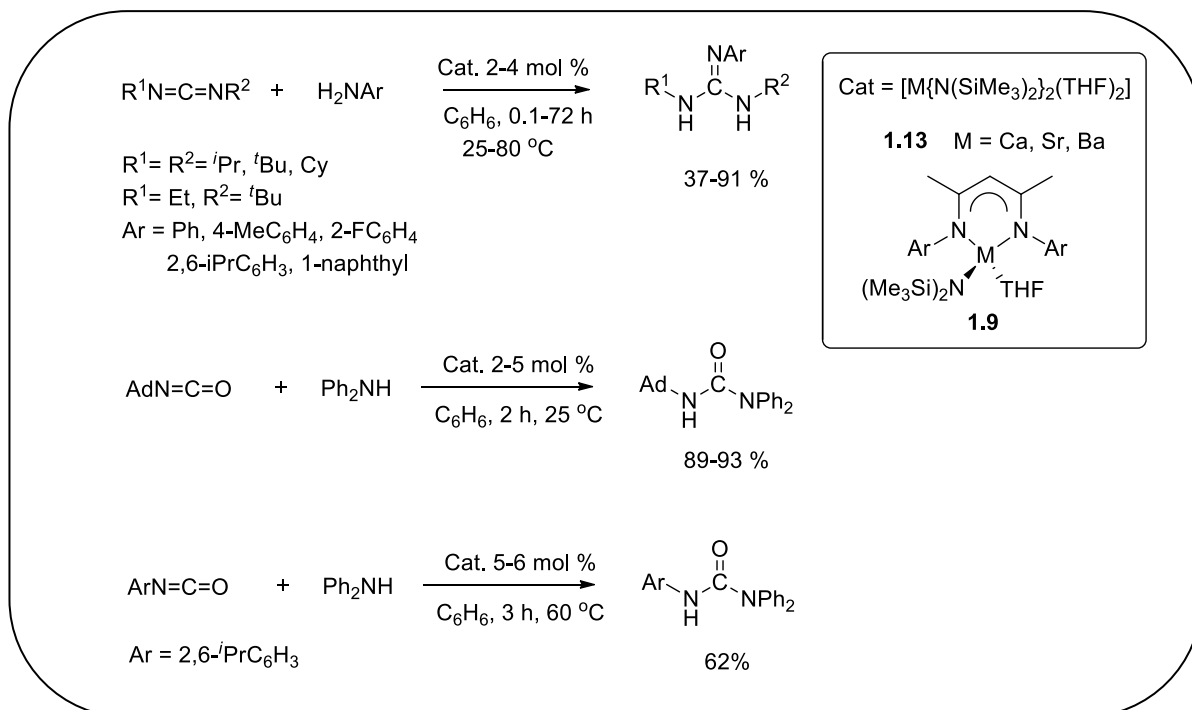
Scheme 1.8: Catalytic hydroamination of carbodiimides and isocyanates.

1.2.2: Organocalcium mediated hydrophosphination reactions

Hydrophosphination is an atom economical reaction involving the addition of P–H bond of phosphine to an unsaturated C–C bond. Based on the success of hydroamination of aminoalkene

with various alkaline earth metal based catalysts, Hill and co-workers utilized the heteroleptic calcium complex for the intermolecular hydrophosphination of activated alkenes and alkynes with diphenylphosphine (Scheme 1.9).[63] The reaction proceeded via anti-Markovnikov pathway with stereoselective syn addition of P–H bond across the unsaturated C–C bond of alkene. The first step involved is a σ bond metathesis between calcium amide and diphenylphosphine to result into a β-diketiminato stabilized diphenyphosphine moiety (Scheme 1.10). Similar stoichiometric σ bond metathesis between alkaline earth metal amides and phosphines to yield homoleptic metal phosphides has been extensively studied by Westerhausen and co-workers.[64] The β-diketiminato stabilized diphenylphosphine moiety further undergoes insertion of unsaturated C–C bond to give $LCaCH_2CH(Ph)PR_2$ via *syn*-addition. In the final catalytic step involve σ bond metathesis reaction with diphenylphosphine to yield phosphinated product and active catalyst.
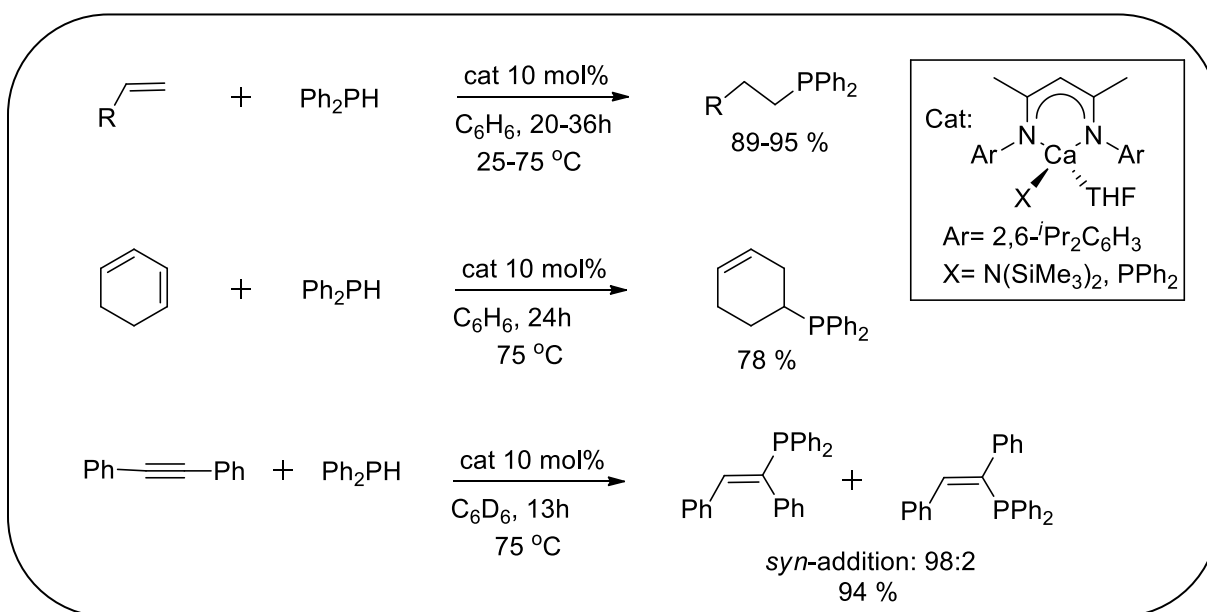
Scheme 1.9: Organocalcium catalyzed intermolecular hydrophosphination of activated alkenes and alkynes.

Subsequently, Westerhausen and co-workers utilized a homoleptic calcium complex $[(thf)_4Ca(PPh_2)_2]$ as an active catalyst for the hydrophosphination of phenyl substituted alkyne.[65] The alkaline earth metal based hydrophosphophination strategy was further extended to cabodiimides. A series of homoleptic amides complexes $[[M\{N(SiMe_3)_2\}_2(THF)_2]$, M = Ca, Sr,

Ba](**1.13**) were used for the hydrophosphination of both symmetric and unsymmetric carbodiimide.[66] Similar to hydroboration of carbodiimides, the reaction proceeds *via* insertion of carbodiimde moiety into the metal-phosphide bond. Further addition of cabodiimide leads to phosphaguanidine and active catalyst. Following this, the group of Westerhausen and Hill reported homoleptic calcium phosphide complex [(thf)$_4$Ca(PPh$_2$)$_2$] and *β*-diketiminate stabilized calcium amide insertion with carbodiimdes.[67] Sarazin and co-workers showed selective hydrophosphonylation of aldehydes and unactivated ketones.[68]
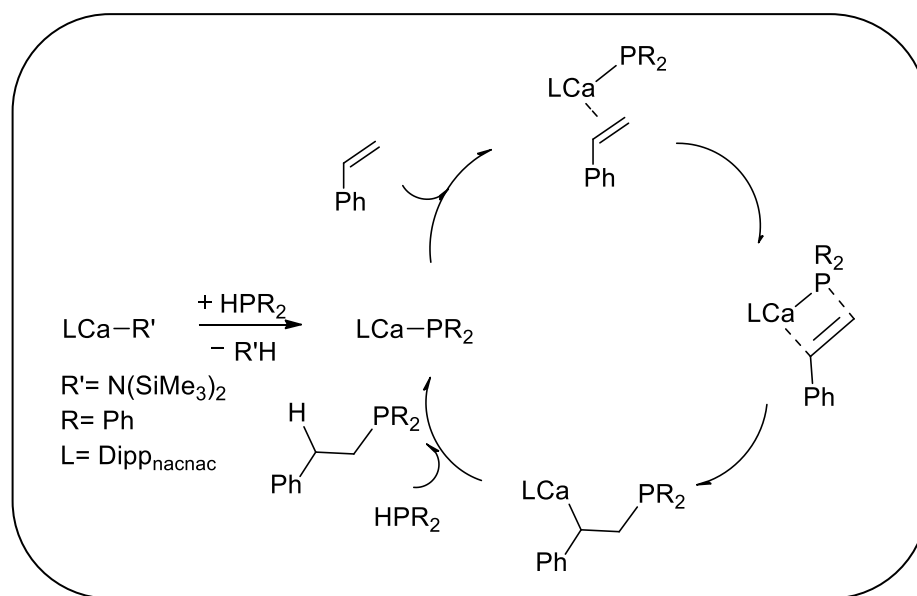
Scheme 1.10: Proposed mechanism for the catalytic hydrophosphination of alkenes.

1.2.3: Organocalcium mediated hydrosilylation reactions

In 2006, Harder and co-workers, introduced the first well defined alkaline earth metal based catalyst [M(DMAT)$_2$(THF)$_2$] (M=Ca, Sr, DMAT=2-dimethylamino-2-trimethylsilylbenzyl)(**1.7**) for the hydrosilylation of alkenes.[69] The larger strontium metal based catalyst showed higher turnover frequencies compared to its smaller calcium counterpart. Notably, the regioselectivity depended upon the choice of solvent; in non-polar benzene solvent, Markovnikov product was obtained, whereas in polar THF solvent exclusively anti-Markovnikov product was observed. In calcium catalyzed reaction, mixture of isomers were observed while using diethyl ether as reaction solvent, however, in case of strontium catalyzed reaction, only terminal silylated product was observed. The solvent dependent regioselectivity indicates two possible catalytic

cycles, one similar to lanthanides catalysis and second one is concerned with metal silyl moiety *via* deprotonation of silane by in-situ generated metal hydride pathway (Scheme 1.11).
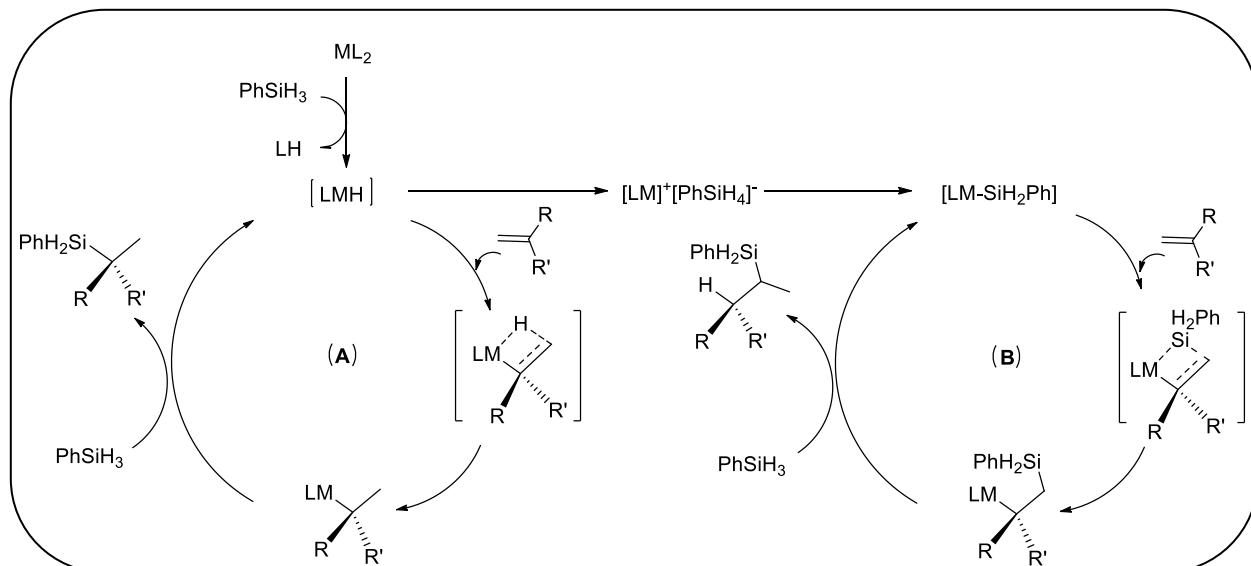
Scheme 1.11: The solvent dependent catalytic cycles for the hydrosilylation of activated alkenes.

Subsequently, the same group utilized dimeric calcium hydride complex [(Dipp$_{nacnac}$)CaH·thf]$_2$ {Dipp$_{nacnac}$=CH[(CMe)(2,6-iPr$_2$C$_6$H$_3$N)]$_2$} as an efficient catalyst for the hydrosilylation of ketones.[70] The first step involves the addition of calcium hydride to the ketone to form the calcium alkoxide complex. In the second step, addition of PhSiH$_3$ leads to the formation of a hypervalent intermediate, which undergoes further elimination to give hydrosilylated product and regenerates the active catalyst. Okuda and co-workers, synthesized alkaline earth metal silyl complex, bis(triphenylsilyl)calcium [Ca(SiPh$_3$)$_2$(thf)] by salt metathesis of CaI$_2$ and two equivalent of [KSiPh$_3$(thf)].[71] It was used as a catalyst for the hydrosilylation of activated olefins under ambient reaction conditions.

1.3: Organocalcium hydride complexes and their application in alkene hydrogenation

During the catalytic cycle of alkene hydrosilylation using [Ca(DMAT)$_2$(THF)$_2$] (DMAT=2-dimethylamino-2-trimethylsilylbenzyl)(**1.7**), existence of a heteroleptic calcium hydride species was observed by Harder and co-workers.[69] However, due to the high instability of the organocalcium hydride complex, it could not be isolated and characterized. Inspired from this observation, Harder and co-workers isolated the first organocalcium hydride

[(Dipp$_{nacnac}$)CaH]$_2$(**1.14**) complex by the reaction of (Dipp$_{nacnac}$)CaN(SiMe$_3$)$_2$(thf) ((Dipp$_{nacnac}$=(2,6-*i*Pr$_2$C$_6$H$_3$)NC(Me)C(H)C(Me)N(2,6-*i*Pr$_2$C$_6$H$_3$)) with PhSiH$_3$ in hexane (Scheme 1.12).[72] The Ca–H bond lengths were found in the range of 2.09(4)–2.21(3) Å and a sharp singlet at δ=4.45 ppm was observed in ^{1}H NMR.
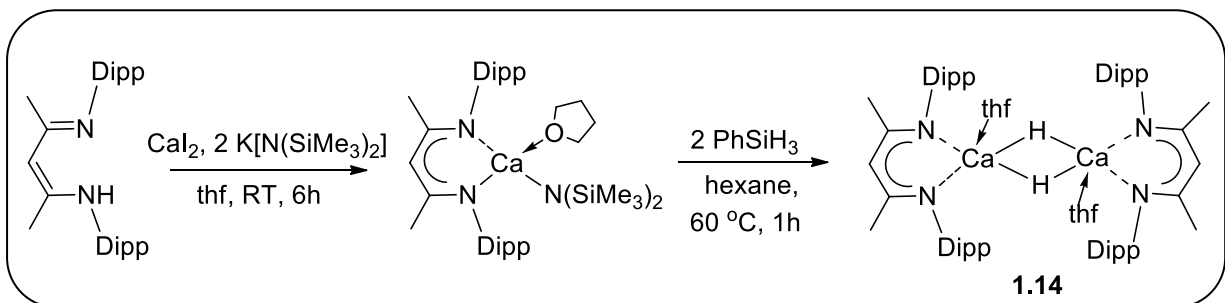
Scheme 1.12: Synthesis of organocalcium hydride [Dipp$_{nacnac}$-CaH(THF)]$_2$

Later, Okuda and coworkers isolated a cationic calcium hydride complex [(Me$_3$TACD)$_3$Ca$_3$(μ_3-H)$_2$](**1.15**) by the of reaction chelating N-macrocyclic ligand Me$_3$TACD-H and Ca-N(SiMe$_3$)$_2$ precursor.[73] The same group further reported a dimeric cationic calcium hydride complex [Ca$_2$H$_3$(Me$_4$TACD)$_2$](SiPh$_3$)(**1.16**) using a neutral N-macrocyclic ligand, Ca-SiR$_3$ precursor and H$_2$ (Scheme 1.13).[74]
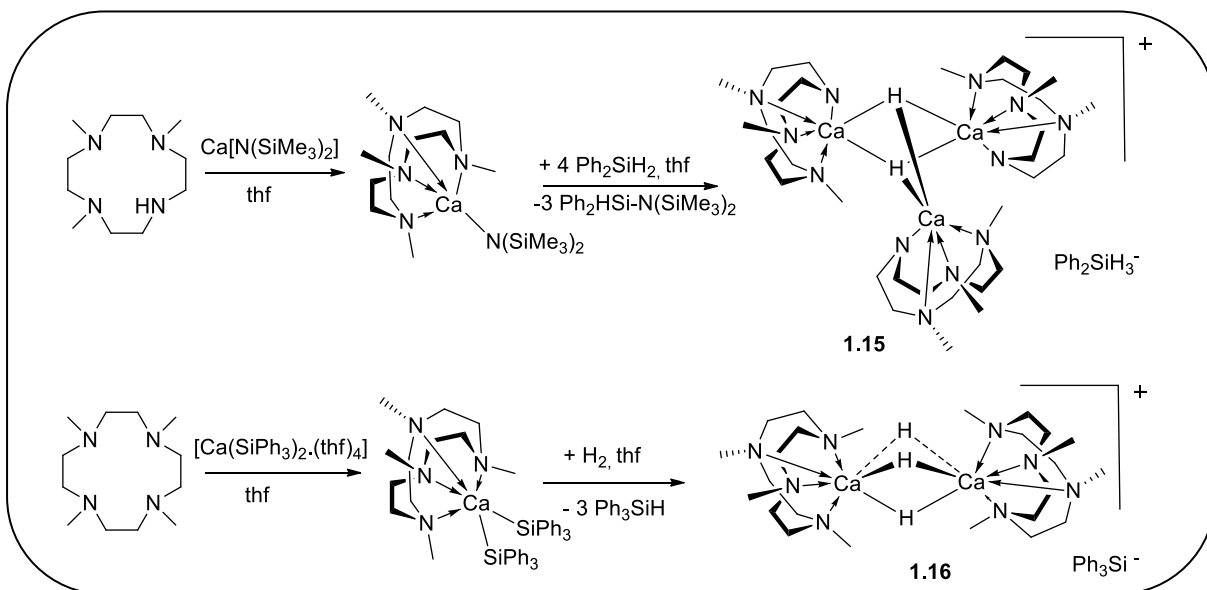
Scheme 1.13: The synthesis pathways employed to isolate cationic calcium hydride complex.

In another work, Harder and coworkers synthesized calcium hydride complexes by the fine tuning of amidinate ligands (**1.17**).[75] Different amidinate ligands were investigated by changing the substituents on the nitrogen and the backbone of the amidinate system. Only the Dipp (2,6-diisopropylphenyl) substituted on nitrogen was found to be stable towards the ligand exchange. Amidiante system having *t*Bu and adamantyl groups on the back bone helped access the dimeric calcium hydride complexes (Scheme 1.14). The aryl···Ca interaction also plays an important role in stabilizing the complex.
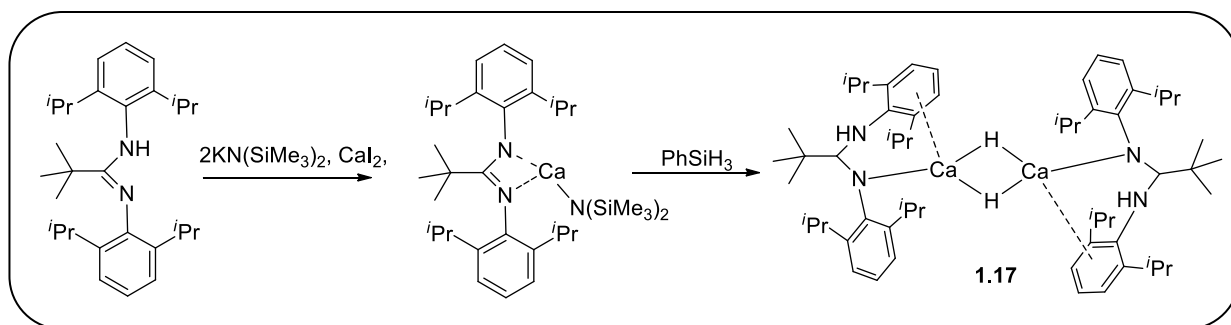
Scheme 1.14: Synthesis of calcium hydride complexes by tuning of amidinate ligand system.

Harder and co-workers described the catalytic hydrogenation of conjugated alkenes with $(Dipp_{nacnac}CaH)_2 \cdot THF$ and dibenzylcalcium complex.[76] These catalysts are observed to be effective under mild conditions (20 °C, 20 bar). The first reaction step involves the addition of $(Dipp_{nacnac}CaH)_2.THF$ to alkene, which was verified by the stoichiometric reaction of alkene and catalyst. The second step involved in catalytic cycle is the σ bond metathesis between organocalcium intermediate and H_2 (Scheme 1.15).

Stoichiometric reaction of $(Dipp_{nacnac}CaH)_2.THF$ with 1,1-diphenylethylene (DPE) yielded expected calcium benzylic complex. It further undergoes protonation by H_2 to give hydrogenated DPE. The uses of polar solvents accelerate the reaction but lead to undesired oligomerization reactions.
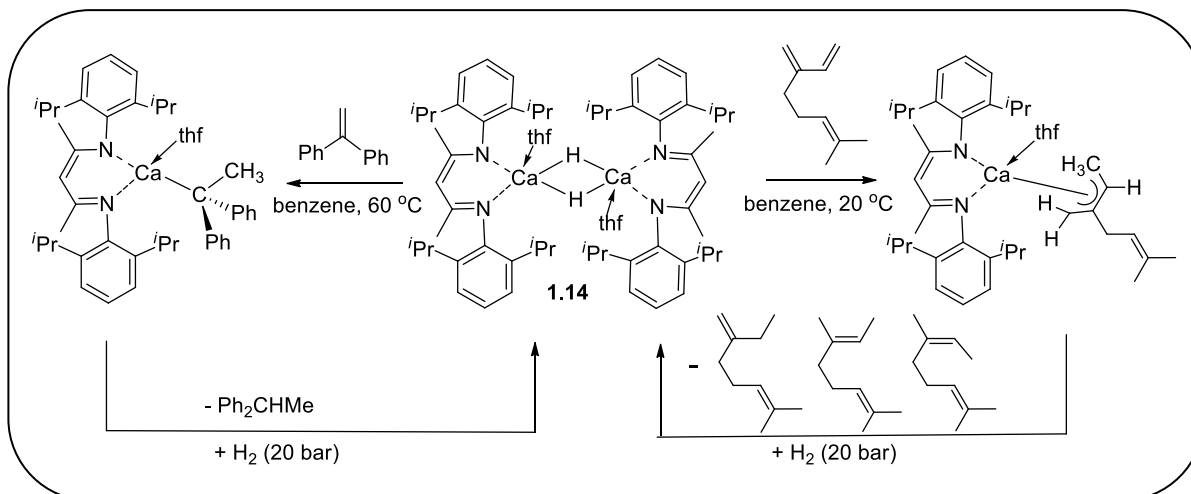
Scheme 1.15: Calcium hydride catalyzed hydrogenation of activated alkenes.

1.4: Organocalcium catalyzed carbon-carbon bond formation

In 2001, Noyori and co-worker used a chiral calcium alkoxide based catalyst for the asymmetric cross-aldol reaction of acetophenone and various aldehydes.[77] More than 91 % enantiomeric excess was observed while using the 1:3:1 molar ratio of $Ca[N\{Si(CH_3)_3\}_2]_2(THF)_2$, (*S,S*)-hydrobenzoin and KSCN as catalyst (Scheme 1.16). This approach was found to be more effective than the previously reported systems, with good enantioselectivity (66-91%).
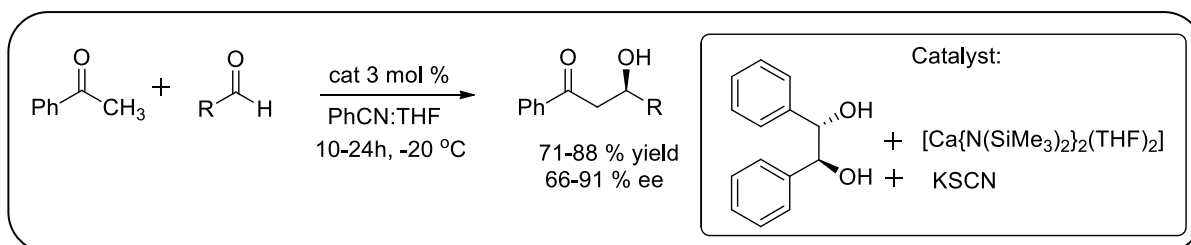
Scheme 1.16: Calcium mediated asymmetric aldol reactions.

Kumarswamy and coworkers reported an enantioenriched, $CaCl_2$/[KO*t*Bu]/(*R*)-BINOL catalyst for asymmetric Michael reaction.[78] Solvent screening sudies demonstrated that toluene provided the highest enantiomeric excess and addition of EtOH accelerated the reaction yield and *ee*'s. Later in 2005, the same group improved the enantioslectivity and reaction yield by using calcium-octahydro-BINOL (H_8-BINOL) complex system for asymmetric Michael reaction.[79] The catalyst system not only acts as a Lewis acid but also as a Bronsted base. Kobayashi and co-

workers developed calcium Pybox catalyst [Ca{O(4-OMe-C$_6$H$_4$)}$_2$]/[anti-5,4-diphenyl-Pybox] for the catalytic asymmetric 1,4-addition of 1,3-dicarbonyl compounds to nitroalkenes in good yields and enantioselectivites.[80]   The same group used chiral calcium catalyst {[Ca(OiPr)$_2$] chiral+Ph-box} ligand which show notable diastereo- and enantioselective 1,4-addition reaction of glycine derivatives to $\alpha\,\beta$-unsaturated esters to give desired glutamic acid derivatives.[81]

This catalyst system was also utilized for asymmetric [3+2] cycloaddition reactions of crotonate derivatives with α-amino acid derivatives to give enantio- and diastereomerically substituted pyrrolidines in 41-98% yield and > 85% *ee* (Scheme 1.17). Due to high yield and excellent selectivity, it was successfully utilized for the synthesis of optical active pyrrolidine core of hepatits-C virus RNA-dependent polymerase inhibitors.
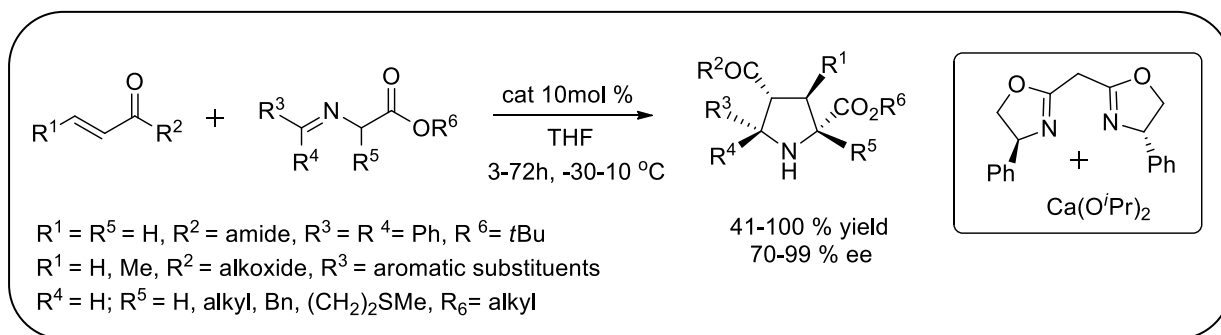
Scheme 1.17: Calcium-mediated [2+3] cycloaddition reactions of crotonate derivatives with α-amino acid derivatives.

Kobayashi and co-workers also used chiral [Ca(OiPr)$_2$]/[Pybox] complex in the Mannich reaction of dibenzylmalonates with N-Boc imines with excellent yield and moderate selectivity (54-77% *ee*). [82]

1.5: Aim and outline of this thesis

The introduction part has accounted that the synthesis of soluble organocalcium complex is a challenge in organometallic chemistry due to Schlenk equilibrium and solubility issues. Despite these issues, various organocalcium complexes have been synthesized and employed in catalysing a number of important reactions such as hydrophosphination, hydrosilylation, and hydrogenation reactions. Calcium based catalysts may be a key player in organometallic

chemistry due to its cost effectiveness, large abundance and biocompatibility. Despite the impressive progress made in recent years, there is still scope to develop easy synthesizable calcium based catalysts with improved stability and catalytic efficiency.

Main aim of the thesis is to extend our understanding on the synthesis, structural property and reactivity of organocalcium complexes. The following points were focused during the thesis work.

1) Designing of new monomeric multidenate ligand systems, to overcome Schlenk equilibrium.

2) Synthesis of monomeric organocalcium complex.

3) The utilization of these soluble organocalcium complexes in homogenous catalysis such as hydroboration and cyanosilylation.

4) To study the mechanism of catalytic cycle both experimentally and theoretically
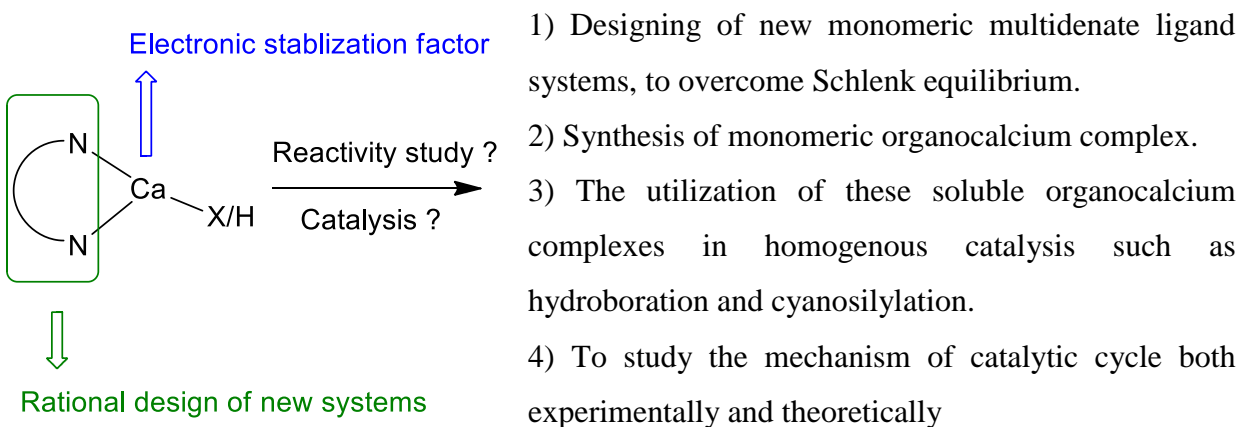
The following thesis chapters will cover all these aspects. All the investigations are based on the combination of synthetic and mechanistic investigations using NMR analysis and crystallographic determination of solid state structure.

Chapter 2 presents the synthesis and characterization of benz–amidinato stabilized monomeric calcium iodide complex [{PhC(NiPr)$_2$}CaI(thf)$_3$] and Li-calciate(II) cluster of composition L$_2$Ca$_4$I$_8$Li$_4$O (L=PhC(NiPr)$_2$). The structural and the bonding arrangement of both complexes were determined by single crystal XRD studies. Furthermore, [{PhC(NiPr)$_2$}CaI(thf)$_3$] catalyzed hydroboration of a wide range of aldehydes, ketones and imines using pinacolborane (HBpin) is discussed. The catalyst shows excellent functional group tolerance even towards OH and NH groups.

Chapeter 3 describes the utilization of the same well-defined amidinatocalcium iodide, [PhC(NiPr)$_2$CaI] for cyanosilylation of a variety of aldehydes and ketones with Me$_3$SiCN under ambient conditions without the need of any co-catalyst. It is the first organocalcium compound catalyzed transformation in which none of the precursors has a polar E–H bond. The reaction

mechanism and catalytic cycle were confirmed by NMR and IR spectroscopy. Also, the quantum chemical calculations have also been discussed to support the catalytic cycle.

Chapter 4 contains the synthesis and structural characterization of well-defined homoleptic compound of magnesium and calcium; [C$_6$H$_3$NC(Me)CHC(Me)NH(CH$_2$py))$_2$M, M= Mg, Ca] using tridentate monoanionic ligand. Further, the hydroboration reaction of aldehydes and ketones catalyzed by these two catalysts is explored. DFT studies have been performed to understand the reaction mechanism.

Chapter 5 accounts the synthesis, and structures of monomeric [PhC(N*t*Bu)$_2$Si{N(SiMe$_3$)$_2$} → ZnI$_2$]·THF and dimeric [{PhC(N*t*Bu)$_2$}(N(SiMe$_3$)$_2$)SiZnI,(μ-I)]$_2$ adduct of silylene and ZnI$_2$. The monomeric and dimeric silylene-ZnI$_2$ metal adducts are inter-convertible by changing the crystallization solvents. Furthermore, NBO analysis is described to understand the nature of bonding in these complexes and inter-conversion mechanism.

1.6: References

1. V. Grignard, *Ann. Chim.*, **1901**, *24*, 433-490.

2. C. Elschenbroich, A. Salzer, *Organometallics*: A Concise Introduction, 2nd ed., Weinheim, VCH, **1992**; Grignard Reagents New Developments (Ed.: H. G. Richey) *Wiley*, Chichester, **2000**.

3. (a) J. J. Eisch, *Organometallics,* **2002**, *21*, 5439–5463; (b) B. J. Wakefield, *Organomet. Chem. Rev.* **1966**, *1*, 131−156; (c) H. Normant, *Bull. Soc. Chim. Fr.*, **1972**, 2161−2175.

4. C. Lambert, P. V. R. Schleyer, *Angew. Chem. Int. Ed.,* **1994**, *33*, 1129−1140.

5. (a) J. S. Alexander, K. Ruhlandt-Senge, *Angew. Chem. Int. Ed.*, **2001**, *40*, 2658−2660; (b) J. S. Alexander, K. Ruhlandt-Senge, H. Hope, *Organometallics,* **2003**, *22*, 4933−4937.

6. (a) R. Fischer, M. Gärtner, H. Görls, M. Westerhausen, *Organometallics*, **2006**, *25*, 3496−3500; (b) J. S. Alexander, K. Ruhlandt-Senge, *Chem. Eur. J.*, **2004**, *10*, 1274−1280.

7. (a) P. R. Markies, T. Nomoto, G. Schat, O. S. Akkerman, F. Bickelhaupt, W. J. J. Smeets, A. L. Spek, *Organometallics*, **1991**, *10*, 3826−3837; (b) M. Gaertner, H. Goerls M. Westerhausen, *Synthesis*, **2007**, 725−730.

8. W. Schlenk, W. Jr. Schlenk, *Chem. Ber.*, **1929**, *B62*, 920.

9. R. D. Shannon, *Acta Crystallogr.*, **1976**, *A32*, 751.

10. R. Zerger, G. Stucky, *J. Organomet. Chem.*, **1974**, *80*, 7−17.

11. F. G. N. Cloke, P. B. Hitchcock, M. F. Lappert, G. A. Lawless, B. Royo, *J. Chem. Soc. Chem. Commun.*, **1991**, 724−726.

12. (a) C. Eaborn, S. A. Hawkes, P. B. Hitchcock, J. D. Smith, *Chem. Commun.*, **1997**, 1961−1962; (b) M. R. Crimmin, A. G. M. Barrett, M. S. Hill, D. J. MacDougall, M. F. Mahon, P. A. Procopiou, *Chem. Eur. J.*, **2008**, *14*, 11292−11295; (c) F. Feil, S. Harder, *Organometallics,* **2000**, *19*, 5010−5015; (d) S. Harder, F. Feil, A. Weebe, *Organometallics*, **2001**, *20*, 1044−1046.

13. E. Beckmann, *Ber. Dtsch. Chem. Ges.*, **1905**, *38*, 904−906.

14. H. Gilman, F. Schulze, *J. Am. Chem. Soc.*, **1926**, *48*, 2463−2467.

15. C. Ruspic, S. Harder, *Organometallics*, **2005**, *24*, 5506−5508.

16. R. Fischer, M. Gaertner, H. Goerls, M. Westerhausen, *Organometallics*, **2006**, *25*, 3496−3500.

17. (a) G. J. Moxey, F. Ortu, L. G. Sidley, H. N. Strandberg, A. J. Blake, W. Lewis, D. L. Kays, *Dalton Trans.,* **2014**, *43*, 4838−4846; (b) R. J. Schwamm, B. M. Day, N. E. Mansfield, W. Knowelden, P. B. Hitchcock, M. P. Coles, *Dalton Trans.*, **2014**, *43*, 14302−14314; (c) B. M. Day, W. Knowelden, M. P. Coles, *Dalton Trans.*, **2012**, *41*, 10930−10933; (d) J. Schwamm, M. P. Coles, *Organometallics,* **2013**, *32*, 5277–5280; (e) B. M. Day, N. E. Mansfield, M. P. Coles, P. B. Hitchcock, *Chem. Commun.*, **2011**, *47*, 4995–4997; (f) C. Jones, *Coord. Chem. Rev.,* **2010**, *254*, 1273−1289; (g) C. Glock, C. Loh, H. Goerls, S. Krieck, M. Westerhausen, *Eur. J. Inorg. Chem.,* **2013**, 3261−3269; (h) M. K. Barman, A. Baishya, S. Nembenna, *J. Organomet. Chem.,* **2015**, *785*, 52−60; (i) S.-O. Hauber, F. Lissner, G. B. Deacon, M. Niemeyer, *Angew. Chem. Int. Ed.,* **2005**, *44*, 5871−5875; (j) A. G. M. Barrett, M. R. Crimmin, M. S. Hill, P. B. Hitchcock, G. Kociok-Köhn, P. A. Procopiou, *Inorg. Chem.,* **2008**, *47*, 7366−7376; (k) S. Nembenna, H. W. Roesky, S. Nagendran, A. Hofmeister, J. Magull, P.-J. Wilbrandt, M. A. Hahn, *Angew. Chem. Int. Ed.,* **2007**, *46*, 2512−2514; (l) A. G. M. Barrett, M. R. Crimmin, M. S. Hill, P. B. Hitchcock, P. A. Procopiou, *Angew. Chem. Int. Ed.,* **2007**, 46, 6339−6342; (m) C. Ruspic, S. Harder, *Inorg. Chem.,* **2007**, *46*, 10426−10433; (n) M. Westerhausen, M. H.

Digeser, C. Gückel, H. Nöth, J. Knizek, W. Ponikwar, *Organometallics,* **1999**, *18*, 2491−2496; (o) S. P. Sarish, A. Jana, H. W. Roesky, T. Schulz, M. John, D. Stalke, *Inorg. Chem.,* **2010**, *49*, 3816−3820; (p) S. P. Sarish, S. Nembenna, S. Nagendran, H. W. Roesky, *Acc. Chem. Res.,* **2011**, *44*, 157−170; (q) F. Ortu, G. J. Moxey, A. J. Blake, W. Lewis, D. L. Kays, *Inorg. Chem.,* **2013**, *52*, 12429−12439.

18. S. Harder, *Angew. Chem. Int. Ed.*, **2004**, *43*, 2714−2718.

19. S. Hong, T. J. Marks, *Acc. Chem. Res.*, **2004**, *37*, 673−686.

20. A. Molander, J. A. C. Romero, *Chem. Rev.*, **2002**, *102*, 2161−2186.

21. Y. W. Li, T. J. Marks, *Organometallics,* **1996**, *15*, 3770−3772.

22. M. R. Gagné, T. J. Marks, *J. Am. Chem. Soc.*, **1989**, *111*, 4108−4109.

23. S. W. Hong, S. Tian, M. V. Metz, T. J. Marks, *J. Am. Chem. Soc.*, **2003**, *125*, 14768−14783.

24. S. D. Wobser, C. J. Stephenson, M. Delferro, T. J. Marks, *Organometallics,* **2013**, *32,* 1317−1327.

25. B. D. Stubbert, T. J. Marks, *J. Am. Chem. Soc.*, **2007**, *129*, 4253−4271.

26. X. H. Yu, S. Seo, T. J. Marks, *J. Am. Chem. Soc.*, **2007**, *129*, 7244−7245.

27. A. Dzudza, T. J. Marks, *Org. Lett.*, **2009**, *11*, 1523−1526.

28. P. W. Roesky, U. Denninger, C. L. Stern, T. J. Marks, *Organometallics,* **1997**, *16*, 4486−4492.

29. A. Motta, I. L. Fragala, T. J. Marks, *Organometallics,* **2005**, *24*, 4995−5003.

30. A. M. Kawaoka, M. R. Douglass, T. J. Marks, *Organometallics,* **2003**, *22*, 4630−4632.

31. S. Y. Seo, X. H. Yu, T. J. Marks, *J. Am. Chem. Soc.*, **2009**, *131*, 263−273.

32. S. Hong, A. M. Kawaoka, T. J. Marks, *J. Am. Chem. Soc.*, **2003**, *125*, 15878−15892.

33. M. R. Douglass, C. L. Stern, T. J. Marks, *J. Am. Chem. Soc.*, **2001**, *123*, 10221−10238.

34. C. J. Weiss, S. D. Wobser, T. J. Marks, *Organometallics,* **2010**, *29*, 6308−6320.

35. A. Dzudza, T. J. Marks, *J. Org. Chem.*, **2008**, *73*, 4004−4016.

36. S. Seo, T. J. Marks, *Chem. Eur. J.*, **2010**, *16*, 5148−5162.

37. C. J. Weiss, T. J. Marks, *Dalton Trans.*, **2010**, *39*, 6576−6588.

38. A. M. Seyam, B. D. Stubbert, T. R. Jensen, J. J. O'Donnell, C. L. Stern, T. J. Marks, *Inorg. Chim. Acta*, **2004**, *357*, 4029−4035.

39. A. Motta, I. L. Fragala, T. J. Marks, *Organometallics,* **2006**, *25*, 5533−5539.

40. V. M. Arredondo, S. Tian, F. E. McDonald, T. J. Marks, *J. Am. Chem. Soc.*, **1999**, *121*, 3633−3639.

41. Y. W. Li, T. J. Marks, *J. Am. Chem. Soc.*, **1998**, *120*, 1757−1771.

42. J. S. Ryu, T. J. Marks, F. E. McDonald, *J. Org. Chem.*, **2004**, *69*, 1038−1052.

43. A. M. Kawaoka, T. J. Marks, *J. Am. Chem. Soc.*, **2005**, *127*, 6311−6324.

44. J. S. Ryu, G. Y. Li, T. J. Marks, *J. Am. Chem. Soc.*, **2003**, *125*, 12584−12605.

45. X. H. Yu, T. J. Marks, *Organometallics*, **2007**, *26*, 365−376.

46. L. Jia, X. M. Yang, A. M. Seyam, I. D. L. Albert, P. F. Fu, S. T. Yang, T. J. Marks, *J. Am. Chem. Soc.*, **1996**, *118*, 7900−7913.

47. S. Seo, X. H. Yu, T. J. Marks, *Tetrahedron Lett.*, **2013**, *54*, 1828−1831.

48. G. Jeske, H. Lauke, H. Mauermann, H. Schumann, T. J. Marks, *J. Am. Chem. Soc.*, **1985**, *107*, 8111−8118.

49. G. Jeske, H. Lauke, H. Mauermann, P. N. Swepston, H. Schumann, T. J. Marks, *J. Am. Chem. Soc.*, **1985**, *107*, 8091−8103.

50. A. S. Dudnik, V. L. Weidner, A. Motta, M. Delferro, T. J. Marks, *Nature Chem.*, **2014**, *6*, 1100−1107.

51. A. Yaroshevsky, *Geochem. Int*., **2006**, *44*, 48−55.

52. Anastas, P. T.; Crabtree, R. H. *Handbook of Green Chemistry*; Wiley- VCH: Weinheim, Germany, **2009**; Vol. 1.

53. (a) A. Togni, H. Grutzmacher, *Catalytic Heterofunctionalization*; VCH: Weinheim, Germany, **2001**; (b) M. Nobis, B. Drie*ss*en-Hölscher, *Angew. Chem., Int. Ed.,* **2001**, *40*, 3983−3985; (c) G. A. Molander, J. A. C. Romero, *Chem. Re*v.*,* **2002**, *102*, 2161−2186; (d) S. Hong, T. J. Marks, *Acc. Chem. Res.,* **2004**, *37*, 673−686; (e) R. Severin, S. Doye, *Chem. Soc. Re*v.*,* **2007**, *36*, 1407−1420; (f) T. E. Müller, K. C. Hultzsch, M. Yus, F. Foubelo, T. Tada, *Chem. Re*v., **2008**, *108*, 3795−3892; (g) P. W. Roesky, *Angew. Chem., Int. Ed.*, **2009**, *48*, 4892−4894.

54. M. R. Crimmin, I. J. Casely, M. S. Hill, *J. Am. Chem. Soc.*, **2005**, *127*, 2042−2043.

55. S. Datta, P. W. Roesky, S. Blechert, *Organometallics*, **2007,** *26,* 4392−4394.

56. (a) A. G. M. Barrett, M. R. Crimmin, M. S. Hill, P. B. Hitchcock, G. Kociok-Köhn, P. A. Procopiou, *Inorg. Chem.*, **2008**, *47*, 7366−7376.; (b) M. Arrowsmith, M. S. Hill, G. Kociok-Köhn, *Organometallics*, **2009,** *28,* 1730−1738

57. J. E. Baldwin, *J. Chem. Soc., Chem. Commun.*, **1976**, 734−736.

58. M. E. Jung, G. Piizzi, *Chem. Rev.*, **2005**, *105*, 1735−1766.

59. F. Buch, S. Harder, *Z. Naturforsch.*, **2008**, *63b,* 169−177.

60. A. G. M. Barrett, C. Brinkmann, M. R. Crimmin, M. S. Hill, P. Hunt, P. A. Procopiou, *J. Am. Chem. Soc.*, **2009**, *131*, 12906−12907.

61. M. R. Crimmin, M. Arrowsmith, A. G. M. Barrett, I. J. Casely, M. S. Hill, P. A. Procopiou, *J. Am. Chem. Soc.*, **2009**, *131*, 9670−9685.

62. (a) A. G. M. Barrett, T. C. Boorman, M. R. Crimmin, M. S. Hill, G. Kociok-Köhn, P. A. Procopiou, *Chem. Commun*., **2008**, 5206−5208; (b) J. Lachs, A. Barrett, M. Crimmin, G. Kociok-Köhn, M. Hill, M. Mahon, P. Procopiou, *Eur. J. Inorg. Chem.*, **2008**, 4173−4179.

63. M. R. Crimmin, A. G. M. Barrett, M. S. Hill, P. B. Hitchcock, P. A. Procopiou, *Organometallics*, **2007,** *26,* 2953−2956.

64. T. M. A. Al-Shboul, H. Görls, M. Westerhausen, *Inorg. Chem. Commun.*, **2008**, *11*, 1419−1421.

65. T. M. A. Al-Shboul, V. K. Pálfi, L. Yu, R. Kretschmer, K. Wimmer, R. Fischer, H. Görls, M. Reiher, M. Westerhausen, *J. Organomet. Chem.*, **2011**, *696* , 216−227.

66. M. R. Crimmin, A. G. M. Barrett, M. S. Hill, P. B. Hitchcock, P. A. Procopiou, *Organometallics,* **2008,** *27,* 497−499.

67. T. M. A. Al-Shboul, G. Volland, H. Gorls, M. Westerhausen, *Zeit. Anorg. Allg. Chem.* **2009**, *635*, 1568−1572.

68. B. Liu, J.-F. Carpentier, Y. Sarazin, *Chem. Eur. J.,* **2012**, *18*, 13259−13264.

69. F. Buch, J. Brettar, S. Harder, *Angew. Chem. Int. Ed.*, **2006**, *45*, 2741−2745.

70. J. Spielmann, S. Harder, *Eur. J. Inorg. Chem.,* **2008**, 1480−1486.

71. V. Leich, T. P. Spaniol, L. Maronb, J. Okuda, *Chem. Commun.,* **2014**, *50*, 2311−2314.

72. S. Harder, J. Brettar, *Angew. Chem. Int. Ed.,* **2006**, *45*, 3474−3478.

73. P. Jochmann, J. P. Davin, T. P. Spaniol, L. Maron, J. Okuda, *Angew. Chem. Int. Ed.,* **2012**, *51*, 4452−4455.

74. V. Leich, T. P. Spaniol, J. Okuda, *Angew. Chem. Int. Ed.,* **2016**, *55*, 4794−4797.

75. A. Causero, G. Ballmann, J. Pahl, H. Zijlstra, C. Färber, S. Harder, *Organometallics,* **2016**, *35*, 3350−3360.

76. J. Spielmann, F. Buch, S. Harder, *Angew. Chem. Int. Ed*., **2008**, *47*, 9434−9438.

77. T. Suzuki, N. Yamagiwa, Y. Matsuo, S. Sakamoto, K. Yamaguchi, M. Shibasaki, R. Noyori, *Tetrahedron Lett*., **2001**, *42*, 4669−4671.

78. G. Kumaraswamy, M. N. V. Sastry, N. Jena, *Tetrahedron Lett*., **2001**, *42*, 8515−8517.

79. G. Kumaraswamy, N. Jena, M. N. V. Sastry, M. Padmaja, B. Markondaiah, *Adv. Synth. Catal*., **2005**, *347*, 867−871.

80. T. Tsubogo, Y. Yamashita, S. Kobayashi, *Angew. Chem. Int. Ed*., **2009**, *48*, 9117−9120.

81. (a) S. Kobayashi, T. Tsubogo, S. Saito, Y. Yamashita, *Org. Lett*., **2008**, *10*, 807−809; (b) T. Tsubogo, S. Saito, K. Seki, Y. Yamashita, S. Kobayashi, *J. Am. Chem. Soc*., **2008**, *130*, 13321−13332; (c) S. Kobayashi, Y. Yamashita, *Acc. Chem. Res*., **2011**, *44*, 58−71; (d) T. Tsubogo, Y. Kano, K. Ikemoto, Y. Yamashita, S. Kobayashi, *Tetrahedron Asymm*., **2010**, *21*, 1221−1225.

82. T. Poisson, T. Tsubogo, Y. Yamashita, S. Kobayashi, *J. Org. Chem*., **2010**, *75*, 963−965.

Chapter 2: Synthesis of Amidinate Stablized Organocalcium Complexes and Their Application in Hydroboration of Aldehydes and Ketones
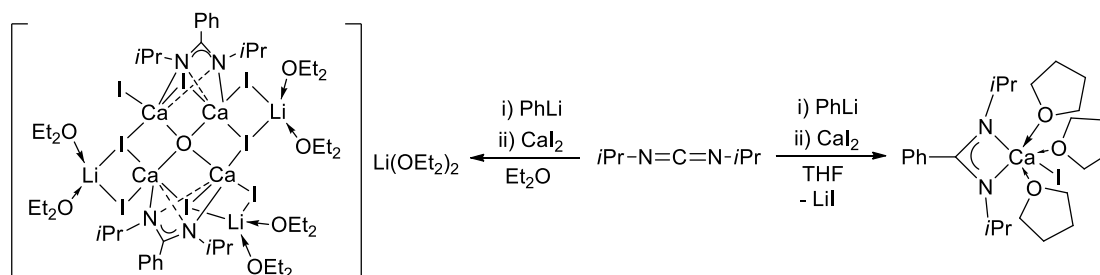
Abstract:

A monomeric calcium iodide $[\{PhC(NiPr)_2\}CaI(thf)_3]$ and Li calciate(II) cluster of composition $L_2Ca_4I_8Li_4O$ (L=$PhC(NiPr)_2$) are synthesized by using benz-amidinato ligand with iPr substituents on the nitrogen atoms. The monomeric calcium iodide $[\{PhC(NiPr)_2\}CaI(thf)_3]$ is used as a catalyst for the hydroboration of a range of aldehydes and ketones.

**2.1: Synthesis of benz-amidinato stabilized calcium iodide complexes**

2.1.1: Introduction

The synthesis of monomeric calcium halide complexes has been a challenge for the main group chemists. As pointed by Gilman and Schulze,[1] and various other groups,[2] the preparation of a well-defined organocalcium iodide is extremely difficult due to: (a) Würtz type coupling (2RI + Ca → R–R + CaI$_2$), (b) Schlenk equilibrium (2RCaX = R$_2$Ca + CaX$_2$), and (c) poor solubility arising from the large ionic radii of Ca (1.00 Å). More than 100 years ago, Beckmann unsuccessfully attempted the reduction of alkyl or aryl iodides by calcium to make an organocalcium iodide.[3] The existence of the organocalcium halides was only affirmed by quenching experiments. Nevertheless, the last two decades have witnessed remarkable growth in the structural elucidation of σ-bonded alkaline earth metal complexes[4] as well as functionalized heteroleptic calcium complexes.[5] A majority of the Ca halide complexes reported so far are either stabilized by β-diketiminato or related ligands, which reduce the electrophilicity of the Ca atom as well as provide steric shielding to the Ca–X bond.[5e] Winter and co-workers realized the calcium iodide complex (**2.1** and **2.2**)[6a] (Scheme 2.1.2) where β-diketiminate ligands exhibit η^5 binding mode with the metal center. The groups of Roesky and Jones independently reported calcium iodide complexes **2.3**[6b] and **2.4** using the same β-diketiminate ligand,[6c] which are dissimilar only from coordinating solvents. Hill's group synthesized another dimeric calcium iodide compound, **2.5**[6d] using bulkier diaryltriazenide ligand. The group of Roesky obtained a [I-Ca-I-Ca-I]$^{2+}$ chain (**2.6**) stabilized by two chelating β-diketiminate ligands.[7] Important to note here that the majority of the *N*-donor supported Ca-halide complexes reported so far are dimeric in nature. The only exception is the aminotroponiminate calcium iodine complex [{(*i*Pr)$_2$ATI}CaI(THF)$_3$] (**2.7**) reported by Roesky et al.[8] The dimerization occurs from the instability of the putative [LCa-X] complexes as well as disfavored bonding between the hard group 2 cation and the soft donor ligand. The dimerization allows an extra coordination of the ligand to the Ca atom and thereby hinder the ligand redistribution.

The previous reports on calcium chemistry indicate that among the array of N-donor ligands with intramolecular stabilization potentials, amidinate ligand system has slightly greater donor tendency than the β-diketiminate ligands. It was reflected from Niemeyer and co-workers' NPA

analysis studies on the energy-minimized structures of the model anions [1,3-diphenyl-1,3-diketiminate and 1,3-diphenyl-1,3-diazaallyl], for which the NPA charge of the N atoms are –0.54 and –0.60, respectively (Scheme 2.1.1).[9]
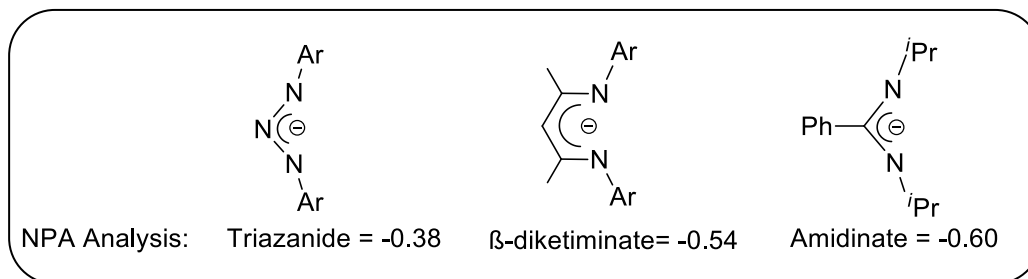
Scheme 2.1.1: NPA of various monoanionic ligands

Recently, Roesky and co-workers have extensively used amidinato ligand with the N-tertbutyl C-phenyl substitution pattern for the synthesis of a range of compounds with low valent Si,[10a–e] Ge,[10f] and Sn[10g] atoms. Utilizing the related guanidinate ligands Jones et al. have synthesized a compound with a Mg(I)–Mg(I) bond.[11] In spite of these accomplishments, amidinate or related four membered ligands have been given much less attention in alkaline earth metal chemistry.[12]
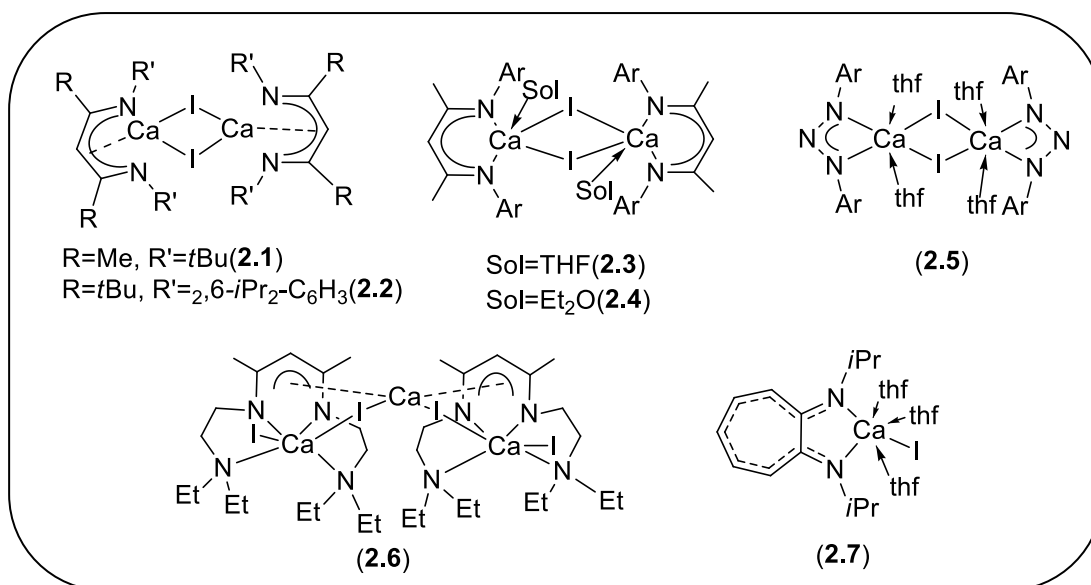
Scheme 2.1.2: Molecular structures of various calcium iodide complexes (2.1–2.7) (Ar = 2,6-iPr$_2$-C$_6$H$_3$).

2.1.2: Synthesis and characterization of monomeric calcium complex

The reaction of N,N-diisopropyl carbodiimide with PhLi led to the *in situ* formation of the lithiated compound, [PhC(N*i*Pr)$_2$Li]. The latter was added to the suspension of CaI$_2$ in THF and stirred for 3 days (Scheme 2.1.3). Upon removal of the solvent, the residue was extracted in toluene. Subsequent recrystallization in THF yielded colorless crystalline blocks of **3**. It crystallizes in the monoclinic space group *Pn*[13] and represents a N-donor supported monomeric calcium iodide complex (Figure 2.1.1). Benz-amidinate moiety provides electronic and steric support to the metal center, and three THF molecules coordinated to calcium center help in the monomerization of Ca-I bond. The Ca atom is hexacoordinated and exhibits distorted octahedral geometry. The distortion from octahedral geometry is mainly due to the restricted bite angle of the amidinate ligand, as derived from the N–Ca–N angle of 57.3(4)°. THF molecules occupy the three sites, two N atoms from the amidinato ligand occupy two sites, and the iodide ligand fills the remaining coordination site. The Ca–I bond length is of 3.084(3)Å, which is shorter than those in **2.7** (3.1365(8)Å and 3.1533(8)Å),[8] Westerhausen's [(thp)$_4$Ca(I)(CH$_2$SiMe$_3$)] (thp = tetrahydropyrran) (3.191(3)Å),[14] and the average Ca–I bond distances in **2.1** (3.144Å),[6a] and **2.3** (3.106Å).[6b] The decrease in the bond length is most likely a result of slightly increased donor ability of the amidinates relative to the *β*-diketiminates as well as a weak steric shielding of the calcium center by the ligands. The Ca–N bond lengths are of 2.383(11) and 2.363(13) Å, which are shorter than the Ca–N bond in [{PhC(NSiMe$_3$)$_2$}$_2$Ca(thf)$_2$] (2.431(2)Å)[15,16] but in good agreement with the average Ca–N bond lengths reported for **2.1–2.6** complexes (2.34–2.38Å), which contains five or six-coordinate Ca atoms.[5,6] The two THF molecules are in the trans position with the O1−Ca1−O3 bond angle of 169.8(4)°. The deviation from linearity is likely due to the repulsion between the THF molecules and the *i*Pr substituents on the nitrogen atoms.
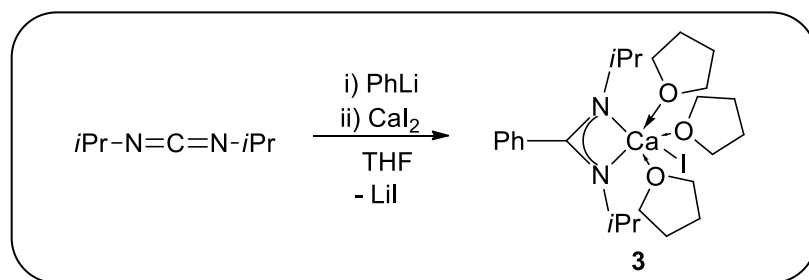
Scheme 2.1.3: Synthesis of monomeric calcium iodide complex **3**.

Crystals of **3** are partially soluble in benzene but still the ^{1}H NMR spectrum of **3** in C$_6$D$_6$ displays resonances for isopropyl groups, coordinated THF solvents, and aromatic protons. However, the characteristic resonances for the THF protons are merged with the resonances for the isopropyl groups and thus leading to a broad signal. Moreover, the integration of aromatic protons cannot be done unambiguously due to the residual peak of C$_6$D$_6$. Therefore, we performed the NMR experiment in DMSO-d$_6$, which unequivocally confirmed the constitution of **3**. Two sets of doublets have appeared at δ 0.90 and 1.06 ppm for the CH$_3$ protons with coupling constants of δ 6.11 and 6.49 Hz, respectively. Two septets for the two isopropyl groups were observed at δ 3.08 and 3.98 ppm, respectively. The resonances corresponding to the THF protons were found at δ 1.79 and 3.59 ppm in the ^{1}HNMR and δ 25.10 and 66.99 ppm in the ^{13}C NMR spectra, respectively. The aromatic protons resonate at δ 7.17–7.37 ppm with an integration of five protons. In the mass spectrum, no molecular ion peak corresponding to **3** was detected, and only fragment ions were observed. However, ions that are in accordance with the proposed formula of **3** were detected. Monitoring the solution of **3** upon exposure to air for 2–3 days by NMR experiments showed no appreciable decomposition.
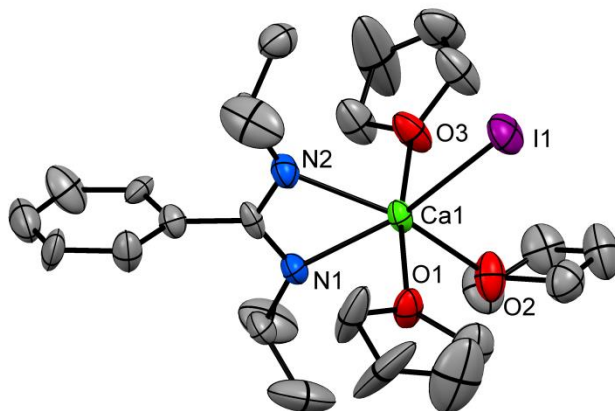
Figure 2.1.1: Crystal structure of monomeric calcium iodide complex **3**. Anisotropic displacement parameters are depicted at the 50% probability level. Hydrogen atoms are not shown for clarity. Selected bond distances (Å) and bond angles (deg): Ca1–I1 3.084(3), Ca1–N1 2.383(11), Ca1–N2 2.363(13), Ca1–O1 2.376(10), Ca1–O2 2.385(12),Ca1–O3 2.391(10); N2–Ca1–O3 89.6(4), N2–Ca1–N1 57.3(4), N1–Ca1–O3 94.2(4), N2–Ca1–O2 156.6(4), O3–Ca1–O2 81.9(5), N1–Ca1–O2 101.5(4), N2–Ca1–O1 100.5(4), O3–Ca1–O1 169.8(4), N1–Ca1–O1

90.3(4), O2–Ca1–O1 88.3(4), N2–Ca1–I1 107.0(3), O3–Ca1–I1 92.8(3), N1–Ca1–I1 162.7(3), O2–Ca1–I1 95.2(3), O1–Ca1–I1 85.5(3).

2.1.3: Synthesis and characterization of calcium iodide cluster

From the formation of **3**, we understood that THF molecules play a role in preventing the formation of homoleptic complex or dimerization. Hence, to check the role of donor solvent, we performed the same reaction in diethyl ether, keeping all other reaction conditions intact. The reaction led to a cluster of composition $L_2Ca_4I_8Li_4O$ (L=PhC(NiPr)$_2$) (**4**) (Scheme 2.1.4), having LiI incorporated into the structure. It represents a metal-rich cluster comprising of both group 1 and group 2 metals. We did not observe the formation of any other product either spectroscopically or structurally. Single crystal X-ray study shows that the cluster consists of a Ca_4O unit in which four Ca^{2+} ions are coordinated to the central O^{2-} ion to give the central oxygen atom a distorted tetrahedral geometry. An analogous Ca_4O unit was found in Harder's $[\{2,6\text{-}(MeO)_2C_6H_3\}_6Ca_4O].$[16] The source of the encapsulated O^{2-} ion is most likely the leakage of oxygen/moisture during the reaction or crystallization.[17] The cluster **4** is reproducible as unit cell constants of several crystals from the same as well as different batches were similar. **4** is insoluble in hydrocarbon solvents such as n-hexane, toluene, and benzene but soluble in diethyl ether, THF, and DMSO.
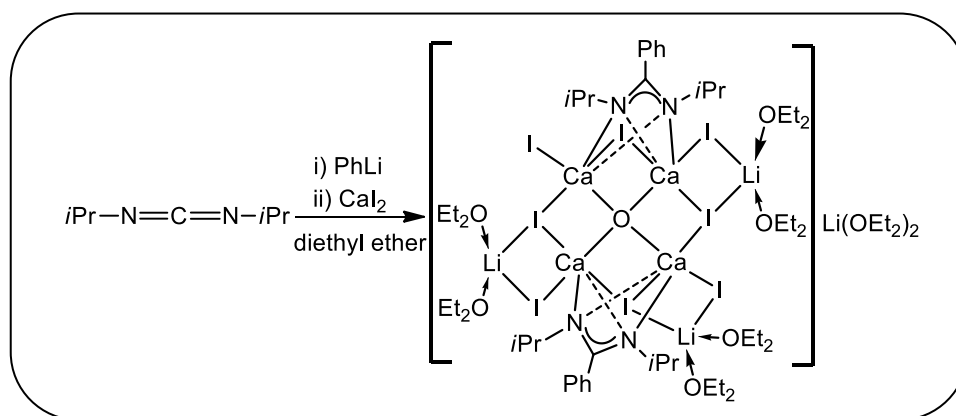

Scheme 2.1.4: Synthesis of calcium iodide cluster **4**.

The ^{1}H and ^{13}C spectra of **4** exhibited one set of resonances that result from the amidinate ligands and another set for the free ether moieties. One doublet is observed at δ 0.88 ppm with a coupling constant of 6.06 Hz whereas the other doublet is overlapped with the triplet resonances

from the CH_3 protons of the coordinated ethers. Two septets for the isopropyl groups are found at δ 3.09 and 3.96 ppm, which is in good agreement with those of **3**.

The molecular structure of **4** and its core structure are shown in Figure 2.1.2, and selected bond lengths and angles are listed in the legends of Figure 2.1.2. Compound **4** crystallizes in the monoclinic space group *C*2/*c*. The Ca-O distances vary within a very narrow range of 2.186(8)–2.216(8) Å, which are in good agreement with the Ca–O bond length found in [{2,6-$(MeO)_2C_6H_3$}$_6$Ca$_4$O] (2.128(3)–2.138(3)Å).[16] Each Ca atom is hexacoordinated and exhibits distorted octahedral geometry. There are four Ca_2IO four-membered rings present in the cluster. The Ca$\cdots$Ca distances lie between 3.196(4) and 3.787(4) Å. The distances between the Ca atoms bound to the same amidinate ligand (e.g. Ca1$\cdots$Ca4 and Ca2$\cdots$Ca3) are shorter than the distances between the two Ca atoms bound to two different amidinate moieties. There are twelve Ca–I bonds in the cluster which range from 3.000(3) to 3.193(4)Å. Out of eight I atoms, one (I2) is dicoordinate bound to only two Ca atoms, three (I4, I5, I7) are dicoordinate bound to one Ca and another Li atoms, three (I3, I6, and I8) are tri-coordinate bound to two Ca atoms and one Li atom and only I1 is monocoordinate with a terminal Ca–I bond. The Li–I bond lengths in these rings vary between 2.56(3) and 2.78(3)Å.
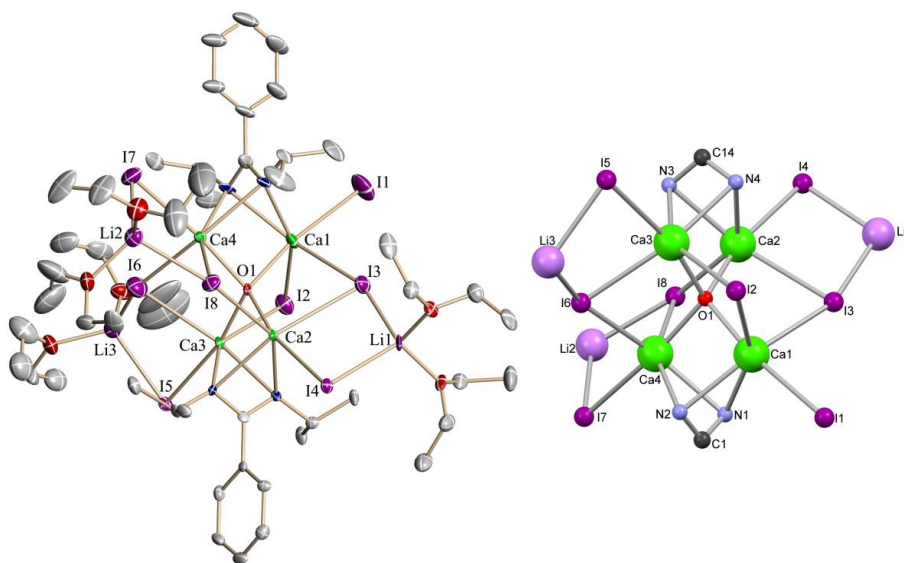

Figure 2.1.2: Molecular structure of calcium iodide cluster **4**. Anisotropic displacement parameters are depicted at the 50% probability level, hydrogen atoms and one Li atom are not shown for clarity. Selected bond distances (Å) and bond angles (deg): Ca1–O1 2.186(8), Ca2–O1

2.187(8), Ca3–O1 2.204(8), Ca4–O1 2.216(8), Ca1–I1 3.116(3), Ca1–I3 3.075(3), Ca1–I2 3.193(3), Ca2–I3 3.161(3), Ca2–I4 3.124(3), Ca2–I8 3.120(3), Ca3–I2 3.170(3), Ca3–I5 3.105(3), Ca3–I6 3.024(3), Ca4–I6 3.000(3), Ca4–I7 3.095(3), Ca4–I8 3.120(3); N2–Ca1–N1 52.5(4), N4–Ca2–N3 52.2(3), N4–Ca3–N3 52.4(3), N2–Ca4–N1 52.8(4), Ca1–O1–Ca2 119.0(4), Ca1–O1–Ca3 118.9(4), Ca2–O1–Ca3 93.4(3), Ca1–O1–Ca4 93.1(3), Ca2–O1–Ca4 118.6(4), Ca3–O1–Ca4 115.8(3).

2.1.4: Bonding mode in monomer and cluster complex

Another important feature is the coordination mode of the amidinate ligand (Scheme 2.1.5). They are flexible to coordinate either as monodentate two-electron donor (η^1) as well as chelating (η^2) or as bridging monodentate (μ-η^1-η^1) four-electron donor (Scheme 2.1.5).[10-12,18-20] In **4**, each N atom of the amidinate ligands is bound to two Ca atoms, leading to bridging and bis-chelating coordination mode. This type of bridging mono-chelating, bridging bis-chelating or analogous coordination was reported for the amidinate complexes of lithium,[21] sodium,[22] potassium,[23] magnesium,[24] strontium, and related guanidinate complexes of lithium, copper, and zinc.[25] Due to the coordination to both Ca atoms, there is a considerable increase in the Ca–N bond in **4** (2.517(11)–2.561(10) Å) than those in **3** (2.363(13) and 2.383(11)Å). In line with this finding, the corresponding N–Ca–N bite angles in **4** (52.2(3)–52.8(4)°) are considerably smaller than that in **3** (57.3(4)°). However, the different coordination modes do not influence the C−N bond lengths in the amidinate groups, which lie between 1.327(18) and 1.351(18)Å.
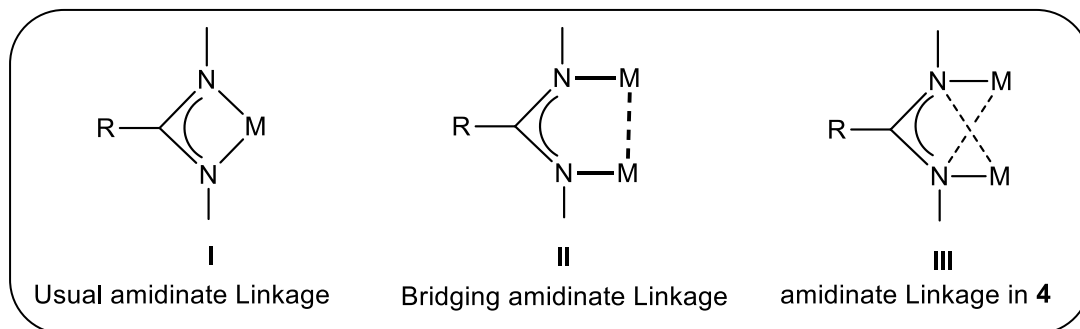
Scheme 2.1.5: Comparison of the usual amidinate linkage with **4**.

2.1.5: Conclusions

In conclusion, we have used a benz-amidinato ligand with *i*Pr substituents on the N atoms to synthesize hydrocarbon soluble calcium iodides. When the salt metathesis reaction between (PhC(N*i*Pr)$_2$Li) and CaI$_2$ were carried out in THF, a monomeric calcium iodide compound, **3** was obtained. The molecular structure of **3** was confirmed by single crystal X-ray studies, which shows a hexa-coordinate Ca(II) center with three THF molecules coordinated to Ca. Instead, when the same reaction was carried out in diethyl ether, a lithium calciate(II) cluster of composition L$_2$Ca$_4$I$_8$Li$_4$O (L=PhC(N*i*Pr)$_2$) (**4**) was obtained. The latter consists of a O^{2-} ion in the middle of a tetrahedron connected by four Ca^{2+} ions. The amidinate bonding mode in **3** is chelating, while in **4** is bridging and bis-chelating. Although it is unquestionable that **4** is a serendipitous product, there is a growing interest in oxygen scavenging by alkaline earth metal clusters,[26] and **4** is another example of oxygen scavenging in alkaline earth metal chemistry. In the next part of this chapter we will discuss about the reactivity of complex **3** in the catalytic hydroboration of aldehydes, ketones, and imines.

2.2: Benz-amidinato calcium iodide catalyzed aldehyde and ketone hydroboration with unprecedented functional group tolerance

2.2.1: Introduction

One of the most important homogeneously catalyzed reactions is the catalytic hydroboration of aldehydes and ketones, i.e. the formal addition of a borane R$_2$BH to a C=O bond to give R$_2$BOCHR$_2$. The transition metal catalyzed hydroboration of carbonyl compounds has been intensively studied.[27] Recently, several research groups have focused on the hydroboration of aldehydes and ketones without the use of transition-metal/rare-earth catalysts such as the groups of Roesky, Nembenna, Jones, Frenking, Zhao, Wesemann, and many others.[28-33] However, majority of these reports focus on *p*-block elements such as Al, Si, Ge, Sn, and P. While Okuda and co-workers reported hydroboration of aldehydes and ketones with alkali metal hydridotriphenylborates M[HBPh$_3$] (M = Li, Na, K) with remarkably high efficiency,[34] among alkaline earth metals, the catalyst scope for carbonyl hydroboration has been reported only with magnesium complexes.[35-39]

Catalytic hydroboration of carbon-heteroatom multiple bond with any calcium compound remains unexplored and deserves attention. A further impetus comes from the recent accomplishment by Marks' group of using organolanthanide catalysts for hydroboration of aldehydes and ketones. Complex **3** can catalyze the hydroboration of aldehydes and ketones by HBpin rapidly at room temperature to afford alkoxypinacolboronate esters.

2.2.2: Hydroboration of aldehydes

Aldehyde (0.25 mmol), pinacolborane (0.25 mmol), LCaI (0.5-2 mol%)(**3**) [benzene (1ml)] were charged in Schlenk tube inside glove box. The reaction mixture was allowed to run at room temperature. The progress of the reaction was monitored by ^{1}H NMR, which indicated the completion of the reaction by the disappearance of the aldehyde proton and appearance of a new CH_2 peak. Upon completion of reaction, the solvent was removed under high vacuum in Schlenk line and mesitylene (0.25 mmol) as internal standard, was added while making the NMR sample in $CDCl_3$. A brief screening of solvents showed that majority of the solvents are suitable for the reaction but benzene gives the best conversion. The reaction yields are calculated based on the integration area of product and starting material signals in the ^{1}H spectra using mesitylene as an internal standard. We assessed the utility of catalyst **3** with a variety of aldehydes and ketones.
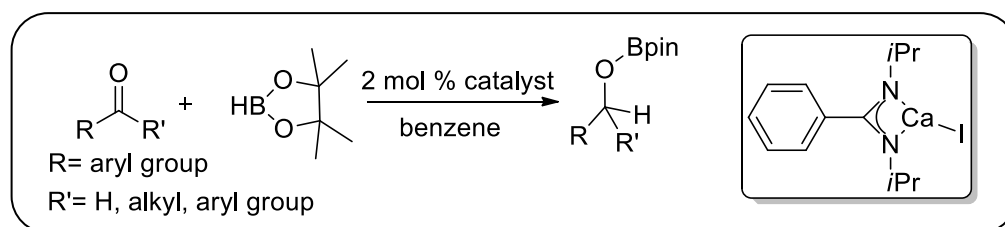
Scheme 2.2.1: Amidinato calcium(II) compound catalyzed hydroboration of aldehydes and ketones

For hydroboration of aldehydes, catalyst loadings are of typically 0.5-2 mol % and the reactions were over approx 40 min. (scheme 2.2.1). In fact, a number of aldehyde hydroboration reactions were over before the reaction mixtures were investigated by NMR spectroscopy. Hydroboration of aromatic aldehydes with electron donating as well as withdrawing substituents at different positions was obtained in good to high yields.[41] Moreover; *ortho* substituents (**5c**, **5f**, and **5n**) do not show any inhibitory effect. The reaction of 4-cyano-benzaldehyde with HBpin led to

exclusive hydroboration at the C=O functionality keeping the nitrile moiety intact (**5k**). The addition of a second equivalent of HBpin did not lead to further hydroboration of the nitrile functionality even after heating. In case of 4-fluorobenzaldehyde (**5l**), the fluoride functionality is well-tolerated. Surprisingly, when salicylaldehyde or 4-hydroxybenzaldehyde was used, hydroboration occurred at the aldehyde functional group instead of hydroxylborane dehydrocoupling, (**5i** and **5h**). No alkali or alkaline earth metal catalyst so far was reported to show tolerance towards OH group. However, when the same reaction is carried out in absence of the catalyst, dehydrocoupled product was observed albeit with low yield which is in line with the recent report by Bertrand and coworkers.[42] When 2 equivalents of HBpin were used, both hydroboration and dehydrocoupling reaction took place. The hydroboration of bromo benzaldehydes are limited with even magnesium based catalysts. Only Okuda et al. reported the hydroboration of 4-bromo benzaldehyde using [Mg(thf)$_6$][HBPh$_3$]$_2$,[37] but the reaction is very sluggish with noticeable amounts of DMSO reduction. On the contrary, we have observed that *o-*, *m-*, and *p*-bromo substituted benzaldehydes underwent almost quantitative hydroboration within 40 minutes (**5c-e**). Hydroboration of *α,β*-unsaturated cinnamaldehyde took place exclusively at the 1,2-position (**5o**) leaving the olefinic functionality intact. No dearomatization of the furan ring was observed when furfural was used, underscoring the catalyst selectivity towards C=O functionality (**5m**). Usually, higher catalyst loading, longer reaction time, heating are required for sterically hindered substrates. However, 2,6-dimethylbenzaldehyde (**5n**) and 1-naphthaldehyde (**5p**) underwent hydroboration under the same condition (room temperature, 40 min, 2 mol% catalyst) (Scheme 2.2.2)
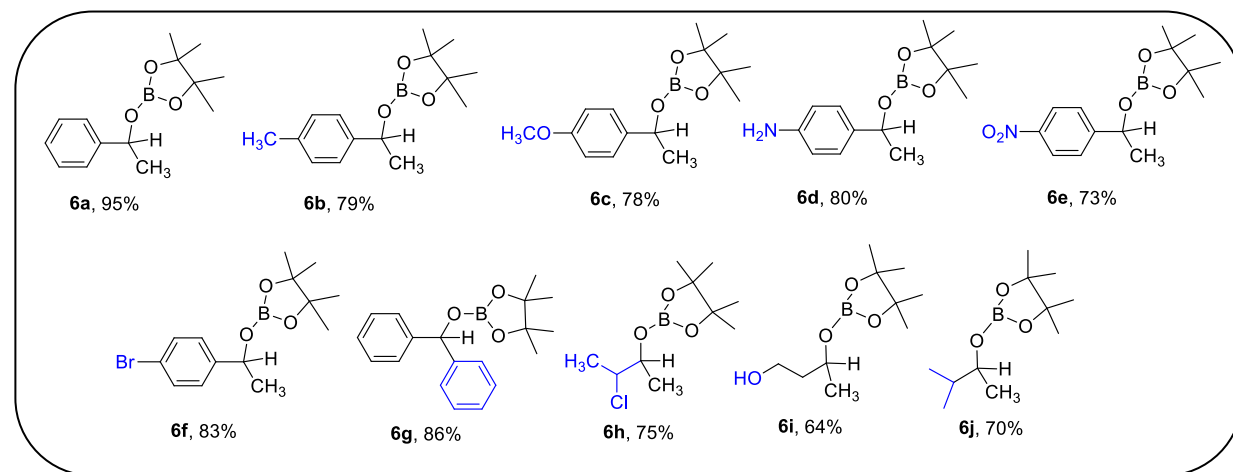
2.2.3: Hydroboration of ketones

Marginally higher catalyst loading (3 mol%) as well as longer reaction time (5 h), were required for ketones hydroboration. Ketone (0.25 mmol), pinacolborane (0. 25 mmol), LCaI (3 mol%)(**3**) [benzene (1 ml)] were charged in Schlenk tube inside glove box. The reaction mixture was allowed to run at room temperature. The progress of the reaction was monitored by ^{1}H NMR, which indicated the completion of the reaction by the appearance of a new CH peak. Upon completion of reaction, the solvent was removed using high vacuum in Schlenk line and mesitylene as internal standard, (0.25 mmol) was added while making the NMR sample in CDCl$_3$. The hydroboration of acetophenone derivatives with electron-withdrawing substituents

(Scheme 2.2.3; **6a-e**) as well as electron-donating substituent (**6f**) proceeded smoothly. The reaction showed excellent functional group tolerance toward NH and OH functionalities: e.g. 4-aminoacetophenone and 4-hydroxy 2-butanone reaction with HBpin led to the corresponding borate esters (**6d** and **6i**) instead of dehydrocoupling products. Aliphatic ketones such as 2-hydroxyethyl methyl ketone, methyl isopropyl ketone, 3-chloro-2-butanone also react with HBpin to afford the corresponding borate esters in moderate yields (**6g-i**).
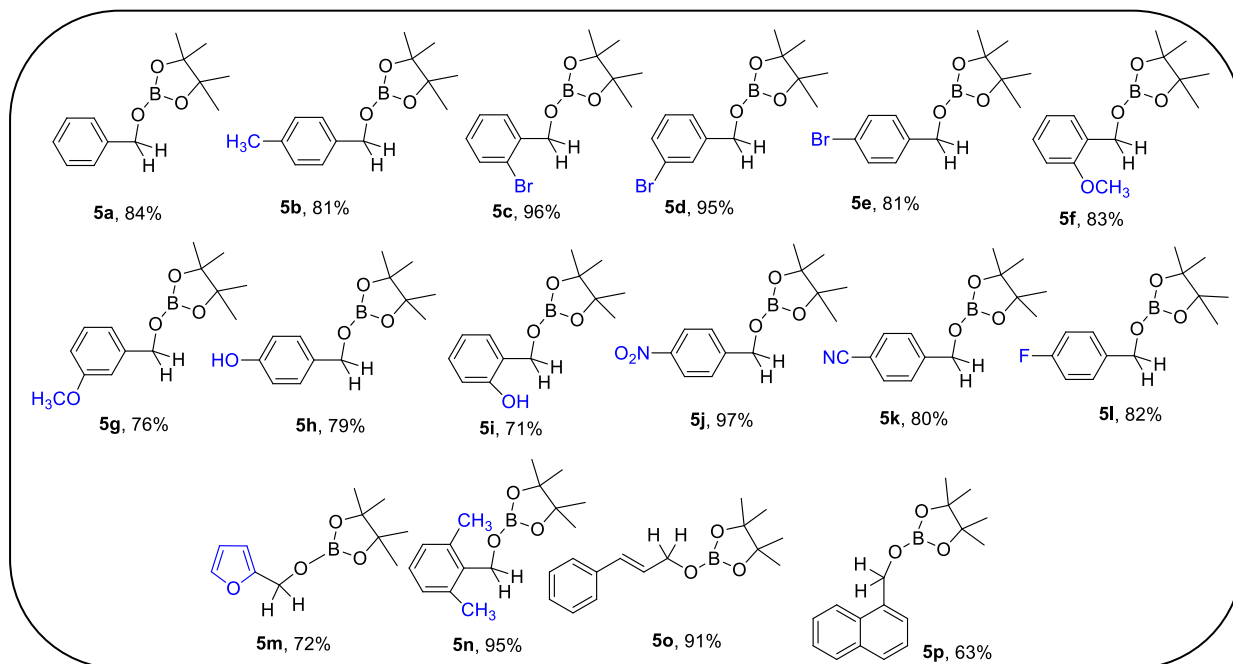

Scheme 2.2.2: Scope of hydroboration with aldehyde substrates

**Scheme 2.2.3**: Scope of hydroboration with ketone substrates

Among the existing magnesium based catalysts reported for hydroboration of aldehydes and ketones, Hill's molecular magnesium catalyst, [CH{C(Me)NAr}$_2$MgnBu, Ar=2,6-iPr$_2$C$_6$H$_3$] showed a TOF of 8×10^3 h^{-1} for PhCHO.[35] In comparison, our catalyst gave a TOF of 249 h^{-1} for PhCHO. However, for benzophenone, Hill's magnesium catalyst,[35] Okuda's [Mg(thf)$_6$][HBPh$_3$]$_2$,[37] Stasch's phosphinoamido-magnesium-hydride[36] are recorded with large TOFs of 500 h^{-1}, 1000 h^{-1} (in absence of DMSO), 1760 h^{-1}, respectively. **3** is also similar in activity but much poor compared to the formers in terms of TOF (8.6 h^{-1}). It is to be noted here that lithium hydridotriphenylborate [(L)Li][HBPh$_3$] [L=tris{2-(dimethylamino)ethyl}amine] has been recorded with the highest TOF of 66.6×10^3 h^{-1} for benzophenone.[8] However, unlike **3**, none of these aforementioned catalysts are reported to show tolerance towards the OH and NH groups. To further assess the competitive hydroboration of aldehydes versus ketones, the competing experiment involving a mixture of benzaldehyde and acetophenone was performed (Scheme 2.2.4), which led to almost quantitative hydroboration of benzaldehyde and complete recovery of acetophenone. Subsequent addition of a second equivalent of HBpin afforded both hydroborated products in more than 90% yield. This experiment shows excellent selectivity of aldehydes over ketones similar to the reports of Nembenna[29] and Marks.[40]
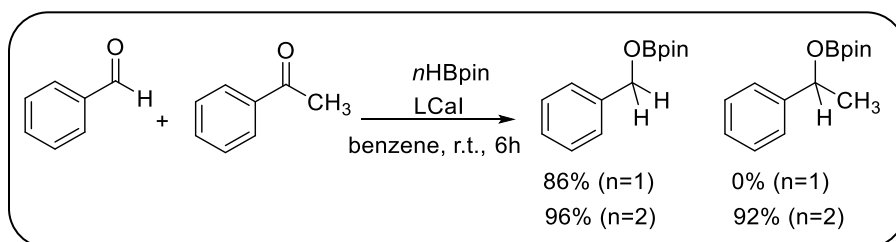
Scheme 2.2.4: Competitive aldehyde/ketone hydroboration selectivity study. Reaction conditions: 3 mol% catalyst. Yields were determined by ^{1}H NMR integration relative to mesitylene.

2.2.4: Hydroboration studies of Imine

A catalytic amount of **3** also promoted the hydroboration of benzylidene aniline with HBpin at 60 °C (Scheme 2.2.5). Previous studies of main group imine hydroboration catalysis typically involve (a) a combination of a Lewis acid and a Lewis base, such as DABCO and B(C$_6$F$_5$)$_3$,[43] (b) NacnacMg–alkyl complex,[44] or (c) PhC(NtBu)$_2$SiHCl$_2$.[32b]
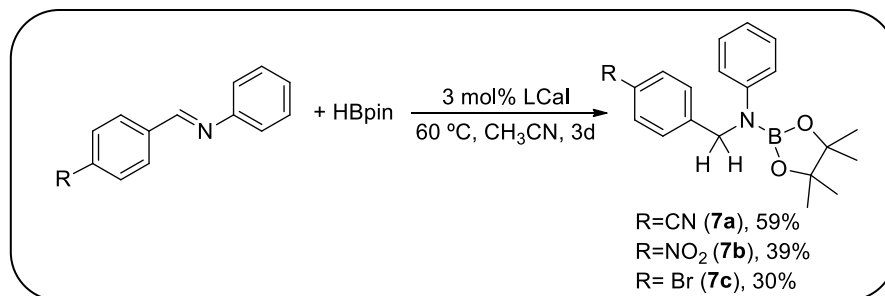
Scheme 2.2.5: Hydroboration of imine using **3** as a catalyst. Yields were determined by ^{1}H NMR integration relative to mesitylene.

2.2.5: Conclusion

In summary, this chapter describes the hydroboration of a range of aldehydes and ketones by using a well-defined calcium compound under mild conditions. The system chemoselectively reduces aldehydes over ketones and exhibits a good functional group tolerance even towards OH and NH groups. It is also believed that many of the organolanthanide catalysts mediated processes can likely be achieved with an organocalcium complex and our results on organocalcium catalyzed hydroboration of aldehydes and ketones testify the concept.

2.3: References

1. a) H. Gilman, F. Schulze, *Ber. Dtsch. Chem. Ges.*, **1926**, *48*, 2463–3467; b) H. Gilman, J. C. Bailie, *J. Org. Chem.*, **1937**, *2*, 84–94.

2. a) K. Mochida, T. Yamanishi, *J. Organomet. Chem.,* **1987**, *332*, 247–262; b) P. R. Markies, T. Nomoto, G. Schat, O. S. Akkerman, F. Bickelhaupt, *Organometallics,* **1991**, *10*, 3826–3837; c) M. L. Hays, T. P. Hanusa, *Tetrahedron Lett.,* **1995**, *36*, 2435–2436.

3. E. Beckmann, *Ber. Dtsch. Chem. Ges.*, **1905**, *38*, 904–906.

4. Selected examples for σ-bonded alkaline earth metal complexes, please see: (a) F. Feil, S. Harder, *Organometallics,* **2000**, *19*, 5010–5015; b) S. Harder, F. Feil, A. Weeber, *Organometallics,* **2001**, *20*, 1044–1046; c) S. Harder, S. Müller, E. Hübner, *Organometallics,* **2004**, *23*, 178–183; d) P. J. Bailey, R. M. Coxall, C. M. Dick, S. Fabre, L. C. Henderson, C. Herber, S. T. Liddle, D. Lorono-Gonzalez, A. Parkin, S. Parsons, *Chem. Eur. J.*, **2003**, *9*, 4820–4828; e) J. Langer, S. Krieck, R. Fischer, H. Görls, D. Walther, M. Westerhausen, *Organometallics,* **2009**, *28*, 5814–5820; f) T. P. Hanusa, *Coord. Chem. Rev.,*

2000, *210*, 329–367; g) J. S. Alexander, K. Ruhlandt-Senge, *Eur. J. Inorg. Chem.,* **2002**, 2761–2774; h) J. S. Alexander, K. Ruhlandt-Senge, *Chem. Eur. J.,* **2004**, *10*, 1274–1280; i) M. Westerhausen, *Dalton Trans.*, **2006**, 4755–4768; j) M. Westerhausen, M. Gärtner, R. Fischer, J. Langer, L. Yu, M. Reiher, *Chem. Eur. J.*, **2007**, *13*, 6292–6306.

5. For Ca-halide complexes other than iodides, please see: a) S. Nembenna, H. W. Roesky, S. Nagendran, A. Hofmeister, J. Magull, P.-J.Wilbrandt, M. A. Hahn, *Angew. Chem. Int. Ed.,* **2007**, *46*, 2512–2514; b) A. G. M. Barrett, M. R. Crimmin, M. S. Hill, P. B. Hitchcock, P. A. Procopiou, *Angew. Chem. Int. Ed.,* **2007**, *46*, 6339–6342; c) C. Ruspic, S. Harder, *Inorg. Chem.,* **2007**, *46*, 10426–10433; d) M. Westerhausen, M. H. Digeser, C. Gückel, H. Nöth, J. Knizek, W. Ponikwar, *Organometallics,* **1999**, *18,* 2491–2496; e) S. P. Sarish, S. Nembenna, S. Nagendran, H. W. Roesky, *Acc. Chem. Res.,* **2011**, *44*, 157–170; f) Heavier Group 2 in Alkaline-Earth Metal Compounds: Oddities and Applications, S. Harder, (Ed.); Springer-Verlag Berlin Heidelberg, 29–72; g) S. Harder, *Chem. Rev.*, **2010**, *110*, 3852–3876; For calcium iodides with non-chelating ligands, please see: h) J. Jenter, R. Köppe, P. W. Roesky, *Organometallics*, **2011**, *30*, 1404–1413; i) T. K. Panda, A. Zulys, M. T. Gamer, P. W. Roesky, *J. Organomet. Chem.*, **2005**, *690*, 5078–5089; j) M. Köhler, A. Koch, H. Görls, M. Westerhausen, *Organometallics*, **2016**, *35*, 242−248.

6. a) H. M. El-Kaderi, M. J. Heeg, C. H. Winter, *Polyhedron,* **2006**, *25*, 224–234; b) S. P. Sarish, A. Jana, H. W. Roesky, T. Schulz, M. John, D. Stalke, *Inorg. Chem.,* **2010**, *49*, 3816–3820; (c) S. J. Bonyhady, C. Jones, S. Nembenna, A. Stasch, A. J. Edwards, G. J. McIntyre, *Chem. Eur. J.*, **2010**, *16*, 938–955; (d) A. G. M. Barrett, M. R. Crimmin, M. S. Hill, P. B. Hitchcock, G. Kociok-Köhn, P. A. Procopiou, *Inorg. Chem.*, **2008**, *47*, 7366–7376.

7. S. P. Sarish, A. Jana, H. W. Roesky, T. Schulz, D. Stalke, *Organometallics*, **2010**, *29*, 2901–2903.

8. S. Datta, M. T. Gamer, P. W. Roesky, *Dalton Trans.*, **2008**, 2839–2843.

9. S.-O. Hauber; F. Lissner, G. B. Deacon, M. Niemeyer, *Angew. Chem. Int. Ed.*, **2005**, *44*, 5871–5875.

10. For reviews on amidinato stabilized silylenes and related compounds, please see: a) S. S. Sen, S. Khan, P. P. Samuel, H. W. Roesky, *Chem. Sci.*, **2012**, *2*, 659–682; b) S. S. Sen, S. Khan, S. Nagendran, H. W. Roesky, *Acc. Chem. Res.*, **2012**, *45*, 578–587; c) M. Asay, C.

Jones, M. Driess, *Chem. Rev.*, **2011**, *111*, 354–396; d) H. W. Roesky, *J. Organometal. Chem.*, **2013**, *730*, 57–62; e) V. S. V. S. N. Swamy, S. Pal, S. Khan, S. S. Sen, *Dalton Trans.*, **2015**, *44*, 12903–12923; f) S. Nagendran, S. S. Sen, H. W. Roesky, D. Koley, H. Grubmüller, A. Pal, R. Herbst-Irmer, *Organometallics*, **2008**, *27*, 5459–5463; g) S. S. Sen, M. P. Kritzler-Kosch, S. Nagendran, H. W. Roesky, T. Beck, A. Pal, R. Herbst-Irmer, *Eur. J. Inorg. Chem.*, **2010**, 5304–5311.

11. S. P. Green, C. Jones, A. Stasch, *Science*, **2007**, *318*, 1754–1757.

12. a) A. G. M. Barrett, M. R. Crimmin, M. S. Hill, P. B. Hitchcock, S. L. Lomas, M. F. Mahon, P. A. Procopiou, K. Suntharalingam, *Organometallics*, **2008**, *27*, 6300–6306; b) R. J. Schwamm, M. P. Coles, *Organometallics*, **2013**, *32*, 5277–5280; c) M. Arrowsmith, M. R. Crimmin, M. S. Hill, S. L. Lomas, M. S. Heng, P. B. Hitchcock, G. Kociok-Köhn, *Dalton Trans.*, **2014**, *43*, 14249–14256.

13. a) T. Kottke, D. Stalke, *J. Appl. Crystallogr.*, **1993**, *26*, 615–619; b) D. Stalke, *Chem. Soc. Rev.*, **1998**, *27*, 171–178.

14. M. Köhler, A. Koch, H. Görls, M. Westerhausen, *Organometallics*, **2016**, *35*, 242−248.

15. M. Westerhausen, W. Schwarz, *Z. Naturforsch.*, **1992**, *47*, 453–459.

16. C. Ruspic, S. Harder, *Organometallics,* **2005**, *24*, 5506–5508.

17. a) C. Ruspic, S. Harder, *Organometallics*, **2005**, *24,* 5506–5508; b) R. Fischer, H. Görls, M. Westerhausen, *Inorg. Chem. Commun.,* **2005**, *8*, 1159–1161; c) R. E. Mulvey, V. L. Blair, W. Clegg, A. R. Kennedy, J. Klett, L. Russo, *Nature Chem.*, **2010**, *2*, 588–591; d) S. Krieck, H. Görls, M. Westerhausen, *J. Organomet. Chem.*, **2009**, *694*, 2204–2209; e) J. Langer, M. Gärtner, R. Fischer, H. Görls, M. Westerhausen, *Inorg. Chem. Commun.*, **2007**, *10,* 1001–1004; f) S. Harder, C. Ruspic, *Eur. J. Inorg. Chem.*, **2015**, 5743–5750.

18. J. Barker, M. Kilner, *Coord. Chem. Rev.*, **1994**, *133*, 219–300.

19. a) F. T. Edelmann, *Chem. Soc. Rev.*, **2009**, *38*, 2253–2268; b) F. T. Edelmann, *Adv. Organomet. Chem.*, **2008**, *57*, 133–352; c) F. T. Edelmann, M. P. Coles, *J. Chem. Soc., Dalton Trans.*, **2006**, 985–1001.

20. P. C. Junk, M. L. Coles, *J. Chem. Soc. Chem. Commun.*, **2007**, 1579–1590.

21. a) C. Knapp, E. Lork, P. G. Watson, R. Mews, *Inorg. Chem.*, **2002**, *41*, 2014–2025; b) D. Stalke, M. Wedler, F. T. Edelmann, *J. Organomet. Chem.*, **1992**, *431*, C1–C5

22. Marcus L. Cole, Aaron J. Davies, Cameron Jones, Peter C. Junk, *J. Organomet. Chem.*, **2004**, *689*, 3093−3107.

23. J. Baldamus, C. Berghof, M. L. Cole, D. J. Evans, E. Hey-Hawkins, P. C. Junk, *J. Chem. Soc., Dalton Trans.*, **2002**, 4185−4192.

24. A. R. Sadique, M. J. Heeg, C. H. Winter, *Inorg. Chem.,* **2001**, *40*, 6349–6355.

25. a) M. P. Coles, P. B. Hitchcock, *Chem. Commun.,* **2002**, 2794–2795; b) M. P. Coles, P. B. Hitchcock, *Eur. J. Inorg. Chem.,* **2004**, 2662–2672; c) S. H. Oakley, M. P. Coles, P. B. Hitchcock, *Inorg. Chem.*, **2003**, *42*, 3154–3156.

26. a) T. Chivers, A. Downard, G. P. A. Yap, *J. Chem. Soc., Dalton Trans.*, **1998**, 2603–2606; b) A. R. Kennedy, R. E. Mulvey, R. B. Rowlings, *Angew. Chem. Int. Ed.*, **1998**, *37*, 3180–3183; c) A. E. H. Wheatley, *Chem. Soc. Rev.*, **2001**, *30*, 265–273.

27. Selected recent examples of transition metal catalyzed hydroboration of aldehydes and ketones, see: (*a*) N. Eedugurala, Z. Wang, U. Chaudhary, N. Nelson, K. Kandel, T. Kobayashi, I. I. Slowing, M. Pruski, A. D. Sadow, *ACS Catal.*, **2015**, *5*, 7399–7414; (*b*) A. Kaithal, B. Chatterjee, C. Gunanathan, *Org. Lett.,* **2015**, *17*, 4790–4793; (*c*) S. Bagherzadeh, N. P. Mankad, *Chem. Commun.,* **2016**, *52*, 3844–3846; (*d*) J. Guo, J. Chen, Z. Lu, *Chem. Commun.*, **2015**, *51*, 5725–5727; (*e*) G. Zhang, H. Zeng, J. Wu, Z. Yin, S. Zheng, J. C. Fettinger, *Angew. Chem. Int. Ed.,* **2016**, *55*, 14369–14372; (*f*) M. W. Drover, L. L. Schafer, J. A. Love, *Angew. Chem. Int. Ed.,* **2016**, *55*, 3181–3186.

28. (*a*) Z. Yang, M. Zhong, X. Ma, S. De, C. Anusha, P. Parameswaran, H. W. Roesky, *Angew. Chem. Int. Ed.,* **2015**, *54*, 10225–10229; (*b*) Z. Yang, M. Zhong, X. Ma, K. Nijesh, S. De, P. Parameswaran, H. W. Roesky, *J. Am. Chem. Soc.,* **2016**, *138*, 2548−2551.

29. V. K. Jakhar, M. K. Barman, S. Nembenna, *Org. Lett.,* **2016**, *18*, 4710−4713.

30. T. J. Hadlington, M. Hermann, G. Frenking, C. Jones, *J. Am. Chem. Soc.,* **2014**, *136*, 3028–3031.

31. (a) C.-C. Chong, H. Hirao, R. Kinjo, *Angew. Chem. Int. Ed.,* **2015**, *54*, 190−194; (b) C. C. Chong, R. Kinjo, *ACS Catal.,* **2015**, *5*, 3238−3259.

32. Y. Wu, C. Shan, Y. Sun, P. Chen, J. Ying, J. Zhu, L. Liu, Y. Zhao, *Chem. Commun.*, **2016**, *52*, 13799−13802.

33. J. Schneider, C. P. Sindlinger, S. M. Freitag, H. Schubert, L. Wesemann, *Angew. Chem. Int. Ed.,* **2017**, *56*, 333–337.

34. D. Mukherjee, H. Osseili, T. P. Spaniol, J. Okuda, *J. Am. Chem. Soc.,* **2016**, *138*, 10790–10793.

35. M. Arrowsmith, T. J. Hadlington, M. S. Hill, G. Kociok-Köhn, *Chem. Commun.,* **2012**, *48*, 4567−4569.

36. L. Fohlmeister, A. Stasch, *Chem. Eur. J.,* **2016**, *22*, 10235–10246.

37. D. Mukherjee, S. Shirase, T. P. Spaniol, K. Mashima, J. Okuda, *Chem. Commun.,* **2016**, *52***, 13155–13158.

38. D. Mukherjee, A. Ellern, A. D. Sadow, *Chem. Sci.,* **2014**, *5*, 959–965.

39. K. Manna, P. Ji, F. X. Greene, W. Lin, *J. Am. Chem. Soc.,* **2016**, *138*, 7488−7491.

40. V. L. Weidner, C. J. Barger, M. Delferro, T. L. Lohr, T. J. Marks, *ACS Catal.*, **2017**, *7*, 1244–1247.

41. We have also investigated whether CaI_2 is the actual catalyst which may be generated during the reaction via ligand exchange of **3**. Hence, we deliberately attempted the hydroboration of benzaldehyde using 5mol% CaI_2 as catalyst. Although the reaction led to the hydroborated products but with longer reaction time (24 h), forcing conditions (heating was required at 60 °C), and in less yield (60%).

42. E. A. Romero, J. L. Peltier, R. Jazzar, G. Bertrand, *Chem. Commun.,* **2016**, *52*, 10563–10565.

43. P. Eisenberger, A. M. Bailey, C. M. Crudden, *J. Am. Chem. Soc.,* **2012**, *134*, 17384–17387.

44. M. Arrowsmith, M. S. Hill, G. Kociok-Köhn, *Chem.–Eur. J*., **2013**, *19*, 2776–2783.

Chapter 3: Beyond Hydrofunctionalisation: A Well-Defined Calcium Compound Catalysed Mild and Efficient Carbonyl Cyanosilylation
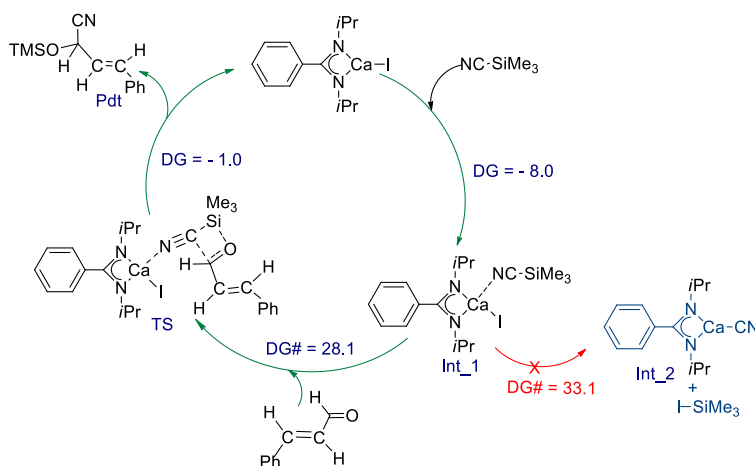

Abstract:

Organocalcium compounds have been reported as efficient catalysts for various transformations, for cases in which one of the substrates contained an E–H (E=B, N, Si, P) bond. In this chapter we have discussed the utilization an organocalcium compound for a transformation in which none of the precursors has a polar E–H bond. We have used a well-defined amidinato calcium iodide, [PhC(NiPr)$_2$CaI] (**3**) for cyanosilylation of a variety of aldehydes and ketones with Me$_3$SiCN under ambient conditions without the need of any co-catalyst. The reaction mechanism involves a weak adduct formation between **3** and Me$_3$SiCN leading to the activation of the Si−C bond, which subsequently undergoes σ-bond metathesis with a C=O moiety. The reaction intermediate has been characterized by multinuclear NMR spectroscopy and IR spectroscopy. Experimental and computational studies support the mechanism.

3.1: Introduction

Due to environmental and economic concerns, there is an urgent demand to explore efficient, sustainable catalysts based on earth-abundant elements that may compete with the precious metal catalysts in high-value transformations.[1-4] Among various earth-abundant elements, organocalcium compounds have recently received considerable interest due to their high terrestrial abundance, cost-effectiveness, non-toxicity, and biocompatibility. A wide range of catalytic processes such as hydroamination, hydroboration, hydrosilylation, hydrophosphination and the hydrogenation of C=C, C=O or C=N bonds involving hydrocarbon soluble calcium compounds has appeared in recent years through the studies from a number of research groups of whom Harder, Hill, Roesky, Westerhausen, Sarazin, and Ward are especially prominent.[5-20] A common feature of all aforementioned reactions is that one of the precursors contains an E–H bond that undergoes σ-bond metathesis with the organocalcium compound to generate the active catalyst. The latter undergoes an insertion reaction with the unsaturated C=X bond to generate a species that subsequently reacts with another molecule of E-H to form the product and regenerate the catalyst (Scheme 3.1). Therefore, the catalytic landscape of organocalcium compounds is primarily restricted to those processes where one of the substrates contains a polar E–H bond and is generally not known for those reactions where neither of the substrates possess an E–H bond.
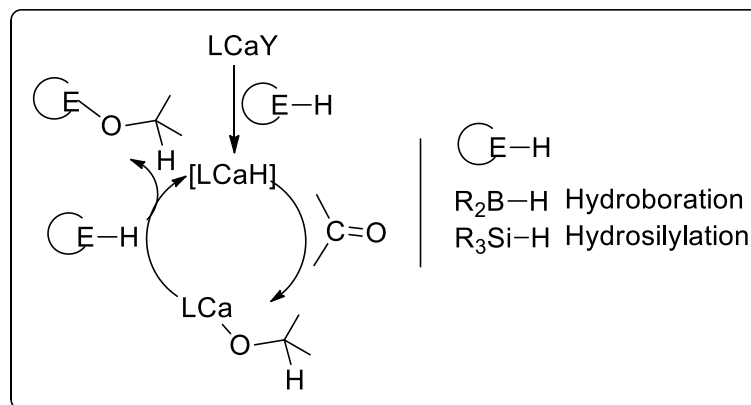
Scheme 3.1: The tentative catalytic cycle for organocalcium catalyzed hydrofunctionalization of carbonyl compounds [Y=H, alkyl]. What happens if there is no E–H bond present in the substrates?

To expand the catalytic regime of hydrocarbon soluble well-defined calcium compounds, we have turned our attention towards the cyanosilylation of carbonyl compounds with Me$_3$SiCN,[21] where none of the substrates possessed an E–H bond. Unlike carbonyl hydroboration by heavier main group compounds, which is increasingly being reported in the literature and discussed in details in the previous chapter,[22] the catalytic carbonyl cyanosilylation by compounds with heavier main group elements has seen only partial success with p-block elements from the groups of Roesky,[23-25] Nagendran,[26,27] and others.[28,29] Furthermore, cyanosilylation of carbonyl compounds has not been achieved till the publication of our work with any alkaline earth metal complex. Subsequent to publication of our work, we have found that the group of Ma reported cyanosilylation with Mg(I) complexes.[30] Our initial entry into the calcium chemistry was through the preparation of soluble and easily accessible [PhC(NiPr)$_2$CaI] (3),[31] which was described in the previous chapter. After observing that 3 efficiently catalyzes the hydroboration of aldehydes, ketones, and imines,[32] we sought to look into the viability of cyanosilylation of carbonyl compounds with the former to enhance the utility of 3 as a catalyst. Incentivized by the seminal works on electrostatic activation of multiple bonds by an early main group element by Clark and others,[33] we hypothesized that the electrostatic interaction between the Ca atom of 3 and Me$_3$SiCN will activate the Si-C bond to such a level that it would permit further nucleophilic attack from the carbonyl moiety. In this chapter, we describe our initial efforts to define a catalytic, molecular cyanosilylation process based upon a calcium complex and provide a mechanistic appraisal based upon stoichiometric reactivity and DFT based calculations.
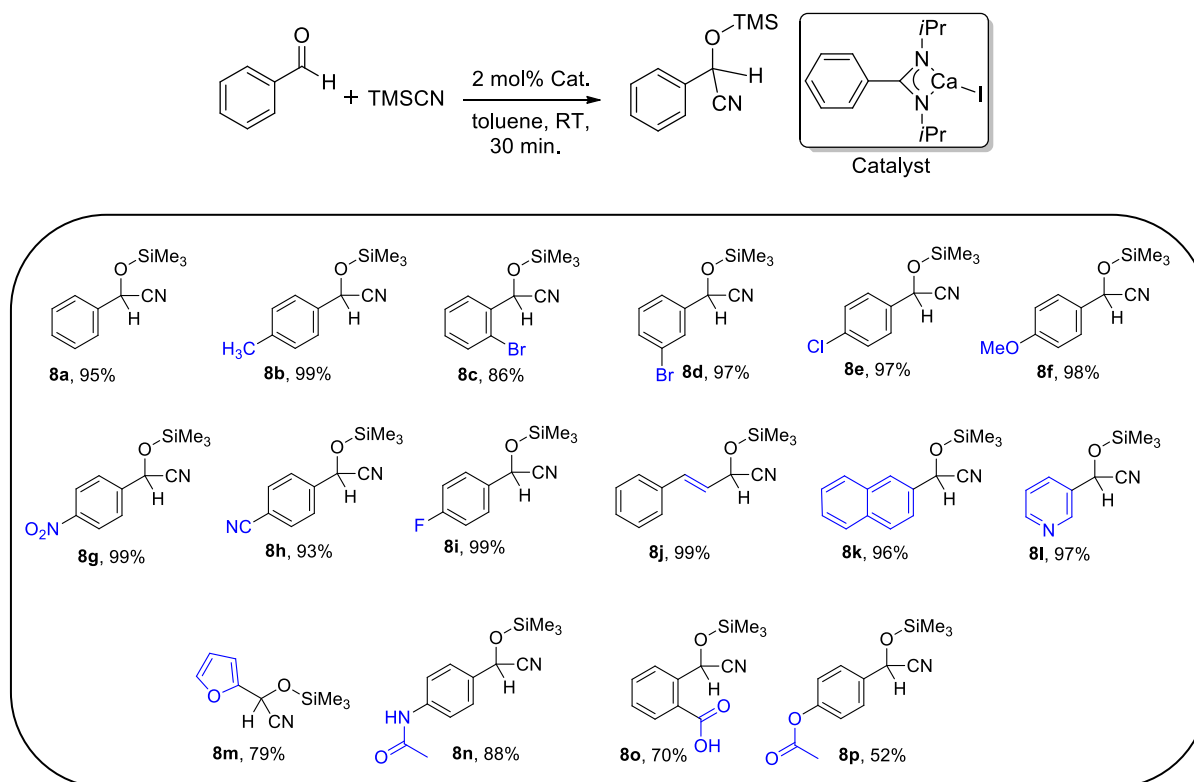
3.2: Cyanosilylation of aldehydes

Complex 3 was examined as a catalyst for cyanosilylation of a variety of aldehydes and ketones with Me$_3$SiCN, as illustrated in Scheme 3.2. A brief screening of solvents showed that most of the organic solvents were suitable for the reaction. However, for aldehydes, toluene and for ketones, THF afforded the best results (Table 3.1). Conversion of aldehydes was efficient at catalyst loadings of 2 mol % within 30 minutes (entries 8a-8p). As the experiments were monitored by ^{1}H NMR spectroscopy, most of the reactions were over before the reaction mixture could be analyzed. In fact, a visual evaluation of all such reactions qualitatively indicated that they were complete in less than 10 min. Electron donating (8b, 8f) as well as withdrawing groups(8c, 8g, 8h, 8i) were well tolerated.

Entry	Catalyst (mol%)	Time(h)	Solvent	NMR Yield%
1.	0.5	0.5	toluene	73
2.	2	0.5	toluene	95
3.	3	0.5	toluene	95
4.	2	1	toulene	96
5.	2	0.5	THF	84
6.	2	0.5	benzene	86
7.	2	0.5	hexane	67

Table 3.1: Optimization table for aldehyde cyanosilylation.

For the analogous reactions with substrates including naphthalene and heterocycles, the desired products were obtained in good yields (**8k**: 96%, **8l**: 97%, **8m**: 79%). Consistent with recent studies, 1,2-addition of Me$_3$SiCN to cinnamaldehyde was observed as a result of the highly electrophilic character of the carbonyl moiety (**8j**). Aldehydes were selectively and exclusively cyanosilylated in the presence of amide (**8n**), acid (**8o**) and ester (**8p**).

Scheme 3.2: The scope of cyanosilylation with aldehyde substrates.

3.3: Cyanosilylation of ketones

Aromatic ketones were identified as equally suitable substrates for cyanosilylation, demonstrated by the conversion of acetophenone although marginally higher catalyst loading (3 mol %) and extended reaction time (2h) were necessary to achieve good conversion. Even the sterically demanding benzophenone was converted to the corresponding cyanosilylated product (**9g**) under the same conditions in 82% yield, which had not been achieved with any other main group catalyst thus far. The cyanosilylation of a wide variety of aromatic ketones bearing various functional groups to the respective cyanohydrin trimethylsilyl ethers was successful under standard reaction conditions. The cyanosilylation of acetophenone derivatives with electron withdrawing substituents (**9c**, **9d**) took place smoothly. In contrast, acetophenone derivatives with electron donating substituents (**9b**, **9e**, **9h**) were not found to be very suitable for productive catalysis (Scheme 3.3). Among the main group catalysts, the catalytic efficiency of **3** was found to be higher than our previously reported silane catalyst [PhC(NtBu)$_2$Si(H)(Me)Cl] and comparable with other known aluminum catalysts reported by Zhi, Nagendran, Roesky and others.[23-27]
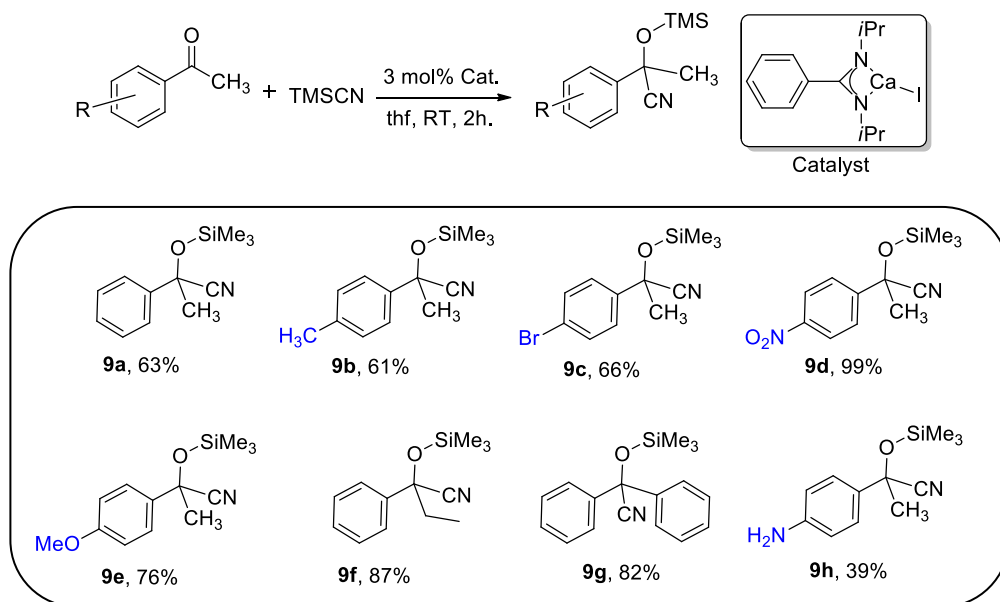
Scheme 3.3: The scope of cyanosilylation with ketone substrates.

3.4: Mechanistic studies of reaction cycle

Efforts to gain some mechanistic insights were next undertaken. Two possible pathways may be considered for the mechanism. By analogy to the mechanism proposed for organolanthanide catalyzed cyanosilylation of ketones,[34] the Ca-catalyst can undergo σ-bond metathesis with Me_3SiCN affording the "Ca-CN complex" (**Int_2**) that acts as the catalyst for the cycle. Alternatively, **3** can form an adduct with Me_3SiCN (**Int_1**) and activates the Si-C bond. As Me_3SiCN is more basic than THF, replacement of one of the THF molecules by Me_3SiCN is viable. The cycloaddition of the Si–C σ bond of the Me_3SiCN fragment to the O=C bond of the carbonyl moiety could result in the formation of cyanohydrin. In order to understand which mechanism is operational, a few stoichiometric reactions were undertaken. The ^{1}H NMR spectrum of the 1:1 reaction of **3** and Me_3SiCN at ambient temperature shows the development of a new $SiMe_3$ peak at δ 0.06 ppm along with the free Me_3SiCN peak at δ 0.23 ppm. In the ^{29}Si NMR, a new peak developed at δ 7.39 ppm with the free Me_3SiCN peak at δ -11.6 ppm. No peak at δ 0.38 ppm in the ^{1}H NMR and δ 10.5 ppm in the ^{29}Si NMR negate the possibility of the metathesis reaction between **3** and Me_3SiCN and the formation of Me_3SiI during the reaction. Monitoring the NMR after 2 h showed the disappearance of the Me_3SiCN resonance and the presence of only one resonance at δ 7.39 ppm in the ^{29}Si NMR (Figure 3.1, left). New resonances appeared at the ^{13}C NMR spectrum at δ 2.1 and 167.2 ppm, which are different from those in Me_3SiCN (δ -1.95 and 127.62 ppm). The new resonances are indicative of the formation of a weakly bound adduct. The IR spectrum of the intermediate showed a CN stretching band at v 2067.7 cm^{-1} (free Me_3SiCN at v 2192 cm^{-1}). The decrease in stretching frequency indicates the decrease of triple bond character, which is anticipated due to electrostatic interaction between the C≡N bond and the calcium atom (Figure 3.1, right). Taken together, these data surmise that Me_3SiI was not formed during the catalytic cycle and suggests the possible formation of a weakly bound adduct, **Int_1**. The role of the calcium complex is to pre-orient the substrate as well as activate the C–Si bond in Me_3SiCN. By monitoring the reaction of **Int_1** with 1 equivalent of benzaldehyde by ^{1}H NMR, we observed the formation of the characteristic C–H resonance of the **Pdt** at δ 4.69 ppm.
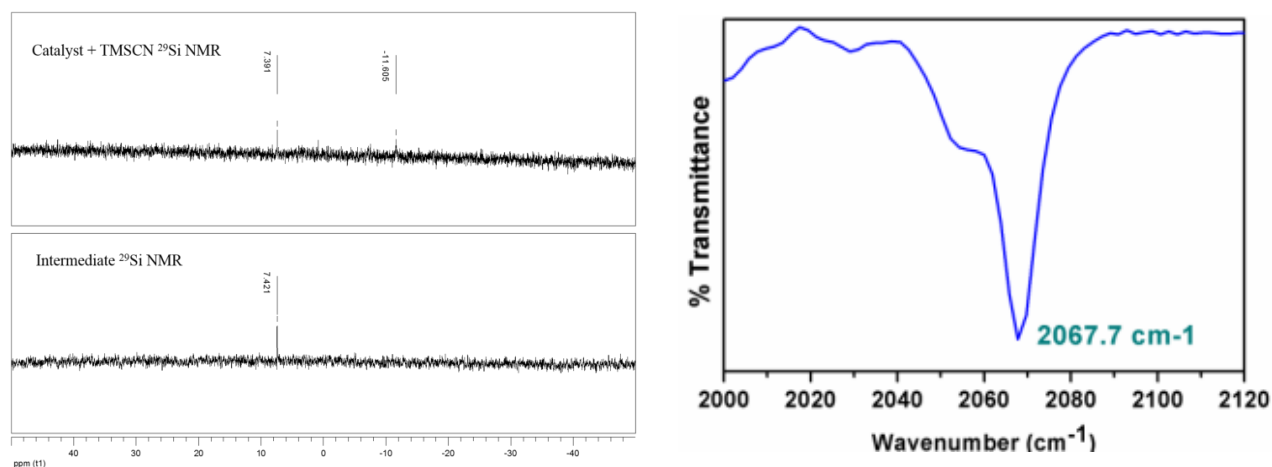
Figure 3.1: ^{29}Si NMR from the reaction the reaction mixture of **3** and Me$_3$SiCN (left). The above NMR was taken after 30 min, when both Me$_3$SiCN and **Int_2** were present; after 2 h all Me$_3$SiCN was consumed and only **Int_2** was left. The IR spectrum of the **Int_2** is on the right.

3.5: Theoretical investigation of mechanism

Full quantum chemical calculations have also been done using density functional theory (DFT) at the PBE/QZVP level of theory. Cinnamaldehyde was chosen as the substrate for the calculations because the obtained product yield was observed to be highest for this case. The mechanism obtained for this is shown in Scheme 3.4.

Complex **3** can react with trimethylsilyl cyanide (Me$_3$SiCN) to give **Int_1**, where the nitrogen of the cyanide group shows a weak interaction with the calcium of catalyst **3**. This intermediate complex, **Int_1**, is seen to being thermodynamically stable ($\Delta G = -8.0$ kcal/mol), (see Scheme 3.4). Subsequent to this, there are two possible pathways that can be followed as the reaction proceeds. In the first possible pathway, Int_1 can transform into Int_2 (Scheme 3.5) *via* a four membered transition state, TS_2, with a free energy barrier ($\Delta G^{\#}$) of 33.1 kcal/mol and a reaction free energy (ΔG) of 2.5 kcal/mol. In the alternative pathway, nucleophilic attack by the carbonyl oxygen of the cinnamaldehyde can occur at the silicon centre of Me$_3$SiCN in **Int_1**. This will lead to the cyanide being transferred from the silicon centre to the electrophilic carbonyl carbon of the cinnamaldehyde, *via* a C-C bond formation reaction. This occurs through a four membered transition state (**TS_1**) and has a barrier of 28.1 kcal/mol.
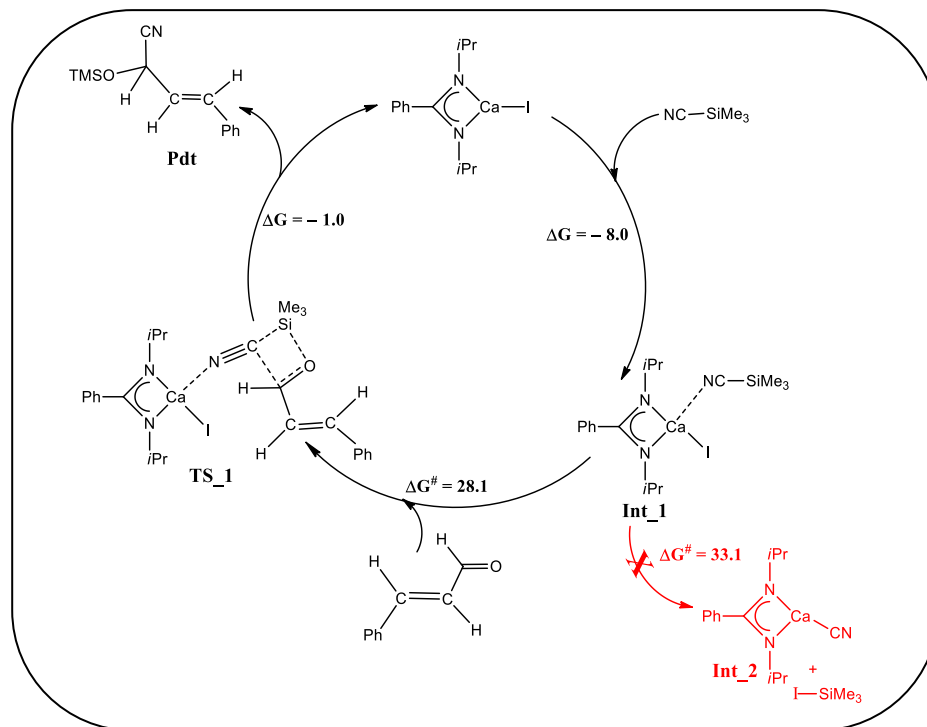
Scheme 3.4: The catalytic cycle and reaction mechanism for the cinnamaldehyde cyanosilylation reaction by catalyst **3**, calculated at the PBE/QZVP level of theory with DFT. ΔG and $\Delta G^{\#}$ represent the Gibbs free energy of reaction and the Gibbs free energy of activation respectively. All values are in kcal/mol.

Therefore, a comparison of the two competing pathways shows that the second pathway is thermodynamically (by 3.5 kcal/mol) and kinetically (by 5.0 kcal/mol) more favourable than the first. Indeed, applying the Arrhenius equation to compare the rates, it is seen that the second pathway would be approximately 4000 times faster than first. Hence, it becomes clear that the reaction would proceed through the second pathway, where the transition state **TS_1** would lead to the formation of the product (**Pdt**) along with the regeneration of the catalyst **3**. The free energy profile with the intermediate and transition state structures are shown in Scheme 3.5.
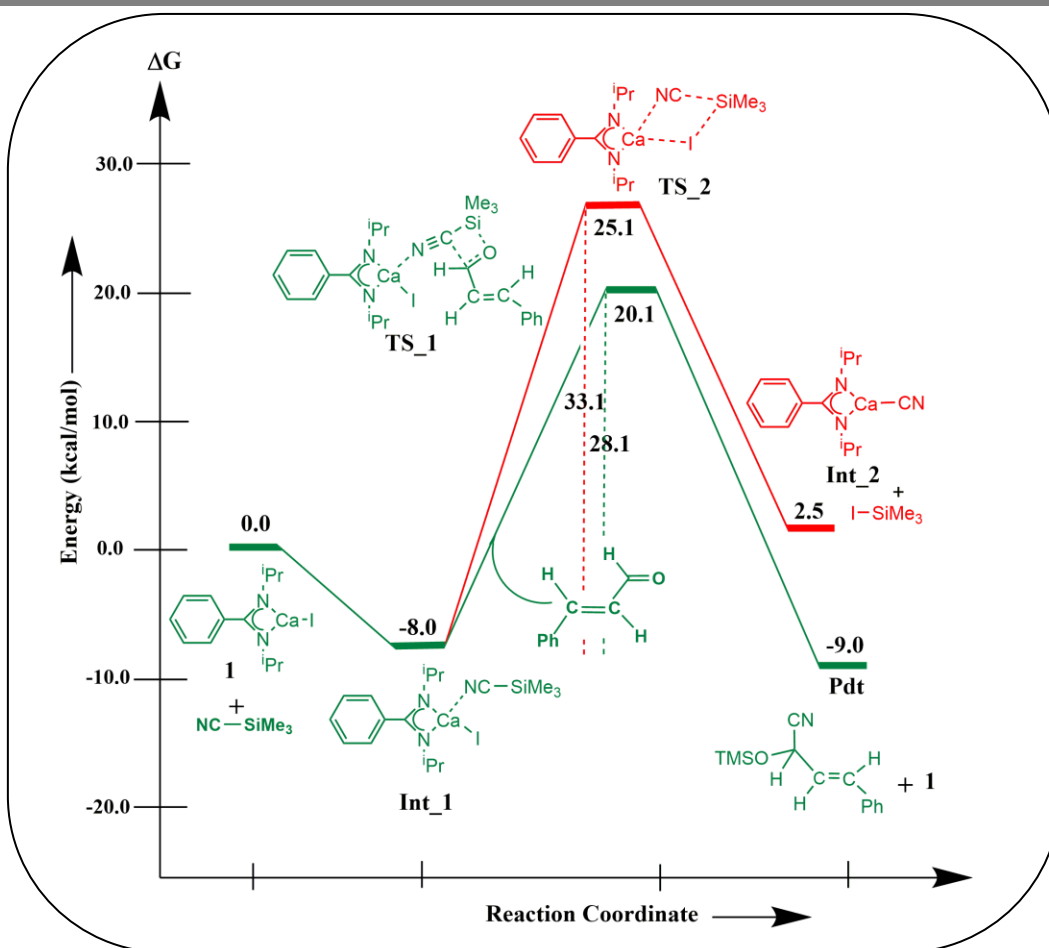
Scheme 3.5: The reaction energy profile diagram for the catalytic cyanosilylation reaction of cinnamaldehyde by catalyst **3**. The values (in kcal/mol)have been calculated at the PBE/QZVP level of theory with DFT.

3.6: Conclusions

In summary, organocalcium compounds are thus far known to catalyze hydroboration, hydroamination, hydrophosphination, and hydrosilylation of multiple bonds. We have introduced a well-defined organocalcium catalyst for cyanosilylation of carbonyl compounds, where none of the precursors contains a polar E–H bond. The catalyst is found to be very effective for the cyanosilyltion of a wide range of aldehydes and ketones under ambient conditions. As neither the precursor or nor the catalyst contains any E–H bond, the mechanism of the reaction is different from that proposed previously for organocalcium catalyzed reactions. Our combined experimental and computational studies (with DFT based calculations) lead us to conclude that the calcium complex forms a weak adduct with trimethylsilyl cyanide, leading to polarization of

the Si-C bond and facilitates the carbonyl attack. The observation of cyanosilylation of carbonyl compounds with **3** will not only expand the catalytic regime of calcium complexes but reduce the gap between the chemistry of alkaline earth metals and transition metals/lanthanides in homogeneous catalysis.

3.7: References

1. Q.−L Zhou, *Angew. Chem. Int. Ed.*, **2016**, *55*, 5352–5353.

2. R. M. Bullock, *Science,* **2013**, *342*, 1054–1055.

3. P. Wender, *Nature,* **2011**, *469*, 23–25.

4. R. M. Bullock, *Catalysis Without Precious Metals* (Wiley, 2010).

5. F. Buch, J. Brettar, S. Harder, *Angew. Chem. Int. Ed.,* **2006**, *45*, 2741–2745.

6. J. Spielmann, F. Buch, S. Harder, *Angew. Chem. Int. Ed.,* **2008**, *47*, 9434–9438.

7. M. R. Crimmin, I. J. Casely, M. S. Hill, *J. Am. Chem. Soc.,* **2005**, *127*, 2042–2043.

8. S. Datta, P. W. Roesky, S. Blechert, *Organometallics,* **2007**, *26*, 4392–4394.

9. S. Datta, M. T. Gamer, P. W. Roesky, *Organometallics,* **2008**, *27*, 1207–1213.

10. F. Buch, S. Harder, *Z. Naturforsch. B,* **2008**, *63*, 169–177.

11. J. Jenter, R. Köppe, P. W. Roesky, *Organometallics*, **2011**, *30*, 1404–1413.

12. M. Arrowsmith, M. R. Crimmin, A. G. M. Barrett, M. S. Hill, G. Kociok- Köhn, P. A. Procopiou, *Organometallics*, **2011**, *30*, 1493–1506.

13. T. D. Nixon, B. D. Ward, *Chem. Commun.,* **2012**, *48*, 11790–11792.

14. B. Liu, T. Roisnel, J.-F. Carpentier, Y. Sarazin, *Chem. Eur. J.,* **2013**, *19*, 2784–2802.

15. C. Glock, F. M. Younis, S. Ziemann, H. Görls, W. Imhof, S. Krieck, M. Westerhausen, *Organometallics,* **2013**, *32*, 2649–2660.

16. M. R. Crimmin, A. G. M. Barrett, M. S. Hill, P. B. Hitchcock, P. A. Procopiou, *Organometallics,* **2007**, *26*, 2953–2956.

17. B. Liu, J.-F. Carpentier, Y. Sarazin, *Chem. Eur. J.,* **2012**, *18*, 13259–13264.

18. S. Harder, *Chem. Rev.,* **2010,** *110*, 3852–3876.

19. M. S. Hill, D. J. Liptrot, C. Weetman, *Chem. Soc. Rev.,* **2016**, *45*, 972–988.

20. M. Westerhausen, *Z. Anorg. Allg. Chem.,* **2009**, *635*, 13–32.

21. For selected examples, please see: (a) S.-K. Tian, L. Deng, *J. Am. Chem. Soc.,* **2001**, *123*, 6195–6196; (b) S.-K. Tian, L. Deng, *J. Am. Chem. Soc.,* **2003**, *125*, 9900–9901; (c) D. H.

Ryu, E. J. Corey, *J. Am. Chem. Soc.,* **2004,** *126*, 8106–8107; (d) D. E. Fuerst, E. N. Jacobsen, *J. Am. Chem. Soc.,* **2005**, *127*, 8964–8965; (e) X. Liu, B. Qin, X. Zhou, B. He, X. Feng, *J. Am. Chem. Soc.,* **2005**, *127*, 12224–12225; (f) G. K. S. Prakash, H. Vaghoo, C. Panja, V. Surampudi, R. Kultyshev, T. Mathew, G. A. Olah, *PNAS,* **2007**, *104*, 3026–3030; (g) J. J. Song, F. Gallou, J. T. Reeves, Z. Tan, N. K. Yee, C. H. Senanayake, *J. Org. Chem.,* **2005**, *71*, 1273–1276; (h) Y. N. Belokon, W. Clegg, R. W. Harrington, V. I. Maleev, M. North, M. O. Pujol, D. L. Usanov, C. Young, *Chem.−Eur. J.,* **2009**, *15*, 2148−2165; (i) C. Zhu, Q. Xia, X. Chen, Y. Liu, X. Du, Y. Cui, *ACS Catal.,* **2016**, *6*, 7590−7596; (j) T. Kajiwara, H. Higashimura, M. Higuchi, S. Kitagawa, *ChemNanoMat*, **2018**, *4*, 103-111.

22. For selected examples, please see: (a) T. J. Hadlington, M. Hermann, G. Frenking, C. Jones, *J. Am. Chem. Soc.,* **2014**, *136*, 3028–3031; (b) J. Schneider, C. P. Sindlinger, S. M. Freitag, H. Schubert, L. Wesemann, *Angew. Chem. Int. Ed.,* **2017**, *56*, 333–337; (c) C. C. Chong, H. Hirao, R. Kinjo, *Angew. Chem. Int. Ed.,* **2015**, *54*, 190−194; (d) Y. Wu, C. Shan, Y. Sun, P. Chen, J. Ying, J. Zhu, L(Leo). Liu, Y. Zhao, *Chem. Commun.,* **2016**, *52*, 13799−13802; (e) D. Mukherjee, H. Osseili, T. P. Spaniol, J. Okuda, *J. Am. Chem. Soc.,* **2016**, *138*, 10790–10793; (f) M. Arrowsmith, T. J. Hadlington, M. S. Hill, G. Kociok-Köhn, *Chem. Commun.,* **2012**, *48*, 4567−4569; (g) L. Fohlmeister, A. Stasch, *Chem. Eur. J.,* **2016**, *22*, 10235–10246; (h) D. Mukherjee, S. Shirase, T. P. Spaniol, K. Mashima, J. Okuda, *Chem. Commun.,* **2016**, *52*, 13155–13158; (i) D. Mukherjee, A. Ellern, A. D. Sadow, *Chem. Sci.,* **2014**, *5*, 959–965; (j) K. Manna, P. Ji, F. X. Greene, W. Lin, *J. Am. Chem. Soc.,* **2016**, *138*, 7488−7491; (k) M. K. Bisai, S. Pahar, T. Das, K. Vanka, S. S. Sen, *Dalton Trans.,* **2017**, *46*, 2420–2424.

23. Z. Yang, M. Zhong, X. Ma, S. De, C. Anusha, P. Parameswaran, H. W. Roesky, *Angew. Chem. Int. Ed.,* **2015**, *54*, 10225–10229.

24. Z. Yang, Y. Yi, M. Zhong, S. De, T. Mondal, D. Koley, X. Ma, D. Zhang, H. W. Roesky, *Chem. Eur. J.,* **2016**, *22*, 6932–6938.

25. Y. Li, J. Wang, Y. Wu, H. Zhu, P. P. Samuel, H. W. Roesky, *Dalton Trans.,* **2013**, *42*, 13715–13722.

26. R. K. Sitwatch, S. Nagendran, *Chem. Eur. J.,* **2014**, *20*, 13551–13556.

27. M. K. Sharma, S. Sinhababu, G. Mukherjee, G. Rajaraman, S. Nagendran, *Dalton Trans.*, **2017**, *46*, 7672-7676.

28. V. S. V. S. N. Swamy, M. K. Bisai, T. Das, S. S. Sen, *Chem. Commun.,* **2017**, *53*, 6910–6913.

29. A. L. Liberman-Martin, R. G. Bergman, T. D. Tilley, *J. Am. Chem. Soc.,* **2015**, *137*, 5328–5331.

30. W. Wang, M. Luo, J. Li, S. A. Pullarkat, M. Ma, *Chem.Commun.,* **2018**, *54*, 3042-3045.

31. S. Yadav, V. S. V. S. N. Swamy, R. G. Gonnade, S. S. Sen, *ChemistrySelect,* **2016**, *1*, 1066–1071.

32. S. Yadav, S. Pahar, S. S. Sen, *Chem. Commun.,* **2017**, *53*, 4562–4564.

33. (a) T. Clark, *J. Chem. Soc. Chem. Commun.,* **1986**, 1774–1776; (b) H. Hofmann, T. Clark, *Angew. Chem. Int. Ed. Engl.,* **1990**, *29*, 648–650; (c) A. H. C. Horn, T. Clark, *J. Am. Chem. Soc.,* **2003**, *125*, 2809–2816; (d) T. Clark, *J. Am. Chem. Soc.,* **2006**, *128*, 11278–11285.

34. F. Wang, Y. Wei, S. Wang, X. Zhu, S. Zhou, G. Yang, X. Gu, G. Zhang, X. Mu, *Organometallics,* **2015**, *34*, 86−93.

35. R. Ahlrichs, M. Bar, M. Häser, H. Horn, C. Kölmel, *Chem. Phys. Lett.,* **1989**, *162*, 165-169.

36. J. P. Perdew, K. Burke, M. Ernzerhof, *Phys. Rev. Lett*., **1996**, *77*, 3865-3868.

37. F. Weigend, R. Ahlrichs, *Phys. Chem. Chem. Phys.,* **2005**, *7*, 3297-3305.

38. K. Eichkorn, O. Treutler, H. Öhm, M. Haser, R. Ahlrichs, *Chem. Phys. Lett*., **1995**, *240*, 283-289.

39. M. Sierka, A. Hogekamp, R. Ahlrichs, *J. Chem. Phys*., **2003**, *118*, 9136-9148.

40. A. Klamt, G. Schuurmann, *J. Chem. Soc*., *Perkin Trans*. *2,* **1993**, 799-805.

Chapter 4: Alkaline Earth Metal Compounds of Methylpyridinato β-Diketiminate Ligands and their Catalytic Application in Hydroboration of Aldehydes and Ketones
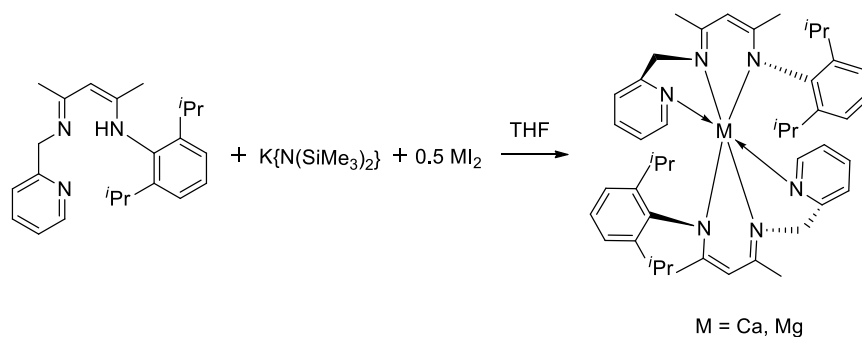
Abstract:

Due to high terrestrial abundance, non-toxicity, and cost-effectiveness, the alkaline earth metals may be a promising option for mimicking the transition and lanthanide metal chemistry. In this chapter, we have used a *β*-diketiminato ligand with methyl–pyridine side arm [(2, 6-*i*Pr-C_6H_3NC(Me)CHC(Me)NH(CH_2py)] to synthesize homoleptic complex of magnesium (**10**) and calcium (**11**). The pendant methyl–pyridine group on one of the nitrogen centers provides steric as well as an addition electronic stabilization to the metal center. Subsequently, we have used them as catalysts for hydroboration of a wide range of aldehydes and ketones using pinacolborane (HBpin) at ambient reaction conditions. The quantum mechanical calculations have been performed to understand the reaction mechanism.

4.1: Introduction

In alkaline earth (Ae) metal chemistry, steric and electronic properties of the ligand system play a vital role for stabilizing of Ae metal complexes. Therefore, the exploration for the new ligands, which can gratify the coordination requirements of the alkaline earth metals, continues to be of significant current interest. Majority of the alkaline earth metal complexes have been synthesized by using monoanionic bidentate ligand systems such as amidinate $[RC\{NR\}_2]^-$,[1] guanidinate $[RNC(NR_2)NR]^-$,[1] trizenide $[(R_2N_3)]^-$,[2] β-diketiminate $[(R)NC(Me)C(H)C(Me)N(R)]^-$,[3] diboxmethanide $[(4,6-R-NCOC_6H_2)_2CH]^-$,[4,5] silylated aminopyridinato $[(2-R_3SiNH-6-MeC_5H_3N)]^-$[6] etc. The efficient binding capacity, easily tunable steric and electronic properties of these ligands have been exploited for the stabilization of a plethora of hydrocarbon soluble alkaline earth metal complexes, including a compound with a Mg(I)-Mg(I) bond.[7] Recently, Roesky's group synthesized a $[LCaI(\mu\text{-}ICaI\text{-}\mu)ICaL]$ chain stabilized by two chelating β-diketiminate ligands $(L=CH\{Et_2NCH_2CH_2N(CMe)\}_2)$.[8] The result shows that an additional N→Ae donation can play an important role in the stabilization of highly electrophilic alkaline earth metal complexes. Kay and coworkers also supported this hypothesis by synthesizing a series of alkaline earth metal complexes of bidentate silylated aminopyridinato ligands as an alternative of amidinate or guanidinate ligands.[6]

The introduction of a methyl-pyridine side arm in the β-diketiminato framework leads to a ligand that is tridentate and monoanionic in its nacnac imino-pyridine state $(2,6\text{-}i\text{Pr}_2\text{-}C_6H_3NC(Me)CHC(Me)NH(CH_2py))$. The pendant pyridine group on one of the nitrogen centres provides steric support as well as an addition electronic stabilization to the metal center. The group of Wolczanski recently employed such tridentate chelating ligand for preparing a variety of iron and chromium complexes.[9] Chen and co-workers reported β-diketiminato rare-earth metal complexes of composition $Ln(CH_2SiMe_3)_3(THF)_2$ (Ln=Sc and Y) using the same ligand.[10] Harder and co-workers have demonstrated the utility of *para*-phenyl and pyridine-bridged bis(β-diketiminate) ligand for the stabilization of multinuclear magnesium hydride complexes.[11] Very recently, Westerhausen and co-workers have used *N*-(2-Pyridylethyl)-substituted bulky amidinates and triazenides ligand system to synthesize magnesium complex.[12] Despite their ongoing popularity and versatility, there are no examples of group 2 complexes supported by nancnac methyl pyridinato ligands in the literature. In this chapter, we report the synthesis and

isolation of homoleptic magnesium and calcium complexes stabilized by nancnac methyl pyridinato ligand. Although homoleptic alkaline earth metal complexes are usually considered catalytically inept, but due to the hemilabile coordination of pyridyl moiety these magnesium and calcium complexes were found to catalyze hydroboration of aldehydes and ketones with HBpin under mild conditions with high yields.

4.2: Synthesis and characterization of Mg and Ca complexes

The ligand was synthesized following the procedures given by Chen and co-workers.[10] Deprotonation of the ligand with $KN(SiMe_3)_2$ in THF at room temperature led to the formation of the potassium salt of the ligand. The latter was subsequently reacted with MgI_2 and CaI_2 to afford homoleptic complexes of composition L_2M {M=Mg (**10**) and Ca (**11**)} (Scheme 4.1). Single crystals suitable for XRD measurement were grown from the concentrated solution of *n*-hexane at −4 °C. The direct addition of $[M\{N(SiMe_3)_2\}_2]$ (M=Mg and Ca) to the ligand has also afforded homoleptic L_2M complexes with concomitant release of $HN(SiMe_3)_2$.
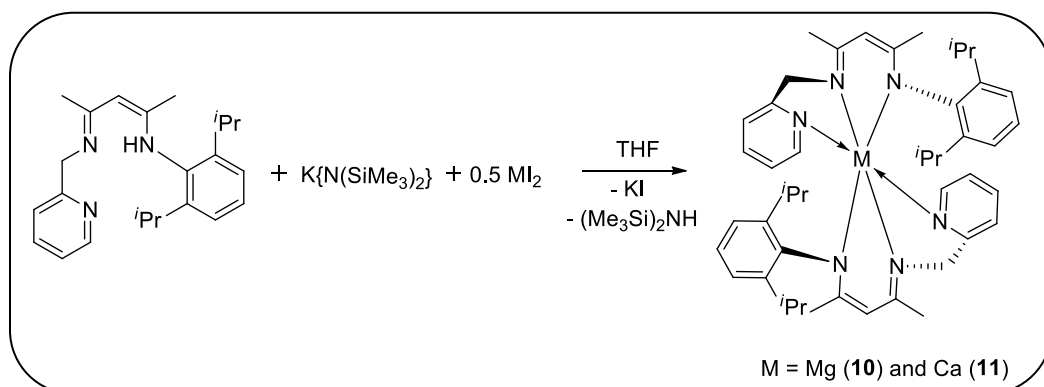
Scheme 4.1: Synthetic approaches for accessing magnesium (**10**) and calcium (**11**) compounds of methylpyridinato *β*-diketiminate ligands.

Complexes **10** and **11** were characterized by multinuclear NMR spectroscopy. The disappearance of an N–H peak in the ^1H NMR spectrum indicates complete deprotonation of the ligand. Both **10** and **11** display two sets of doublets for the isopropyl groups, one septet, and two singlets for the methyl groups in their respective ^1H spectrum. The molecular structures of **10** and **11** were confirmed by single crystal X-ray analysis.[13] It is of note that in **10** and **11**, no solvent molecule is coordinated to metal center. To check the coordination of solvent molecule in the solvent phase, we have performed DOSY NMR of complex **11** and we have observed that the complex

do not interact with THF strongly because the two THF signals show higher diffusion coefficients, indicating THF molecules are moving much faster than the solute. **10** crystallizes in the triclinic space group $P\bar{1}$ (Figure 4.1). The Mg atom is hexa-coordinated and has distorted octahedral geometry, with two nancnac methyl pyridinato ligands completing the environment. The Mg–N_{nacnac} bond lengths are 2.1226(19), 2.1237(19), 2.224(2), 2.2303(19)Å, which are longer than the average Mg–N bond length (2.111(2)Å) in homoleptic β-diketiminato magnesium complex, [((DIPP-nacnac)$_2$Mg), DIPP-nacnac=(2,6-iPr$_2$C$_6$H$_3$)NC(Me)C-(H)C(Me)N(2,6-iPr$_2$C$_6$H$_3$)] complex, reported by Harder and coworkers.[14] The pyridyl group coordinates to the magnesium centre with Mg-Npyridyl bond lengths of 2.270(2) and 2.290(2)Å, which are longer than the Mg–N_{nacnac} bonds. The longer Mg-Npyridyl bond with respect to the Mg–N_{nacnac} bond indicates that the pendant pyridyl groups act as neutral donors while the backbone is an anionic ligand.
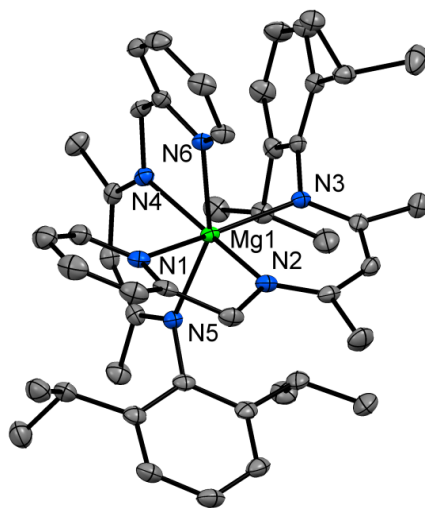
Figure 4.1: Molecular structure of **10** in the solid state with anisotropic displacement parameters depicted at the 50 % probability level. Hydrogen atoms are omitted for clarity. Selected bond lengths [Å] or angles [deg]: Mg1-N2 2.1226(19), Mg1-N4 2.1237(19), Mg1-N3 2.224(2), Mg1-N5 2.2303(19), Mg1-N1 2.270(2), Mg1-N6 2.290(2); N2-Mg1-N4 168.02(8), N2-Mg1-N3 87.75(7), N4-Mg1-N3 99.10(7), N2-Mg1-N5 98.54(7), N4-Mg- N5 88.29(7), N3-Mg1-N5 110.63(7), N2-Mg1-N1 76.31(7), N4-Mg1-N1 94.30(7), N3-Mg1-N1 157.79(7), N5-Mg1-N1 87.28(7), N2-Mg- N6 94.40(7), N4-Mg1-N6 75.88(7), N3-Mg1-N6 90.16(7), N5-Mg1-N6 155.80(7), N1-Mg1-N6 75.99(7) .
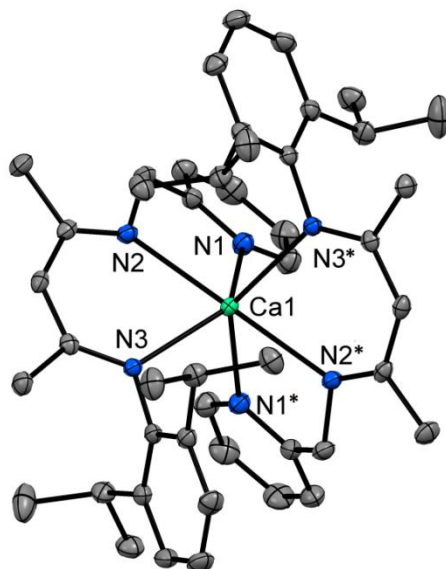
Figure 4.2: Molecular structure of **11** in the solid state with anisotropic displacement parameters depicted at the 50 % probability level. Hydrogen atoms are omitted for clarity. Selected bond lengths [Å] or angles [deg]: Ca1-N2 2.4486(9), Ca1-N2 2.4487(9), Ca1- N3 2.4722(9), Ca1-N3 2.4722(9), Ca1-N1 2.5305(10), Ca1-N1 2.5305(10); N2-Ca1-N2 178.11(5), N2-Ca1-N3 104.22(3), N2-Ca1-N3 76.69(3), N2-Ca1-N3 76.69(3), N2-Ca1-N3 104.22(3), N3-Ca1-N3 124.38(4), N2-Ca1-N1 109.88(3), N2-Ca1-N1 68.52(3), N3-Ca1-N1 135.35(3), N3-Ca1-N1 91.48(3), N2-Ca1-N1 68.52(3), N2-Ca1-N1 109.88(3), N3-Ca1-N1 91.48(3), N3-Ca1-N1 135.35(3), N1-Ca1-N1 75.62(5).

Compound **11** crystallizes in the monomeric space group $C2/c$ and exhibits crystallographic C2−symmetry (Figure 4.2). The molecular structure of **11** is similar to that of **10**, where the calcium atom is coordinated by six nitrogen atoms and is in distorted octahedral geometry. The Ca–N bond lengths range from 2.4486(9) to 2.4722(9)Å, which are longer than the mean Ca–N bond in ((DIPP–nacnac)$_2$Ca) complex (2.379(1)Å).[14] The slight increase in the bond lengths is likely due to the more steric crowding in **11**. The bond distances of pyridine nitrogen to Ca metal center are 2.5305(10) and 2.5305(10)Å, which are longer than the β–diketaminate backbone N–Ca bond lengths. The N–Ae bond distances of Ca are longer as compared to the Mg due to the increase in the metal size.

4.3: Catalytic application of homoleptic alkaline earth metal complexes

The use of transition metal free catalysts for hydroboration of aldehydes and ketones has been recently explored in-depth. Catalysts derived from both s-[15-26] and p-block[27-35] elements have been reported with good success. Inspired from our previous works on amidinato stabilized calcium catalyzed hydroboration of aldehydes and ketones,[24] we have thought to use complexes **10** and **11** as catalysts for the same. Both **10** and **11** are homoleptic in nature. Recently, homoleptic complexes of alkaline earth metals have been shown as potent catalysts. For example, Harder and coworkers demonstrated the catalytic activity of bora-amidinate (bam) complexes ^{DIPP}NBN-Mg·(THF)$_3$ and ^{DIPP}NBN-Ca·(THF)$_4$ in the intramolecular alkene hydroamination, in which the bora-amidinate ligand functions as a non-innocent ligand and partakes in substrate deprotonation and product protonation.[36] The same group reported metal-ligand cooperative catalysis by tetranuclear Sr and Ba complexes for intramolecular alkene hydroamination, alkene hydrophosphination, pyridine hydroboration, pyridine hydrosilylation, and alkene hydrosilylation.[37] In contrast to these above-mentioned non-innocent ligands, amidinates or β-diketiminates are usually traditional spectator ligands which bind to the metal and provide a pocket for the substrate binding in homogeneous catalysis without participating in the catalytic cycle. Usually homoleptic alkaline earth metal complexes having spectator ligands are considered as catalytically incompetent. Nevertheless, the group of Roesky has recently reported benz-amidinate stabilized homoleptic heavier alkaline earth metal complexes as catalysts for hydrophosphination of styrene.[38] A further encouragement comes from the works of Harder and Speilmann, who described β-diketiminate calcium hydride catalyzed hydroboration of 1,1-diphenylethylene although the subsequent mechanistic studies revealed that the calcium hydride complex was not a bonafide catalyst.[39]

4.4: Hydroboration of aldehydes

Preliminary NMR scale experiments revealed the activity of **10** and **11** toward hydroboration reaction at ambient conditions, as evidenced by the clean conversion of benzaldehyde and pinacolborane (HBpin) in benzene to the corresponding alkoxypinacolboronate ester (Table 4.1). Encouraged by these results, we assessed the utility of **10** and **11** in the hydroboration of a variety of aldehydes and ketones by HBpin at ambient conditions to afford the corresponding alkoxypinacolboronate esters.
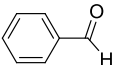
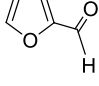| Entry	Catalyst (**10** or **11**) mol%	Time(h)	Solvent	NMR Yield%(**10/11**)
1.	0.5	1	benzene	57/60
2.	1	1	benzene	68/73
3.	1	2	benzene	99/99
4.	2	2	benzene	99/99
5.	1	2	THF	76/80
6.	1	2	toluene	81/84
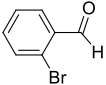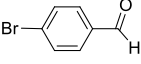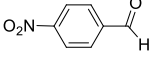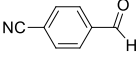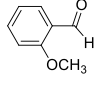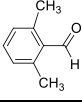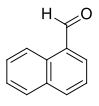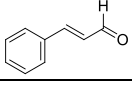
Table 4.1: Optimization table of hydroboration of benzaldehyde catalysed by **10** and **11**.

The *ortho* substituents (entry **12b**, **12g**) do not show any repressing effect on the reaction yield. Benzaldehydes with substitution at *ortho, meta, and para*-position do not have significant impact on the reactivity. Electron withdrawing substituents (Br (entry **12b**, **12c**), NO_2 (entry **12d**), CN (entry **12e**) as well as electron donating substituents (CH_3 (entry **12g**), OCH_3 (entry **12f**) are well-tolerated (Table 4.2). The reaction of furfural with HBpin led to exclusive hydroboration of the carbonyl functionality keeping the furfural ring intact (entry **12j**). Exclusive 1,2-addition of HBpin to cinnamaldehyde was observed as a result of the highly electrophilic character of the carbonyl moiety (entry **12i**), although with a drop in the yield. Hydroboration of sterically hindered 2,6-dimethylbenzaldehyde (entry **12g**) also gave good yield at the same reaction conditions. To demonstrate the applicability of the reported protocol, 4-cyanobenzaldehyde and 4-bromoacetophenone were acid hydrolyzed after completion of reaction and their corresponding alcohols were isolated in quantitative yield.

Table 4.2: Hydroboration of aldehydes using compound **10** and **11**. Reaction condition: aldehyde: 0.25 mmol, Catalyst: 1 mol%, room temperature in benzene. Reaction time: 2 h. Yields are calculated based on the integration area of product and starting material signals in the ^{1}H spectrum using mesitylene as an internal standard.

R= aryl group
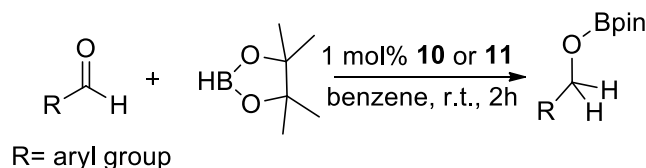
Entry	Substrate	Time (h)	Catalyst	Yield(%)
12a		2	**10**	99
			11	99

12b		2	10	91
			11	90
12c		2	10	99
			11	96
12d		2	10	99
			11	99
12e		2	10	99
			11	99
12f		2	10	98
			11	98
12g		2	10	98
			11	95
12h		2	10	99
			11	97
12i		2	10	78
			11	75
12j		2	10	96
			11	94

4.5: Hydroboration of ketones

Aromatic ketones were also found equally suitable substrates for hydroboration, demonstrated by the clean conversion of acetophenone (entry **13a**), although higher catalyst loadings (2 mol %) and slightly extended reaction times (3h) were required to attain productive conversion. Reduction of a wide variety of aromatic ketones bearing both electron withdrawing {p-Br (entry **13c**)}, p-NO$_2$ (entry **13d**) as well as electron donating {(p-NH$_2$ (entry **13e**)}, p-OMe (entry **13f**) functional groups to the respective boronate esters was successful under the reaction conditions (Table 4.3). Sterically hindered benzophenone was also cleanly converted to the corresponding borate ester (entry **13g**). Even aliphatic ketone was smoothly converted (entry **13h**), revealing the

versatility of our synthetic methodology. However, substrates such as esters, amides, and pyridine were not reduced, even at a higher catalyst loading and under forcing conditions.

Table 4.3: Hydroboration of ketones using compound **10** and **11**. Reaction condition: Ketone: 0.25 mmol, Catalyst: 2 mol%, room temperature in benzene. Reaction time: 3 h. Yields are calculated based on the integration area of product and starting material signals in the ^{1}H spectrum using mesitylene as an internal standard.

R= aryl group
R'= alkyl, aryl group
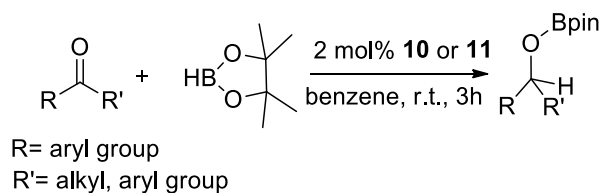
Entry	Substrate	Time	Catalyst	Yield(%)
13a		3h	**10**	95
			11	96
13b		3h	**10**	99
			11	96
13c		3h	**10**	99
			11	99
13d		3h	**10**	99
			11	99
13e		3h	**10**	99
			11	98
13f		3h	**10**	97
			11	95
13g		3h	**10**	99
			11	99
13h		3h	**10**	85
			11	82

We have compared the activity of **10** and **11** with the known alkaline earth metal catalysts for benzophenone. Hill's magnesium catalyst,[20] Okuda's [Mg(thf)$_6$][HBPh$_3$]$_2$,[21] Stasch's

phosphinoamido-magnesium-hydride[22] were recorded with large TOFs of 500 h^{-1}, 1000 h^{-1} (in absence of DMSO), 1760 h^{-1}, respectively. Our previously reported Ca-based catalyst, [PhC(NiPr)$_2$CaI][24] showed a TOF of 8.6 h^{-1}. In comparison, both **10** and **11** are found to give a TOF of 33 h^{-1} for reduction of benzophenone, which is definitely lower than magnesium based heteroleptic catalysts but higher than the calcium one. The decrease in TOF can be attributed to the saturation of coordination sites of **10** and **11**. It should be noted here that analogous β-diketiminato compounds of composition (DIPP-nacnac)$_2$M (M=Mg and Ca)[14] are not reported for the hydroboration of aldehydes and ketones. This indicates the importance of the incorporation of the pyridinato moiety in the ligand framework, which binds to the metal center in a hemilabile manner and assist in improving the catalytic activity.

4.6: DFT studies

To obtain additional mechanistic insight, full quantum chemical calculations were done with density functional theory (DFT) at the dispersion and solvent corrected PBE/TZVP level of theory. In the first step of the reaction, HBPin approaches catalyst **11** and forms **Int_1** (see Scheme 4.2) in which N of one of the pyridine ligand breaks its interaction with catalyst **11** and forms a new N-B bond (likely the Lewis acid base adduct, in which N and B contain positive and negative charges respectively) with the B centre of HBpin. The thermodynamics (ΔG) for this step is unfavourable by 4.8 kcal/mol. This occurs *via* a "two atoms involved transition state" (**TS_1**) where no bond breaking but only N···B bond formation occurs with a very low free energy (ΔG#) barrier of only 6.4 kcal/mol. In the next step, benzaldehyde approaches the B-H bond of **Int_1**. This is the prelude to the nucleophilic attack by the carbonyl oxygen of benzaldehyde to the adjacent sp^2 carbon of pyridine N of **Int_1**, further leading to the neutralization of the charge of N and to the hydride being transferred from the negatively charged centre B to the carbonyl carbon of benzaldehyde which leads to the formation of **Int_2**. This step is favourable by 5.4 kcal/mol. This occurs through a very flexible six membered (C···N···B···H···C···O) transition state (**TS_2**) with a barrier of 29.1 kcal/mol. This is the slowest step of the hydroboration reaction. The ΔG values corresponding to the barriers have been calculated at room temperature. The values are on the higher side, even after volume corrections for the translational entropy term. This is because the entropy loss during the reaction is

overestimated in the calculations, leading to the high values for the barriers. The real values for the barrier heights are, therefore, likely to be much lower.

In the transition state corresponding to this step, there is a significant amount of B-H bond activation (1.47 Å distance in the transition state), which allows the hydride transfer from the boron to the carbonyl carbon centre, along with the simultaneous occurring of C=O bond cleavage and the formation of another C–O bond. In the last step of the reaction, intramolecular bond forming and bond breaking takes place. The O centre of carbonyl group attacks the B centre, along with the formation of the B–O bond and the simultaneously breaking of the N–B and C–O bonds. The last step is very favourable by 26.6 kcal/mol. This occurs after the surmounting of a four membered transition state (**TS_3**) with a barrier of 15.2 kcal/mol, and also leads to the regeneration of catalyst **11**. The fact that the final product is thermodynamically stable, and that the barrier for the slowest step is lower than without the mediation of the catalyst, indicates that the addition of the calcium compound **11** has a salutary effect on the hydroboration reaction. This reaction profile is also shown as a plot of the energy with regard to the reaction coordinate (along with the corresponding figures) in Scheme 4.3. Furthermore, calculations with the energetic span model (ESM), developed by Shaik and co-workers,[40] provide insight into the relative efficiency values for the reactions with and without the calcium catalyst [$2.83*10^{-09}$ s^{-1} (using catalyst **11**) vs $5.48*10^{-12}$ s^{-1} (without catalyst)]. The TOF values are seen to be quite low, but this is due to the overestimation of the entropy loss in the calculations, leading to the higher values for the barriers, as explained earlier. However, since this overestimation affects the barriers for both the catalyst and non-catalyst cases, what is important to note is that the efficiency of the system is increased by a factor of about 500, which shows the distinct effect of the calcium catalyst complex on the efficiency of the hydroboration. We have also investigated the possibility of the calcium center participating in the catalysis process. Several different mechanisms have been studied in this regard, and are discussed below (see scheme 4.4, 4.5, 4.6 and 4.7). However, these mechanisms have not been seen to be as favourable as the mechanism that is discussed above. We have also investigated the possibility of de-coordinating the sidearm, i.e., the methylene bridged pyridyl moiety, so as to leave one coordination site free for the aldehyde reactant to approach the calcium center. However, this was found to be significantly unfavourable: by 8.6 kcal/mol (ΔE value). Hence, the calculations suggest that it is the pyridyl

moiety without the methylene bridge that is thermodynamically more likely to open its coordination site and provide space for the incoming reagents, in comparison to the methylene bridged pyridyl moiety. The role of the calcium in the chemistry is therefore to bind two ligands, each of which is then capable of acting as a catalytic site for the hydroboration. Therefore, the calcium enables the formation of a dual site catalyst, which would be more efficient than just employing a pyridine moiety as a single site catalyst in the reaction.
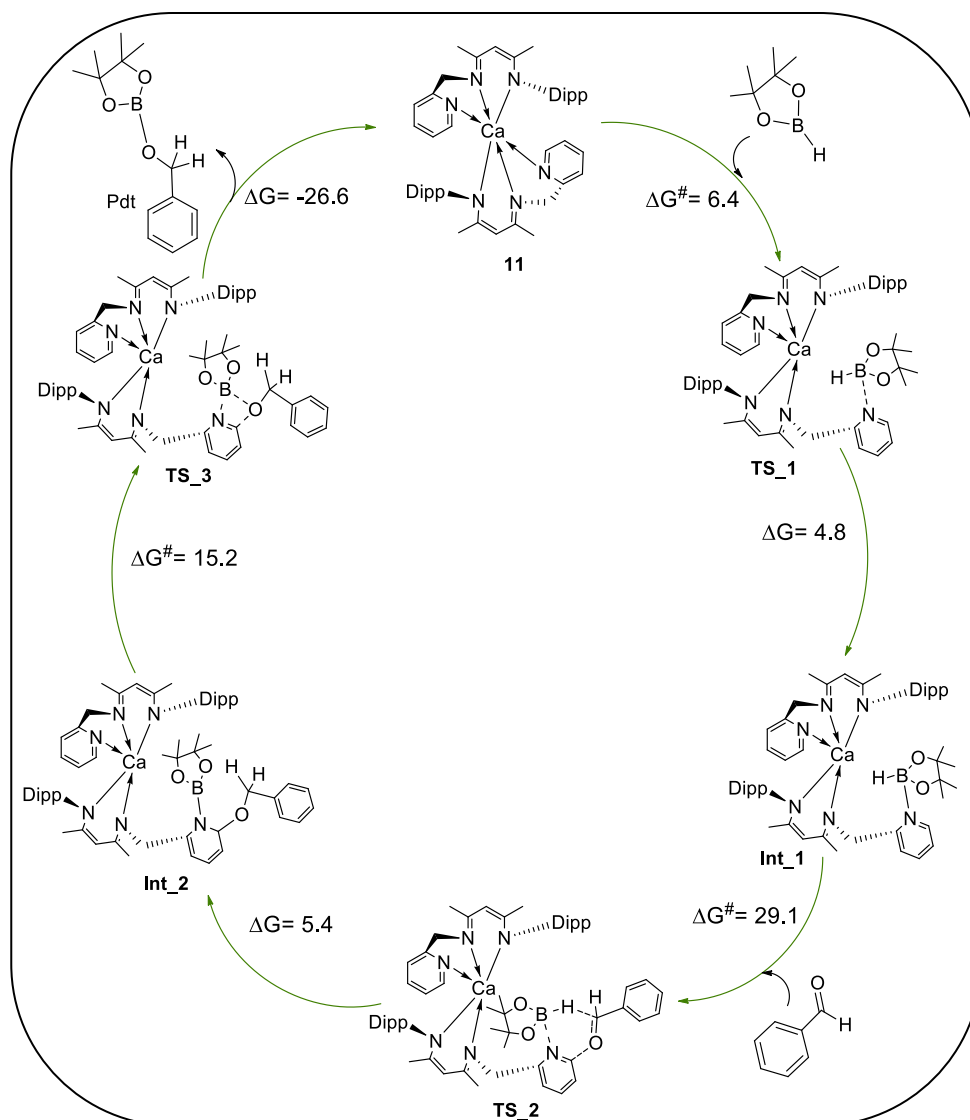
Scheme 4.2: The reaction profile for the hydroboration reaction with the calcium catalyst **11**. The values (in kcal/mol) have been calculated at the PBE/TZVP level of theory.
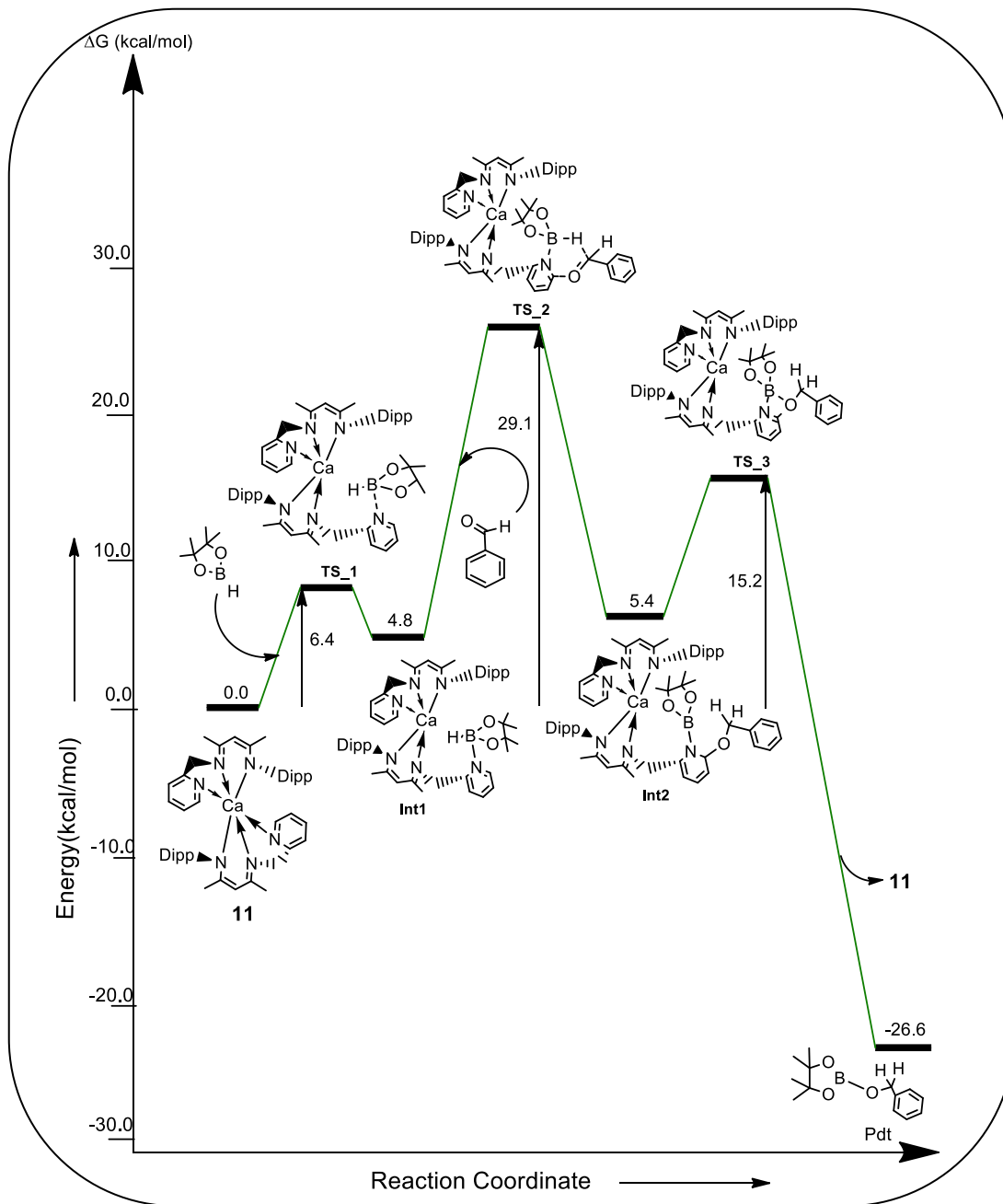
Scheme 4.3: The reaction profile for the hydroboration reaction with the calcium catalyst **11**. The values (in kcal/mol) have been calculated at the PBE/TZVP level of theory.

Discarded Pathways:

Discarded Pathway 1
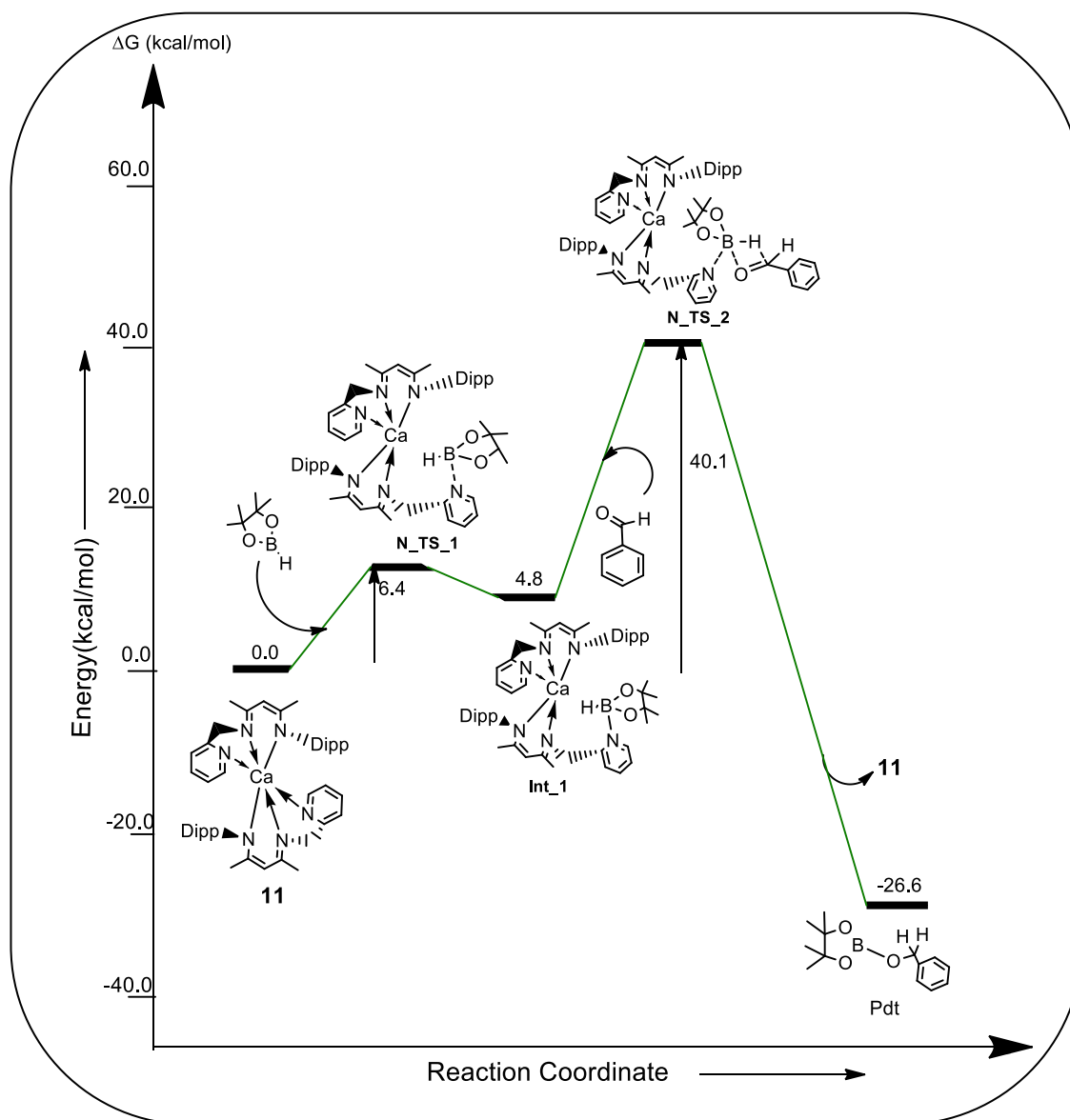
Scheme 4.4: An alternative reaction profile for the hydroboration reaction with the calcium catalyst **11**. The values (in kcal/mol) have been calculated at the PBE/TZVP level of theory.

In the above mechanism, in the first step of the reaction, HBpin approaches catalyst **11** and reacts to form Int_1 in which the nitrogen of one of the pyridine ligand breaks its interaction with the catalyst and forms a new N–B bond (likely the Lewis acid base adduct in which N and B contain positive and negative charges respectively) with the B centre of HBpin. This step is unfavourable by 4.8 kcal/mol. This occurs through a "two atoms involved transition state" (**N_TS_1**), where no bond breaking but only N···B bond formation occurs with a low barrier of only 6.4 kcal/mol.

In the next step, benzaldehyde approaches the B–H bond of **Int_1**. This is the prelude to the nucleophilic attack by the carbonyl oxygen of benzaldehyde to the B centre with the formation of the B–O bond and the simultaneous transferring of hydride from HBpin to carbonyl carbon of benzaldehyde. This occurs through a four membered transition state (**N_TS_2**) having a barrier of 40.1 kcal/mol, leading to the final hydroboration product (pdt) along with the regeneration of the catalyst **11**. Since the barrier for the last step is high, this mechanism has been discarded.

Discarded Pathway 2
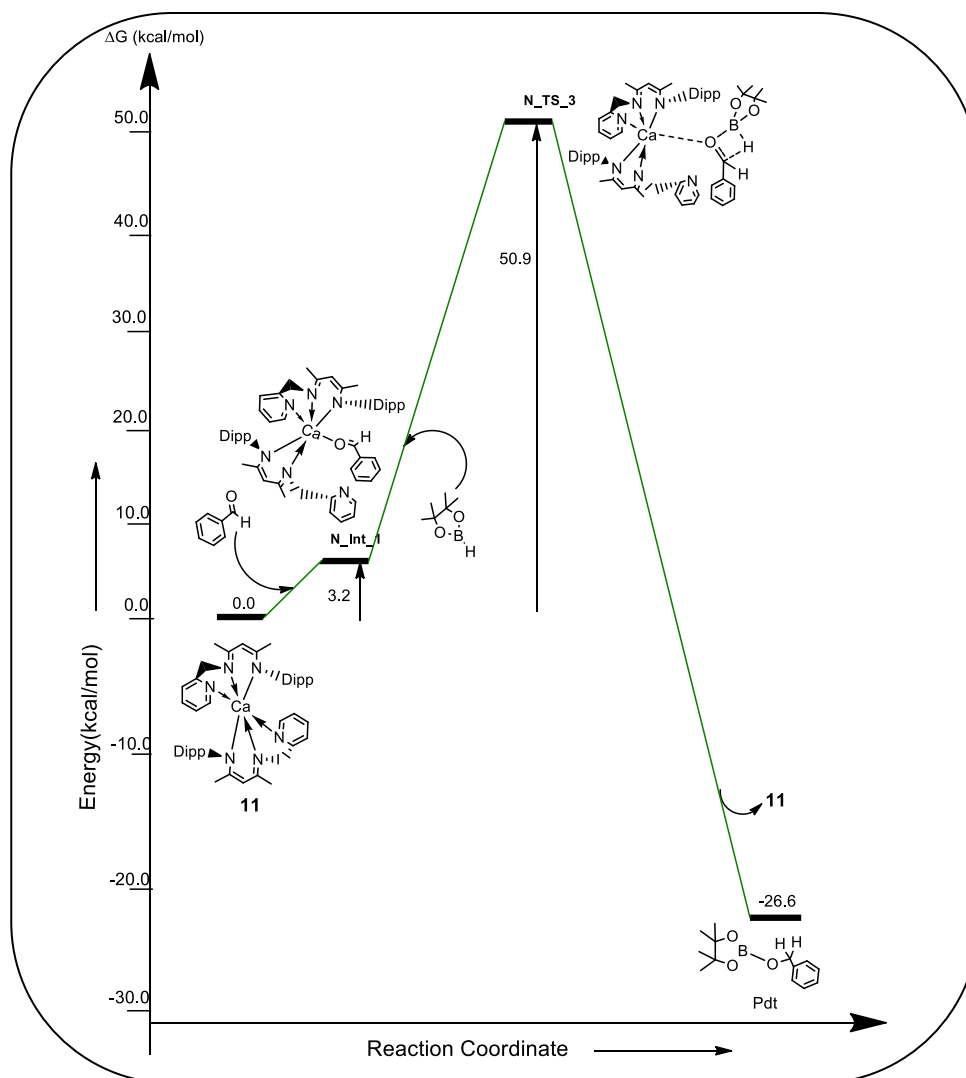
Scheme 4.5: Another alternative reaction profile for the hydroboration reaction with the calcium catalyst **11** in the solvent phase. The values (in kcal/mol) have been calculated at the PBE/TZVP level of theory.

In this investigated alternative pathway, benzaldehyde approaches catalyst **11** and reacts with it to form **N_Int_1**, in which there is a weak interaction between the calcium of the catalyst and the oxygen of benzaldehyde. This is thermodynamically unfavourable by 3.2 kcal/mol. In the next step, HBpin approaches **N_Int_1**. This is the prelude to the nucleophilic attack by the carbonyl O of the benzaldehyde to the B of HBpin, leading to **N_TS_3** and transferring H from HBpin to the carbonyl carbon of benzaldehyde, which finally leads to the formation of the product. As the barrier for the **N_TS_3** ($\Delta G^{\#}$) is very high: 50.9 kcal/mol, this mechanism has also been discarded.

Discarded Pathway 3
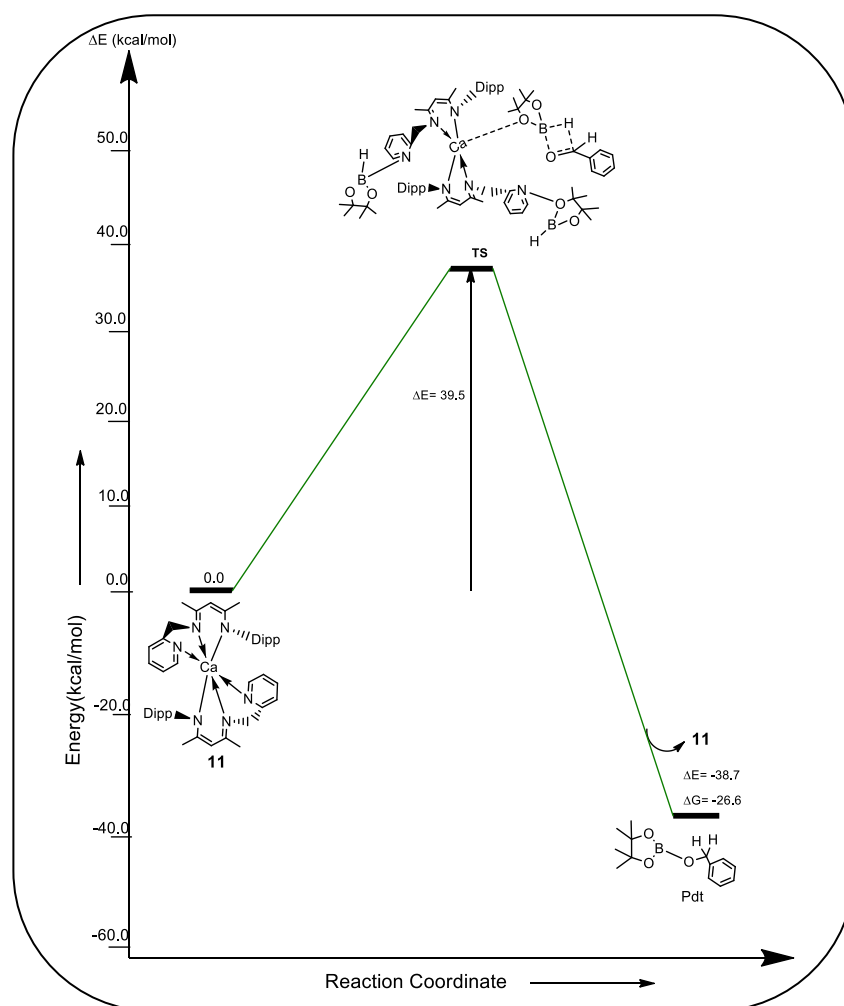
Scheme 4.6: Another alternative reaction profile for the hydroboration reaction with the calcium catalyst **11** in the solvent phase. The values (in kcal/mol) have been calculated at the PBE/TZVP level of theory.

In this investigated alternative pathway, HBpin approaches catalyst **11** and reacts with it to form **Int_1**, in which there is a weak interaction between the calcium of the catalyst and the oxygen of HBpin. This is thermodynamically unfavourable by 7.0 kcal/mol. In the next step, benzaldehyde approaches **Int_1**. This is the prelude to the nucleophilic attack by the carbonyl O of the benzaldehyde to the B of HBpin, leading to **TS** and transferring H from HBpin to the carbonyl carbon of benzaldehyde, which finally leads to the formation of the product. As the barrier for the TS ($\Delta E^{\#}$) is very high: 48.0 kcal/mol, this mechanism has also been discarded.

Discarded Pathway 4
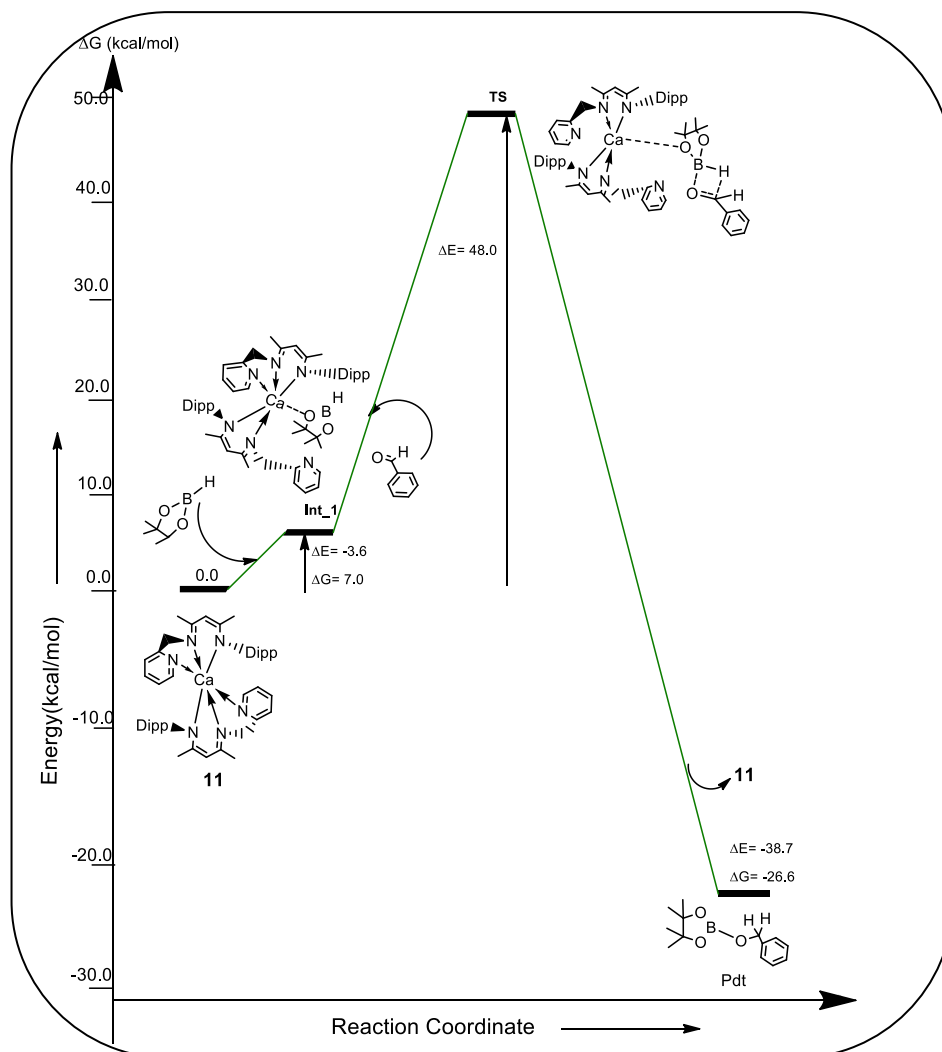
Scheme 4.7: Another alternative reaction profile for the hydroboration reaction with the calcium catalyst **11** in the solvent phase. The values (in kcal/mol) have been calculated at the PBE/TZVP level of theory.

In this investigated alternative pathway, three molecules of HBpin and one molecule of benzaldehyde approaches catalyst **11** and reacts with it to give a transition state **TS**. As the barrier for the TS ($\Delta E^{\#}$) is very high: 39.5 kcal/mol, this mechanism has also been discarded

4.7: Conclusions

The search for new chelating ligands having good steric and electronic properties is ongoing in alkaline earth metal chemistry. Here, in this chapter we have described the synthesis of well-defined homoleptic compounds of Mg (**10**) and Ca (**11**) using a tridentate monoanionic *β*-diketiminate ligand with a pendant pyridyl moiety. Single crystal X-ray studies show both **10** and **11** are six-coordinated and exhibit distorted octahedral geometry. Despite being homoleptic, both **10** and **11** are active toward the hydroboration of a variety of aldehydes and ketones under mild conditions. The introduction of pyridyl moiety in the nacnac system led to increase the catalytic activity presumably due to its hemilabile bonding with the metal center.

4.8: References

1. (a) G. J. Moxey, F. Ortu, L. G. Sidley, H. N. Strandberg, A. J. Blake, W. Lewis, D. L. Kays, *Dalton Trans.*, **2014**, *43*, 4838-4846; (b) R. J. Schwamm, B. M. Day, N. E. Mansfield, W. Knowelden, P. B. Hitchcock, M. P. Coles, *Dalton Trans*., **2014**, *43*, 14302–14314; (c) B. M. Day, W. Knowelden, M. P Coles, *Dalton Trans*., **2012**, *41*, 10930–10933; (d) J. Schwamm, M. P. Coles, *Organometallics*, **2013**, *32*, 5277–5280; (e) S. Yadav, V. S. V. S. N. Swamy, R. G. Gonnade, S. S. Sen, *ChemistrySelect*, **2016**, *1*, 1066–1071; (f) B. M. Day, N. E. Mansfield, M. P. Coles, P. B. Hitchcock, *Chem. Commun.,* **2011**, *47*, 4995–4997; (g) C. Jones, *Coord. Chem. Rev.*, **2010**, *254*, 1273–1289; (h) C. Glock, C. Loh, H. Goerls, S. Krieck, M. Westerhausen, *Eur. J. Inorg. Chem.*, **2013**, 3261–3269; (i) M. K. Barman, A. Baishya, S. Nembenna, *J. Organomet. Chem.*, **2015**, *785*, 52–60.

2. (a) S.-O.,Hauber, F. Lissner, G. B. Deacon, M. Niemeyer, *Angew. Chem. Int. Ed.*, **2005**, *44*, 5871–5875; (b) A. G. M. Barrett, M. R. Crimmin, M. S. Hill, P. B. Hitchcock, G. Kociok-Köhn, P. A. Procopiou, *Inorg. Chem.*, **2008**, *47*, 7366–7376.

3. (a) S. Nembenna, H. W. Roesky, S. Nagendran, A. Hofmeister, J. Magull, P.-J. Wilbrandt, M. A Hahn, *Angew. Chem. Int. Ed.,* **2007**, *46*, 2512–2514; (b) A. G. M. Barrett, M. R. Crimmin, M.

S. Hill, P. B. Hitchcock, P. A. Procopiou, *Angew. Chem. Int. Ed.,* **2007**, *46*, 6339–6342; (c) C. Ruspic, S. Harder, *Inorg. Chem.,* **2007**, *46*, 10426–10433; (d) M. Westerhausen, M. H. Digeser, C. Gückel, H. Nöth, J. Knizek, W. Ponikwar, *Organometallics,* **1999**, *18*, 2491–2496; (e) S. P. Sarish, A. Jana, H. W. Roesky, T. Schulz, M. John, D. Stalke, *Inorg. Chem.,* **2010**, *49*, 3816–3820; (f) S. P. Sarish, S. Nembenna, S. Nagendran, H. W. Roesky, *Acc. Chem. Res.,* **2011**, *44*, 157–170.

4. (a) I. Koehne, R. Herbst-Irmer, D. Stalke, *Eur. J. Inorg. Chem.,* **2017**, 3322–3326; (b) I. Koehne, S. Bachmann, T. Niklas, R. Herbst-Irmer, D. Stalke, *Chem. Eur. J.,* **2017**, *23*, 13141–13149.

5. I. Koehne, N Graw, T. Teuteberg, R. Herbst-Irmer, D. Stalke, *Inorg. Chem.*, **2017**, *56*, 14968−14978.

6. F. Ortu, G. J. Moxey, A. J. Blake, W. Lewis, D. L. Kays, *Inorg. Chem.,* **2013**, *52*, 12429−12439.

7. S. P. Green, C. Jones, A. Stasch, *Science,* **2007**, *318*, 1754−1757.

8. S. P. Sarish, A. Jana, H. W. Roesky, T. Schulz, D. Stalke, *Organometallics,* **2010**, *29*, 2901–2903.

9. W. D. Morris, P. T. Wolczanski, J. Sutter, K. Meyer, T. R. Cundari, E. B. Lobkovsky, *Inorg. Chem.,* **2014**, *53*, 7467−7484.

10. X. Xu, Y. Chen, G. Zou, J. Sun, *Dalton Trans.*, **2010**, *39*, 3952–3958.

11. (a) S. Harder, J. Spielmann, J. Intemann, H. Bandmann, *Angew. Chem. Int. Ed.,* **2011**, *50*, 4156 –4160; (b) S. Harder, J. Spielmann, J. Intemanna, *Dalton Trans.*, **2014**, *43*, 14284–14290.

12. D. Kalden, S. Krieck, H. Görls, M. Westerhausen, *Eur. J. Inrog. Chem.*, **2018**, 4361–4369.

13. (a) T. Kottke, D. Stalke, *J. Appl. Crystallogr.*, **1993**, *26*, 615–619; (b) D. Stalke, *Chem. Soc. Rev.*, **1998**, *27*, 171–178. The CCDC numbers of **10** and **11** are 1836442 and 1836447. These data can be available free of charge from https://www.ccdc.cam.ac.uk/.

14. S. Harder, *Organometallics,* **2002**, *21*, 3782–3787.

15. D. Mukherjee, H. Osseili, T. P. Spaniol, J. Okuda, *J. Am. Chem. Soc.,* **2016**, *138*, 10790–10793.

16. R. McLellan, A. R. Kennedy, R. E. Mulvey, S. A. Orr, S. D. Robertson, *Chem. Eur. J.,* **2017**, *23*, 16853–16861.

17. H. Osseili, D. Mukherjee, T. P. Spaniol, J. Okuda, *Chem. Eur. J.,* **2017**, *23*, 14292–14298.

18. H. Osseili, D. Mukherjee, K. Beckerle, T. P. Spaniol, J. Okuda, *Organometallics,* **2017**, *36*, 3029–3034.

19. M. K. Bisai, T. Das, K. Vanka, S. S. Sen, *Chem. Commun.,* **2018**, *54*, 6843–6846.

20. M. Arrowsmith, T. J. Hadlington, M. S. Hill, G. Kociok-Köhn, *Chem. Commun.,* **2012**, *48*, 4567−4569.

21. D. Mukherjee, S. Shirase, T. P. Spaniol, K. Mashima, J. Okuda, *Chem. Commun.,* **2016**, *52*, 13155–13158.

22. L. Fohlmeister, A. Stasch, *Chem. Eur. J.,* **2016**, *22*, 10235–10246.

23. A. Harinath, J. Bhattacharjee, H. P. Nayek, T. K. Panda, *Dalton Trans.,* **2018**, *47*, 12613–12622.

24. S. Yadav, S. Pahar, S. S. Sen, *Chem. Commun.,* **2017**, *53*, 4562–4564.

25. V. A. Pollard, S. A. Orr, R. McLellan, A. R. Kennedy, E. Hevia, R. E. Mulvey, *Chem. Commun.,* **2018**, *54*, 1233–1236.

26. S. Harder, *Chem. Rev.,* **2010**, *110,* 3852–3876.

27. J. R. Lawson, L. C. Wilkins, R. L. Melen, *Chem. Eur. J.,* **2017**, *23*, 10997–11000.

28. Z. Yang, M. Zhong, X. Ma, S. De, C. Anusha, P. Parameswaran, H. W. Roesky, *Angew. Chem. Int. Ed.,* **2015**, *54*, 10225–10229.

29. V. K. Jakhar, M. K. Barman, S. Nembenna, *Org. Lett.,* **2016**, *18*, 4710−4713.

30. V. A. Pollard, M. A. Fuentes, A. R. Kennedy, R. McLellan, R. E. Mulvey, *Angew. Chem., Int. Ed.,* **2018**, *57*, 10651–10655.

31. M. K. Bisai, S. Pahar, T. Das, K. Vanka, S. S. Sen, *Dalton Trans.,* **2017**, *46*, 2420–2424.

32. T. J. Hadlington, M. Hermann, G. Frenking, C. Jones, *J. Am. Chem. Soc.,* **2014**, *136*, 3028–3031.

33. J. Schneider, C. P. Sindlinger, S. M. Freitag, H. Schubert, L. Wesemann, *Angew. Chem., Int. Ed.,* **2017**, *56*, 333–337.

34. Y. Wu, C. Shan, Y. Sun, P. Chen, J. Ying, J. Zhu, L. (Leo) Liu, Y. Zhao, *Chem. Commun.,* **2016**, *52*, 13799−13802.

35. C. C. Chong, H. Hirao, R. Kinjo, *Angew. Chem. Int. Ed.,* **2015**, *54*, 190−194.

36. B. Freitag, C. A. Fischer, J. Penafiel, G. Ballmann, H. Elsen, C. Färber, D. F. Piesik, S. Harder, *Dalton Trans.*, **2017**, *46*, 11192–11200.

37. B. Freitag, P. Stegner, K. Thum, C. A. Fischer, S. Harder, *Eur. J. Inorg. Chem.,* **2018**, 1938–1944.

38. M. He, M. T. Gamer, P. W. Roesky, *Organometallics,* **2016**, *35*, 2638−2644.

39. S. Harder, J. Spielmann, *J. Organomet. Chem.,* **2012**, *698*, 7−14.

40. S. Kozuch, S. Shaik, *Acc. Chem. Res.,* **2011**, *44*, 101−110.

Chapter 5: Investigation of Silylene/Germylene and Zinc bonding
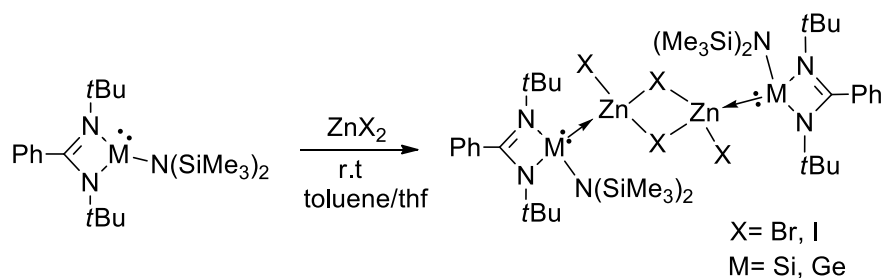
Abstract:

Usually the reaction between silylene and transition metal Lewis acid leads to the formation of adduct which could be either monomer or dimer. However, we observed that a silylene [PhC(NtBu)$_2$SiN(SiMe$_3$)$_2$] reacts with ZnI$_2$ to form both monomeric [PhC(NtBu)$_2$Si{N(SiMe$_3$)$_2$}→ZnI$_2$]·THF (**14**) and dimeric [{PhC(NtBu)$_2$}(N(SiMe$_3$)$_2$)SiZnI(μ-I)]$_2$ (**15**) adducts depending upon the solvent used for the reaction or crystallization. Both the complexes were structurally authenticated and the nature of the Si–Zn bond in these complexes rationalized by quantum chemical calculations. In addition, an inter-conversion between **14** and **15** by changing the solvents have also been observed. Analogous chemistry has been extended with germylene, [PhC(NtBu)$_2$GeN(SiMe$_3$)$_2$], with ZnX$_2$ (X=Br, I) to synthesize [{PhC(NtBu)$_2$}(N(SiMe$_3$)$_2$)GeZnI(μ-I)]$_2$ (**16**) and [{PhC(NtBu)$_2$}(N(SiMe$_3$)$_2$)GeZnBr(μ-Br)]$_2$ (**17**), although no monomeric adduct formation was observed exemplifying the lesser Lewis basicity of germylene than that of silylene.

5.1: Introduction

The recent facile and high yield isolation of functionalized Si(II) compounds such as [PhC(NtBu)$_2$SiCl][1] and [PhC(NtBu)$_2$SiN(SiMe$_3$)$_2$][2] has led to an emerging area of chemistry centered around their coordination properties towards transition metal (TM) complexes.[3] Although the majority of the adducts contains carbonyl ligands around the transition metal, carbonyl free silylene complexes of 3d transition metals[4-7] and silylene complexes of s- and p-block elements have also been recently explored.[8,9] In a recent review, Cabeza and García-Álvarez described the breadth of use of these silylenes as a ligand for transition metals.[10] While nearly hundred silylene-transition metal complexes were reported these two silylenes, the chemistry of silylene with zinc is surprisingly quite underdeveloped, with a handful of very recent examples first from the group of P. Roesky[11,12] and subsequently from the group of Tacke.[13] Moreover, a thorough survey of such silylene adducts revealed that the combination of a silylene and a Lewis acid exclusively affords either a monomer and or a dimer but not both.[10] In addition, the conversion of silylene adducts from the dimer to the monomer or vice-versa or their inter-conversion is also presently unknown.

In this chapter, we have discussed that the reactions of [PhC(NtBu)$_2$SiN(SiMe$_3$)$_2$] with ZnI$_2$ led to both monomeric and dimeric silylene zinc complexes [PhC(NtBu)$_2$Si{N(SiMe$_3$)$_2$}→ZnI$_2$]·THF(**14**) and [PhC(NtBu)$_2$Si{N(SiMe$_3$)$_2$}→ZnI$_2$]$_2$(**15**) depending upon the use of the solvent. Removal of THF from **14** resulted in **15**, while the latter can be converted to **14** just by the addition of THF. Such an inter-conversion of adducts is not known either for silylene or its lighter congener, N-heterocyclic carbene. The theoretical calculation revealed that the Si(II)→Zn bonds in **14** and **15** are of dative nature.[14-17] Analogous chemistry has been extended with germylene, [PhC(NtBu)$_2$GeN(SiMe$_3$)$_2$], with ZnX$_2$ (X=Br, I) to synthesize [{PhC(NtBu)$_2$}(N(SiMe$_3$)$_2$)GeZnI(μ-I)]$_2$ (**16**) and [{PhC(NtBu)$_2$}(N(SiMe$_3$)$_2$)GeZnBr(μ-Br)]$_2$ (**17**).

5.2: Synthesis and characterization of complex 14 and 15

The synthetic strategy for the title compound involves the one-pot reaction of ZnI$_2$ with [PhC(NtBu)$_2$SiN(SiMe$_3$)$_2$] in toluene, which afforded an immediate suspension of a white solid. The reaction mixture was stirred overnight. Upon removal of toluene and subsequent work up in

THF resulted in the monomeric silylene-ZnI$_2$ adduct, **14** (Scheme 5.1). Comparable monomeric N-heterocyclic carbene zinc iodide adduct IPr·ZnI$_2$·THF has been recently reported.[18] **14** exhibits three resonances in the ^{29}Si NMR spectrum at δ –9.5, 6.6, and 8.6 ppm for the Si(II) atom and Si(IV) atoms in trimethylsilyl substituents, respectively, which are in good agreement with analogous four-coordinate silylene-coinage metal complexes.[6] In the solid-state ^{29}Si NMR spectrum three singlets were observed at δ –13.9, 8.2, and 11.5 ppm, which closely matches with the solution state NMR. The ^{1}H NMR spectrum of **14** in CDCl$_3$ displays resonances for (a) *t*Bu (δ 1.35 ppm), (b) trimethylsilyl protons (δ 0.43 and 0.55 ppm) and (c) phenyl protons (δ 7.48–8.0 ppm). The appearance of two signals for the trimethylsilyl groups in ^{1}H as well as ^{29}Si NMR indicates that they are not equivalent and the diastereotopicity stems from the bulky substituents around the Si(II) atom. The resonances corresponding to the THF protons were found at δ 2.01 and 4.12 ppm with an integration of four protons each in the ^{1}H NMR spectrum and δ 25.5 and 68.9 ppm in the ^{13}C NMR spectrum, respectively. The coordinated THF protons are shifted considerably downfield with respect to those in IPr·ZnI$_2$·THF (δ 3.59 and 1.36 ppm) presumably due to more electrophilic nature of [PhC(N*t*Bu)$_2$SiN(SiMe$_3$)$_2$] than IPr. The molecular ion peak for **14** was not observed in the EI-MS spectrum, but the peak corresponds to [M$^+$–(I+THF)] was detected at *m/z* 610.1 with the highest relative intensity.
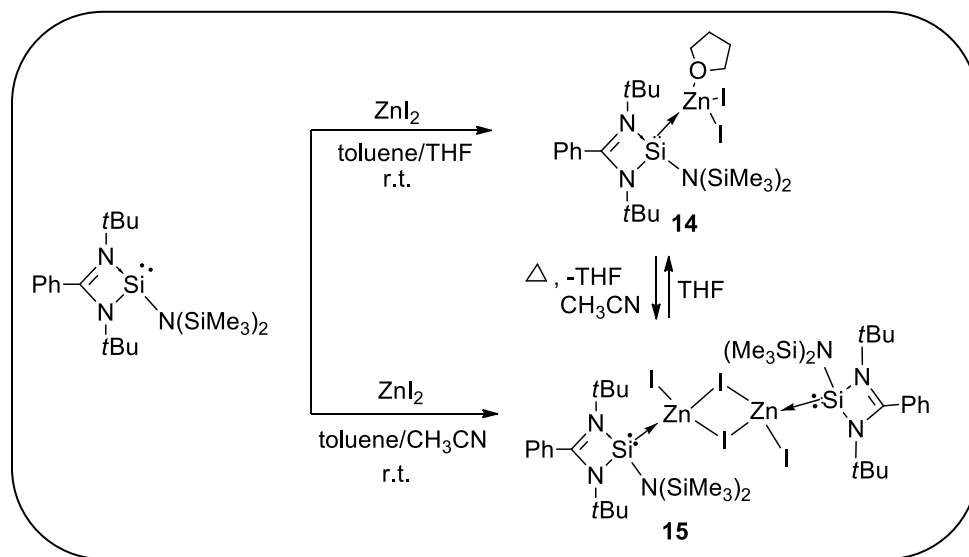
Scheme 5.1: Synthesis of monomeric silylene-ZnI$_2$ adduct (**14**), dimeric silylene-ZnI$_2$ adduct (**15**) and their solvent induced inter-conversion.

The initial realization of **15** was not very straightforward. We intended to isolate silylene-zinc adduct devoid of THF molecule. Hence, we heated **14** under vacuum for 3 h and observed slight changes in the NMR spectroscopy. For example, the ^{29}Si resonances of the new product in CDCl$_3$ appear at δ 10.1 (SiMe$_3$), 8.1 (SiMe$_3$), −6.4 (*Si*N(SiMe$_3$)$_2$) ppm, which are marginally downfield shifted than those of **14**. The solid state ^{29}Si NMR of **15** exhibits very little shift difference (δ 11.5 (SiMe$_3$), 8.3 (SiMe$_3$), −13.3 (*Si*N(SiMe$_3$)$_2$)) with respect to those in **14** emphasizing very similar electronic structures. Similarly, the signals for the Si*Me$_3$* protons are slightly shifted (δ 0.39 and 0.53 ppm) than those of **14** and the signals corresponding to THF disappeared. Subsequent single crystal X-ray studies of a crystal obtained by recrystallization of the residue in acetonitrile confirmed the formation of the dimeric silylene−ZnI$_2$ adduct, [{PhC(N*t*Bu)$_2$}(N(SiMe$_3$)$_2$)SiZnI(μ−I)]$_2$ (**15**), without the coordination of any acetonitrile molecule. Consequently, the general synthetic route to access **15** is developed by reacting [PhC(N*t*Bu)$_2$SiN(SiMe$_3$)$_2$] with ZnI$_2$ in toluene, followed by a work-up in acetonitrile instead of THF (Scheme 5.1). So, the monomerization of **14** can be ascribed to the coordinated THF molecule, which is previously known for stabilization of monomeric calcium iodide complexes.[19] The facile formation of **15** from **14** just by altering the solvents suggests that their inter-conversion could be feasible. This possibility was attempted and found to be true. Gratifyingly, when THF was added to **15**, compound **14** was obtained (Scheme 5.1), which was confirmed by checking the unit cell constants of several crystals of **14** obtained by this synthetic route. Such an inter-conversion between a monomer and a dimer has not been reported for silylene supported adducts yet. In fact, such an inter-conversion has not been reported for analogous IPr·ZnI$_2$·THF as well.
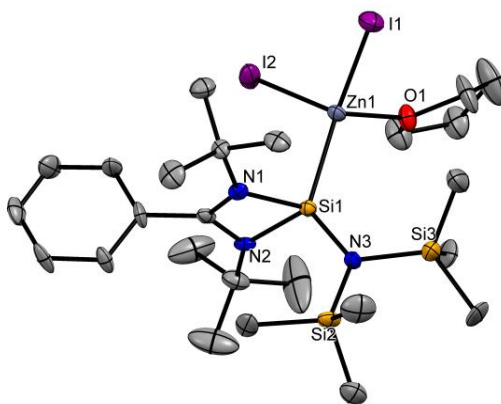
Figure 5.1: Molecular structure of **14** with anisotropic displacement parameters depicted at the 50 % probability level. Hydrogen atoms and solvent of crystallization (1,4-dioxane) are not shown for clarity. Selected bond lengths (Å) and bond angles (°): Zn1–I2 2.6269(11), Zn1–I1 2.5955(11), Zn1–O1 2.092(5), Si1–Zn1 2.434(2), Si1–N3 1.724(6); Si1–N1 1.831(6), Si1–N2 1.840(6); Si1–Zn1–I1 121.70(6), Si1–Zn1–I2 109.01(6), I1–Zn1–I2 107.69(4), Si1–Zn1–O1 115.33(15), O1–Zn1–I1 100.10(14), O1–Zn1–I2 100.79(14), I1–Zn1–I2 107.69(4), N3–Si1–N1 114.2(3), N3–Si1–N2 112.3(3), N1–Si1–N2 70.8(3), N3–Si1–Zn1 128.2(2), N1–Si1–Zn1 104.66(19), N2–Si1–Zn1 111.98(19).
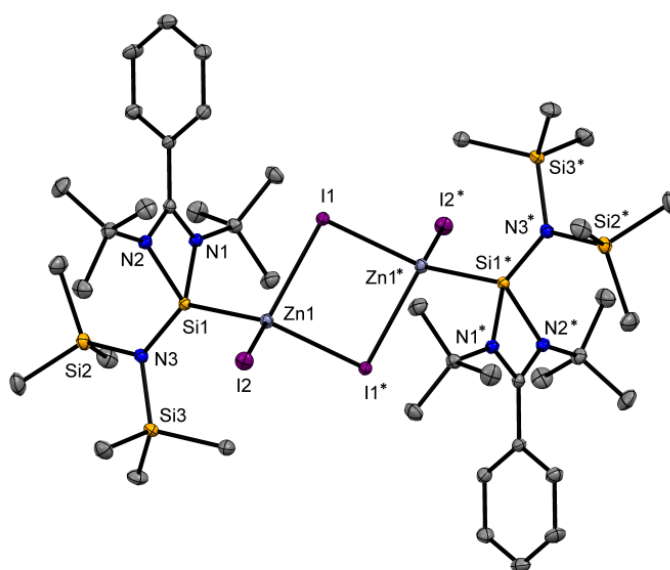
Figure 5.2: Molecular structure of **15** with anisotropic displacement parameters depicted at the 50 % probability level. Hydrogen atoms are not shown for clarity. Selected bond lengths (Å) and bond angles (°): Zn1–I1 2.72225(15) and 2.73727(15), Zn1–I2 2.58023(16), Zn1–Si1 2.4096(3), Si1–N3 1.7163(8), Si1–N1 1.8393(9), Si1–N2 1.8418(9); Si1–Zn1–I2 115.971(8), Si1–Zn1–I1 120.442(8), I2–Zn1–I1 111.409(5), Si1–Zn1–I1 109.284(8) and 120.442(8), I2–Zn1–I1 104.569(5), I1–Zn1–I1 90.861(4), N3–Si1–N1 114.22(4), N3–Si1–N2 114.35(4), N1–Si1–N2 71.28(4), N3–Si1–Zn1 125.84(3), N1–Si1– Zn1 111.29(3), N2–Si1–Zn1 106.76(3). Symmetry generator *: 1-x, 1-y, 1-z.

The slow cooling of saturated THF-dioxane solution of **14** to −35 °C resulted in the formation of highly air sensitive colorless crystals, suitable for single-crystal X-ray diffraction studies. The

molecular structure of **14** is shown in Figure 5.1. Selected bond lengths and angles are provided in the legends of the Figure 5.1. **14** crystallizes in the triclinic space group $P1$.[20] The silicon(II) atom is coordinated by three nitrogen atoms and a zinc atom in a distorted tetrahedral geometry. The Si(II)–Zn bond length in **14** [2.434(2) Å] is comparable to those in silyl-zinc complexes such as $Zn[Si(SiMe_3)_3]_2$ [2.342(4) Å],[21] $tBu_3SiZnBr$ [2.384(1) Å],[22] $[Zn(Si(SiMe_3)_3)Br(thf)]_2$ [2.352(1) Å],[23] $[\{(Me_3Si)_3Si\}(SiMe_3)_2Si]_2Zn$ [2.4028(15) and 2.4066(15) Å],[24] where the formal oxidation state of silicon is +4. The Si(II)–Zn bond length in **14** is longer than those in dimeric zwitter-ionic silylene-zinc iodide adduct, $[\{PhC(NtBu)_2\}(C_5Me_5)SiZnI(\mu-I)]_2$ [2.4116(10) Å],[12] but in good agreement with the Si–Zn bond in $[\{PhC(NtBu)_2\}(C_5Me_5)SiZnPh_2]$ [2.4482(9) Å].[12] The Si–Zn bond length in **14** is also substantially longer than Tacke's silylene-zinc halide complexes $[iPrNC(NiPr_2)NiPr]_2Si·ZnX_2$ [X=Cl {2.3531(9) Å} and Br {2.3564(18) Å}].[13] The zinc atom is coordinated by two iodine atoms, a silicon atom, and a THF molecule and thus adopts a slightly distorted tetrahedral geometry. The Zn–I bond lengths are 2.5955(11) and 2.6269(11) Å, which are comparable to those in Rivard's $IPr·ZnI_2·THF$ [2.6120(3) and 2.5580(3) Å].[18] The Zn–O_{thf} bond distance in **14** [2.092(5)Å] is decreased with respect to the Zn–O bond length in $IPr·ZnI_2·THF$ [2.1252(16) Å][18] but in good agreement with those in $IPr·ZnCl_2·(THF)_2$ [2.077(3) and 2.109(3) Å],[25] and bis(fluorenyl)bis(tetrahydrofuran)zinc complex [2.095(4)–2.114(5) Å].[26] Therefore, the Zn–O_{thf} bond distance in **14**, which is substantially longer than the typical Zn–O covalent bond [1.976(2) Å],[27] indicates an weak coordination of the THF molecule to the Zn(II) center, which is in accordance with earlier observations on donor complexes of diorganozinc compounds.[25,28]

Colorless crystals were obtained upon standing overnight the super-saturated acetonitrile solution of **15** at room temperature. It crystallizes in the monoclinic space group $P2_1/n$. The crystal structure (Figure 5.2) of **15** shows a dimeric complex with the terminal as well as symmetrically bridging iodide ligands with a Zn_2I_2 four-membered ring that results from the μ-iodide bridged dimerization. The iodine atom bridges the two Zn^{2+} ions behaving essentially as a bidentate ligand, a feature very common in alkaline earth metal chemistry.[29,30] The geometry around the zinc can be best described as distorted tetrahedral featuring two bridging and one terminal iodine atoms and the silylene moiety. Similarly, both the Si(II) atoms are four-coordinated and adopt distorted tetrahedral geometry. The mean Si–Zn bond length is 2.4096(3) Å, which is shorter than that in **14** but in good agreement with those in

[{PhC(N*t*Bu)$_2$}(C$_5$Me$_5$)SiZnI(μ−I)]$_2$ (*vide supra*).[12] The terminal Zn–I bond lengths are 2.58023(16) Å. The bridging Zn–I bond lengths are 2.72225(15) and 2.73727(15) Å that are substantially longer than those in [C$_6$H$_3$-2,6-(2,4,6-*i*Pr$_3$C$_6$H$_2$)$_2$ZnI]$_2$ [2.6180(6) to 2.6355(10) Å][31]

6.3: DFT studies to understand dimerization process

The stabilization and bonding of **14** and **15** were investigated computationally by Density Functional Theory using quantum chemistry packages –Q–Chem–4.2 and Gaussian–09.[32] For the calculations, PBE/def2–TZVP[33] level of theory was used. The optimized geometries are shown in the Figure 5.3 with the important bond lengths. The structures obtained computationally are in good agreement with the single crystal XRD data. The HOMO is located on the Si(II) center, Zn and I moieties, while the LUMO is located away from the Zn, on the phenyl groups of the amidinate ligands (shown in Figure 5.4), which is in good agreement with the previously reported coinage metal adducts of [PhC(N*t*Bu)$_2$SiN(SiMe$_3$)$_2$] by Khan et al.[6]
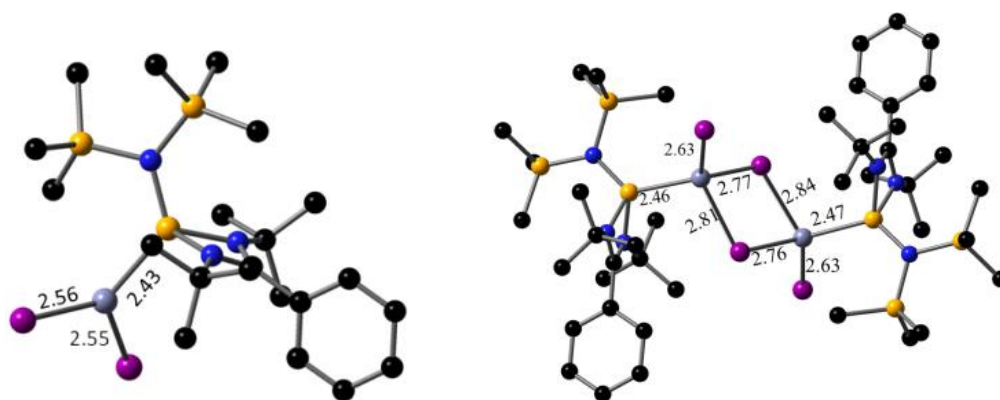
Figure 5.3: The optimized geometry of **14** (left) and **15** (right). The important structural parameters are shown. Hydrogen atoms in **14** and **15** and THF molecule in **14** are not shown for clarity.

To understand the nature of the Si–Zn bond, we used bond dissociation energy (BDE) and bond lengths, as well as partial charges on the atoms. The Si–Zn BDE of the monomer was computed and found to be 34.45 kcal/mol, while the effect of dimerization is an extra stabilization (dimerization energy of 10.9 kcal/mol with respect to formation of one mol of dimer). We have calculated the interaction energy between the adduct with THF and find that the Zn…THF interaction energy is ~6.2 kcal/mol (i.e., 12.4 kcal for two mol of 1*THF complex, which compete with the formation of one mol of dimer). Hence, the similar energies associated with

dimerization and THF–Zn interaction can be seen as the cause of this rather easy conversion between dimer and THF complex in case of this particular ZnI_2–silylene system. We have calculated the interaction energy between the adduct with THF and find that the interaction energy is ~6.23 kcal/mol which is much lower. Here it should be noted that the binding energies are a measure of the bond strength between Si and ZnI_2. Since the binding energy of the monomer is considerably lower than a covalent bond (~50 kcal/mol),[12] the Si–Zn bond is assumed to have a dative character. Furthermore, the dimerization energy as well as the comparison of Si–Zn bond lengths in the monomer and dimer points toward formation of a weak adduct. The Si–Zn bond lengths are 2.43 Å (longer than the single bond), while the Zn-I bonds are 2.55 Å (as compared to 2.43 Å in ZnI_2) in the monomers. This further point towards weaker than single bond character of the Zn–Si bond.
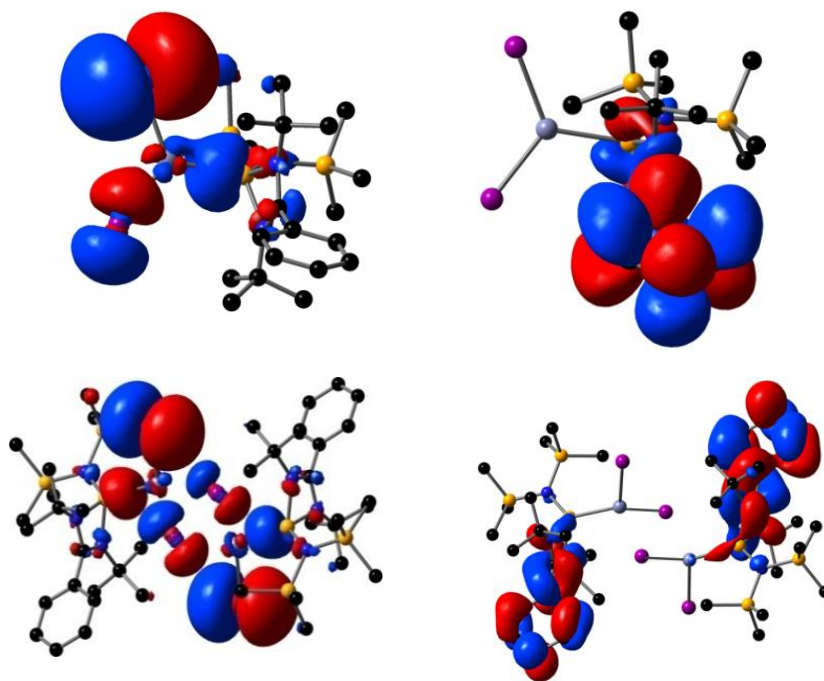
Figure 5.4: The HOMO and LUMO of the monomer and dimer (with an isosurface value of 0.02). (A) HOMO of **14**, (B) LUMO of **14**, (C) HOMO of **15** and (D) LUMO of **15**. The hydrogen atoms are not shown for clarity

The NBO analysis[34] was used to understand the nature of bonding in the complexes. The net natural charges on the relevant parts of the monomer are: +0.39 a.u. (on Zn), –0.44 a.u. (on each I), 1.38 a.u. (on Si adjacent to Zn), 1.81 a.u. (on the other Si atoms), –0.68 a.u. (on the amidinate

Ns) and −1.73 a.u. on the amide N. In case of the dimer, the overall magnitude of the charges are similar with small changes on the I atoms (−0.02 a.u. and −0.1 a.u. respectively), which experience the effect of the adjacent monomer, and reduction in positive charge on the Zn atom (+0.33 a.u.), possibly due to small amount of electron donation from both the Si atoms. The difference in partial charge between Si and Zn points towards small amount of ionic character. The individual monomers in the dimer structure are almost neutral (+/− 0.007 a.u.).

The strongest interactions were noticed between the Si–N bonding and the antibonding orbitals of the adjacent C atoms (14.69 and 14.70 kcal/mol), and also between the Zn–Si bonding orbital (which is predominantly located on Si) with the Zn–I antibonding orbital (which is predominantly located on the Zn atom). This interaction energy between the Si–Zn and the Zn–I bonding and antibonding orbitals is 5.73–5.98 kcal/mol.

5.4: Synthesis and characterization of complex 16 and 17

Analogous chemistry has been extended to germylene, $[PhC(NtBu)_2GeN(SiMe_3)_2]$ with ZnX_2 (X=Br, I), although no monomeric adduct formation was observed exemplifying the lesser Lewis basicity of germylene that that of silylene. A 1:1 mixture of $[PhC(NtBu)_2GeN(SiMe_3)_2]$ and ZnI_2 was stirred overnight using thf as the reaction solvent. The removal of solvent and futher washing with *n*–hexane afforded a dimeric germylene–zinc adduct, $[\{PhC(NtBu)_2\}(N(SiMe_3)_2)GeZnI(\mu–I)]_2$ (**16**) (scheme 5.2). Single crystals suitable for X-ray diffraction studies were grown in the thf–toulene mixture. The molecular structure of **16** is shown in figure 5.5. **16** crystallizes in the monoclinic '*P*21/*n*' space group. The amidinate Ge(II) atom is tetracoordinated and shows distorted tetrahedral geometory. The Ge(II)−Zn bond length in **16** is 2.4460(9) Å, which is comparable to aminotroponiminatogermylene–ZnCl$_2$ adduct, *i.e* 2.425(3).[37]
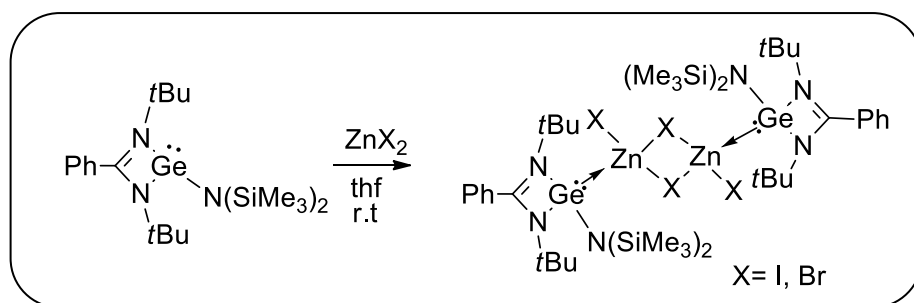
Scheme 5.2: Synthesis of Germylene–ZnX$_2$(X=I, Br) adducts.
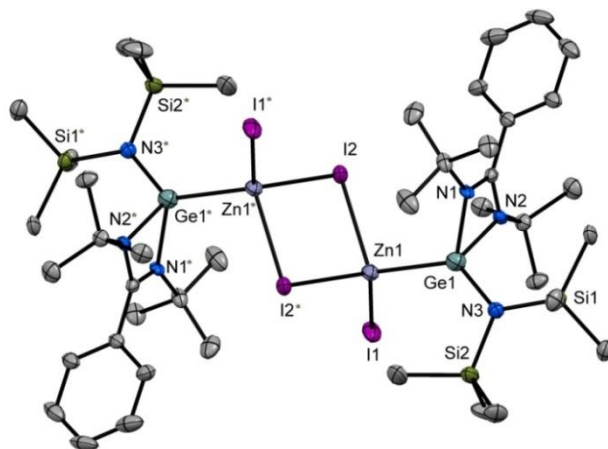
Figure 5.5: Molecular structure of **16** with anisotropic displacement parameters depicted at the 50 % probability level. Hydrogen atoms are not shown for clarity. Symmetry generator *: 1−x, 1−y, 1−z. Selected bond lengths (Å) and bond angles (°): I2−Zn1 2.6986(8) and 2.7128(8), I1−Zn1 2.5572(8), Zn1−Ge1 2.4460(9), Ge1−N3 1.826(5), Ge1−N1 1.941(4), Ge1−N2 1.949(4); Zn1−I2−Zn1 86.84(2), Ge1−Zn1−I1 114.15(3), Ge1−Zn1−I2 119.09(3), I1−Zn1−I2 113.55(3), Ge1−Zn1−I2 105.94(3), I1−Zn1−I2 107.74(3), I2−Zn1−I2 93.17(2), N3−Ge1−N1 109.9(2), N3−Ge1−N2 110.6(2), N1−Ge1−N2 67.73(19).

The similar procedure as of **16** was performed for the synthesis of [{PhC(N*t*Bu)$_2$}(N(SiMe$_3$)$_2$)GeZnBr(μ–Br)]$_2$(**17**) using ZnBr$_2$ instead of ZnI$_2$. The molecular structure of **17** is shown in Figure 5.6. It crystallizes in the triclinic '*P*-1' space group. The Ge(II)–Zn bond length in **17** is 2.4587(6) Å, which is in good agreement with that in **16**.
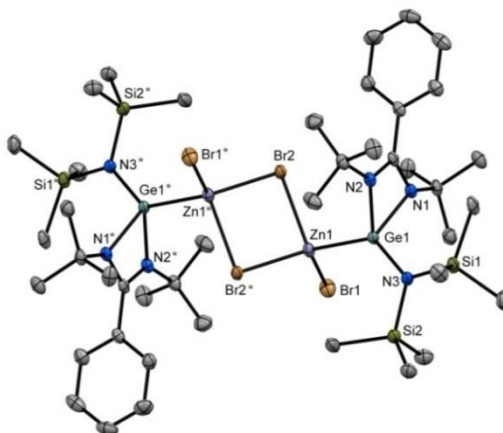
Figure 5.6: Molecular structure of **17** with anisotropic displacement parameters depicted at the 50 % probability level. Hydrogen atoms are not shown for clarity. Symmetry generator *: 1–x, 1–y, 1–z. Selected bond lengths (Å) and bond angles (°): Br2−Zn1 2.4800(5) and 2.5143(5), Ge1−N3 1.838(3), Ge1−N2 1.959(2), Ge1−N1 1.972(2), Ge1−Zn1 2.4587(6), Br1−Zn1 2.3445(5), Zn1−Br2 2.5143(5); Zn1−Br2−Zn1 87.456(16), N3−Ge1−N2 111.48(12), N3−Ge1−N1 110.94(12), N2−Ge1−N1 66.73(10), N3−Ge1−Zn1 130.29(9), N2−Ge1−Zn1 112.13(9), N1−Ge1−Zn1 107.30(9), Br1−Zn1−Ge1 113.38(2), Br1−Zn1−Br2 115.07(2), Ge1−Zn1−Br2 117.743(18), Br1−Zn1−Br2 110.504(19), Ge1−Zn1−Br2 104.722(18), Br2−Zn1−Br2 92.543(16).

5.5: Conclusions

At the beginning of this chapter, we pointed out that (a) no silylene is reported to afford both monomer and dimer upon reacting with a Lewis acid and (b) inter-conversion between monomeric and dimeric silylene-transition metal adducts is hitherto unknown. We have tried to address these issues in our studies. The results of our studies can be summarized as follows: (a) [PhC(N*t*Bu)$_2$SiN(SiMe$_3$)$_2$] (B) forms both monomeric [PhC(N*t*Bu)$_2$Si{N(SiMe$_3$)$_2$}→ZnI$_2$]·THF (**14**) and dimeric [{PhC(N*t*Bu)$_2$}(N(SiMe$_3$)$_2$)SiZnI(μ-I)]$_2$ (**15**) adducts upon reacting with ZnI$_2$, (b) a unique inter-conversion between **14** and **15** just by altering the solvents has been observed. The isolation of **14** and **15** adds to the family of silylene-zinc complexes, which are very limited in number. The ligation chemistry of germylene is not very developed as compared to carbenes and silylenes. Hence, analogous chemistry has been extended with germylene, [PhC(N*t*Bu)$_2$GeN(SiMe$_3$)$_2$] to sythesize [{PhC(N*t*Bu)$_2$}(N(SiMe$_3$)$_2$)GeZnI(μ-I)]$_2$ (**16**) and [{PhC(N*t*Bu)$_2$}(N(SiMe$_3$)$_2$)GeZnBr(μ-Br)]$_2$ (**17**). The failure to obtain a monomeric adduct can be attributed to the lesser Lewis basicity of germylene than that of silylene.

5.6: References

1. (a) C.–W. So, H. W. Roesky, J. Magull, R. B. Oswald, *Angew. Chem. Int. Ed.*, **2006**, *45*, 3948–3950; (b) S. S. Sen, H. W. Roesky, D. Stern, J. Henn, D. Stalke, *J. Am. Chem. Soc.*, **2010**, *132*, 1123–1126.

2. S. S. Sen, J. Hey, R. Herbst-Irmer, H. W. Roesky, D. Stalke, *J. Am. Chem. Soc.,* **2011**, *133*, 12311–12316.

3. (a) M. Haaf, R. Hayashi, R. West, *J. Chem. Soc., Chem. Commun.*, **1994**, 33–34; (b) R. West, M. Denk, *Pure Appl. Chem.,* **1996**, *68*, 785–788; (c) B. Gehrhus, P. B. Hitchcock, M. F. Lappert, H. Maciejewski, *Organometallics,* **1998**, *17*, 5599–5601; (d) S. H. A. Petri, D. Eikenberg, B. Neumann, H.–G. Stammler, P. Jutzi, *Organometallics*, **1999**, *18*, 2615–2618; (e) T. A. Schmedake, M. Haaf, B. J. Paradise, D. Powell, R. West, *Organometallics*, **2000**, *19*, 3263–3265; (f) J. M. Dysard, T. D. Tilley, *Organometallics*, **2000**, *19*, 4726–4732; (g) A. Fürstner, H. Krause, C. W. Lehmann, *Chem. Commun.*, **2001**, 2372–2373; (h) S. B. Clendenning, B. Gehrhus, P. B. Hitchcock, D. F. Moser, J. F. Nixon, R. West, *J. Chem. Soc., Dalton Trans.*, **2002**, 484–490; (i) D. Amoroso, M. Haaf, G. P. A. Yap, R. West, D. E. Fogg, *Organometallics*, **2002**, *21*, 534–540; (j) A. G. Avent, B. Gehrhus, P. B. Hitchcock, M. F. Lappert, H. Maciejewski, *J. Organomet. Chem.*, **2003**, *686*, 321–331; (k) W. Yang, H. Fu, H. Wang, M. Chen, Y. Ding, H. W. Roesky, A. Jana, *Inorg. Chem.*, **2009**, *48*, 2058–2060; (l) W. Wang, S. Inoue, S. Yao, M. Driess, *J. Am. Chem. Soc.,* **2010**, *132*, 15890–15892; (m) J. Li, S. Merkel, J. Henn, K. Meindl, A. Döring, H. W. Roesky, R. S. Ghadwal, D. Stalke, *Inorg. Chem.*, **2010**, *49*, 775–777; (n) G. Tavčar, S. S. Sen, R. Azhakar, A. Thorn, H. W. Roesky, *Inorg. Chem.*, **2010**, *49,* 10199–10202; (o) R. Azhakar, S. P. Sarish, H. W. Roesky, J. Hey, D. Stalke, *Inorg. Chem.*, **2011**, *50*, 2897–2900; (p) R. Azhakar, S. P. Sarish, H. W. Roesky, J. Hey, D. Stalke, *Inorg. Chem.*, **2011**, *50*, 5039–5043; (q) W. Wang, S. Inoue, E. Irran, M. Driess, *Angew. Chem. Int. Ed.,* **2012**, *51*, 3691–3694; (r) W. Wang, S. Inoue, S. Enthaler, M. Driess, *Angew. Chem. Int. Ed.,* **2012**, *51*, 6167–6171; (s) A. Brück, D. Gallego, W. Wang, E. Irran, M. Driess, J. F. Hartwig, *Angew. Chem. Int. Ed.*, **2012**, *51*, 11478–11482; (t) B. Blom, S. Enthaler, S. Inoue, E. Irran, M. Driess, *J. Am. Chem. Soc.,* **2013**, *135*, 6703–6713; (u) C. I. Someya, M. Haberberger, W. Wang, S. Enthaler, S. Inoue, *Chem. Lett.*, **2013**, *42*, 286–288; (v) N. C. Breit, T. Szilvási, T. Suzuki, D. Gallego, S. Inoue, *J. Am. Chem. Soc.*, **2013**, *135*, 17958–17968; (w) M. Stoelzel, C. Praesang, B. Blom, M. Driess, *Aust. J. Chem.*, **2013**, *66*, 1163–1170; (x) B. Blom, D. Gallego, M. Driess, *Inorganic Chemistry Frontiers*, **2014**, *1*, 134–148; (y) D. Gallego, B. Blom, G. Tan, M. Driess, *Chelating N-Heterocyclic Silylenes as Steering Ligands in Catalysis. Structure and Bonding*, In: J. Reedijk, (Ed.) Elsevier Reference Module in Chemistry, Molecular Sciences and Chemical Engineering. Waltham, MA. **2014**.

4. (a) G. Tan, S. Enthaler, S. Inoue, B. Blom, M. Driess, *Angew. Chem. Int. Ed.*, **2015**, *54*, 2214–2218; (b) D. Gallego, S. Inoue, B. Blom, M. Driess, *Organometallics*, **2014**, *33*, 6885–6897; (c) D. Gallego, A. Brück, E. Irran, F. Meier, M. Kaupp, M. Driess, J. F. Hartwig, *J. Am. Chem. Soc.*, **2013**, *135*, 15617–15626.

5. R. Azhakar, R. S. Ghadwal, H. W. Roesky, J. Hey, L. Krause, D. Stalke, *Dalton Trans.*, **2013**, *42*, 10277–10281.

6. (a) S. Khan, S. Pal, N. Kathewad, P. Parameswaran, S. De, I. Purushothaman, *Chem. Commun.*, **2016**, *52*, 3880–3882; (b) S. Khan, S. K. Ahirwar, S. Pal, N. Parvin, N. Kathewad, *Organometallics,* **2015**, *34*, 5401–5406; (c) N. Parvin, R. Dasgupta, S. Pal, S. S. Sen, S. Khan, *Dalton Trans.*, **2017**, *46*, 6528–6532; (d) N. Parvin, S. Pal, S. Khan, S. Das, S. K. Pati, H. W. Roesky, *Inorg. Chem.*, **2017**, *56*, 1706–1712.

7. F. M. Mück, J. A. Baus, A. Ulmer, C. Burschka, R. Tacke, *Eur. J. Inorg. Chem.*, **2016**, 1660–1670.

8. (a) F. M. Mück, J. A. Baus, R. Bertermann, C. Burschka, R. Tacke, *Organometallics,* **2016**, *35*, 2583−2588; (b) K. Junold, J. A. Baus, C. Burschka, C. F. Guerra, F. M. Bickelhaupt, R. Tacke, *Chem. Eur. J.,* **2014**, *20*, 12411−12415; (c) B. Blom, G. Klatt, D. Gallego, G. Tan, M. Driess, *Dalton Trans.*, **2015**, *44*, 639–644.

9. (a) S.–P. Chia, H.–W. Xi, Y. Li, K. H. Lim, C.-W. So, *Angew. Chem. Int. Ed.*, **2013**, *52*, 6298–6301; (b) Y.–L. Shan, B.–X. Leong, H.–W. Xi, R. Ganguly, Y. Li, K. H. Lim, C.–W. So, *Dalton Trans.*, **2017**, *46*, 3642–3648.

10. For a recent review on silylene-adducts: L. Alvarez-Rodriguez, J. A. Cabeza, P. Garcia-Alvarez, D. Polo, *Coord. Chem. Rev.,* **2015**, *300*, 1–28.

11. S. Schäfer, R. Köppe, M. T. Gamer, P. W. Roesky, *Chem. Commun.,* **2014**, *50*, 11401–11403.

12. S. Schäfer, R. Köppe, P. W. Roesky, *Chem. Eur. J.*, **2016**, *22*, 7127–7133.

13. J. A. Baus, F. M. Meck, H. Schneider, R. Tacke, *Chem. Eur. J.*, **2017**, *23*, 296–303.

14. D. Himmel, I. Krossing, A. Schnepf, *Angew. Chem. Int. Ed.*, **2014**, *53*, 370–374.

15. G. Frenking, *Angew. Chem. Int. Ed.,* **2014**, *53*, 6040–6046.

16. D. Himmel, I. Krossing, A. Schnepf, *Angew. Chem. Int. Ed.*, **2014**, *53*, 6047–6048.

17. A. Haaland, *Angew. Chem. Int. Ed.*, **1989**, *28*, 992–1007.

18. S. M. I. Al-Rafia, P. A. Lummis, A. K. Swarnakar, K. C. Deutsch, M. J. Ferguson, R. McDonald, E. Rivard, *Aust. J. Chem.*, **2013**, *66*, 1235–1245.

19. (a) S. Datta, M. T. Gamer, P. W. Roesky, *Dalton Trans.,* **2008**, 2839–2843; (b) S. Yadav, V. S. V. S. N.; Swamy, R. G. Gonnade, S. S. Sen, *ChemistrySelect*, **2016**, *1*, 1066-1071.

20. (a) T. Kottke, D. Stalke, *J. Appl. Crystallogr.*, **1993**, *26*, 615–619; (b) D. Stalke, *Chem. Soc. Rev.*, **1998**, *27*, 171–178; (c) G. M. Sheldrick, *Acta Crystallogr.*, **2008**, *A64*, 112–122; (d) T. Schulz, K. Meindl, D. Leusser, D. Stern, J. Graf, C. Michaelsen, M. Ruf, G. M. Sheldrick, D. Stalke, *J. Appl. Crystallogr.*, **2009**, *42*, 885−891; (e) L. Krause, R. Herbst-Irmer, G. M. Sheldrick and D. Stalke, *J. Appl. Crystallogr.*, **2015**, *48*, 3−10.

21. J. Arnold, T. D. Tilley, A. L. Rheingold, S. J. Geib, *Inorg. Chem.*, **1987**, *26*, 2106-2109.

22. N. Wiberg, K. Amelunxen, H.-W. Lerner, H. Nöth, A. Appel, J. Knizek, K. Polborn, *Z. Allg. Anorg. Chem.*, **1997**, *623*, 1861–1870.

23. C. T. Sirimanne, M. M. Kerrigan, P. D. Martin, R. K. Kanjolia, S. D. Elliott, C. H. Winter, *Inorg. Chem.*, **2015**, *54*, 7−9.

24. W. Gaderbauer, I. Balatoni, H. Wagner, J. Baumgartner, C. Marschner, *Dalton Trans.*, **2010**, *39*, 1598–1603.

25. A. Doddi, C. Gemel, R. W. Siedel, M. Winter, R. A. Fischer, *Polyhedron*, **2013**, *52*, 1103–1108.

26. A. Fischer, J. Boersma, G. vanKoten, W. J. J. Smeets, A. L. Spek, *Organometallics*, **1989**, *8*, 667–672.

27. S. Bhattacharyya, S. B. Kumar, S. K. Dutta, E. R. T. Tiekink, M. Chaudhury, *Inorg. Chem.,* **1996**, *35,* 1967–1973.

28. (a) D. Wang, K. Wurst, M. Buchmeiser, *J. Organomet. Chem.,* **2004**, *689*, 2123–2130; (b) M. Weidenbruch, M. Herrendorf, A. Schäfer, S. Pohl, W. Saak, *J. Organomet. Chem.*, **1989**, *361*, 139–145.

29. C. Ruspic, S. Harder, *Inorg. Chem.*, **2007**, *46*, 10426–10433

30. S. P. Sarish, S. Nembenna, S. Nagendran, H. W. Roesky, *Acc. Chem. Res.*, **2011**, *44*, 157–170 and references therein.

31. Y. Wang, B. Quillian, C. S. Wannere, P. Wei, P. v. R. Schleyer, G. H. Robinson, *Organometallics*, **2007**, *26*, 3054–3056.

32. Y. Shao et al. *Mol. Phys.*, **2015**, *113*, 184−215.

33. Gaussian 09, Revision A.02, M. J. Frisch, et al, Gaussian 09, Revision A.02, Gaussian, Inc., Wallingford CT, **2016**.

34. E. D. Glendening, C. R. Landis, F. Weinhold, *J. Comput. Chem.*, **2013**, *34*, 1429−1437.

35. Bruker (**2006**). *APEX2*, *SAINT* and *SADABS*. Bruker AXS Inc., Madison, Wisconsin, USA.

36. L. J. Farrugia, *J. Appl. Cryst.,* **1997**, *30*, 565–565.

37. S. Sinhababu, D. Yadav, S. Karwasara, M. K. Sharma, G. Mukherjee, G. Rajaraman, S. Nagendran, *Angew. Chem. Int. Ed.,* **2016**, *55*, 7742 –7746.

Appendix: Experimental and spectra details

6.2: Chapter 2 experimental details

6.2.1: Synthesis and experimental details of complex **3** and **4**

6.2.2: Crystal structure details of complex **3** and **4**

6.2.3: General procedure for catalytic hydroboration of aldehydes

6.2.4: Spectroscopic data for aldehyde hydroboration products

6.2.5: General procedure for catalytic hydroboration of ketones

6.2.6: Spectroscopic data for aldehyde hydroboration products

6.3: Chapter 3 experimental details

6.3.1: General procedure for the cyanosilylation of aldehydes

6.3.2: Spectroscopic data for cyanosilylated product of aldehydes

6.3.3: General procedure for the cyanosilylation of ketones

6.3.4: Spectroscopic data for cyanosilylated product of ketones

6.3.5: Characterization and isolation of intermediate

6.3.6: Details of DFT calculations

6.4: Chapter 4 experimental details

6.4.1: Synthesis and experimental details of complex **10** and **11**

6.4.2: Crystal structure details of complex **10** and **11**

6.4.3: DOSY NMR of complex **11**

6.4.4: Spectroscopic data for hydroborated product of aldehydes

6.4.5: Spectroscopic data for hydroborated product of ketones

6.4.6: Details of DFT calculations

6.5: Chapter 5 experimental details

6.5.1: Synthesis and experimental details of complex **14** and **15**

6.5.2: Crystal structure details of complex **14** and **15**

6.5.3: Synthesis and experimental details of complex **16** and **17**

6.5.4: Crystal structure details of complex **16** and **17**

6.2: Chapter 2 experimental details

6.2.1: Synthesis and experimental details of complex 3 and 4

Synthesis of complex 3: PhLi (5.26 mL, 10 mmol, 1.9 M solution in di-*n*-butyl ether) was added to a stirring solution of N, N'-diisopropyl carbodiimide (1.26 g, 10 mmol) in THF (30 mL) at –78 °C. The reaction mixture was allowed to warm slowly to room temperature and stirred further for 4 h at this temperature. This solution was transferred by a cannula to a suspension of CaI_2 (2.93 g, 10 mmol) in THF (30 mL) at –78 °C. The reaction mixture was allowed to warm to room temperature and then stirred for 3 days. The solvent was removed under vacuum and the residue was extracted with toluene (50 mL) to remove LiI. Toluene was removed under vacuum and crystallization was performed in THF (15 mL) at –30 °C in a freezer. Yield: 2.16 g (36.8 %). Mp: turns opaque at 80–85 °C (presumably loss of donor solvent), turns dark at 185–190 °C. ^{1}H NMR (200 MHz, DMSO-d_6, 25 °C) δ 0.90 (d, 6H, 6.11 Hz, CH_3), 1.06 (d, 6H, 6.49 Hz, CH_3), 1.79 (m, THF), 3.08 (sept, 1H, CH), 3.59 (m, THF), 3.98 (sept, 1H, CH), 7.17 (dd, 2H, Ph), 7.37 (m, 3H, Ph) ppm; ^{13}C NMR (50.28 MHz, DMSO-d_6, 25 °C) δ 22.1 (CH_3), 25.1 (THF), 48.7 (CHCH_3), 66.6 (THF), 127.1, 128.1, 136.4, 138.4 (Ph), 155.4 (NCN) ppm. LCMS *m/z* (%): 441.2 (25) [M$^+$–2THF], 371.1 (10) [M$^+$–3THF], 243.1 (100) [M$^+$–3THF–I]. For elemental analysis, **3** was treated under vacuum to remove THF molecules. Anal. Calcd for $C_{13}H_{19}CaIN_2$ (370.29): C, 42.17; H, 5.17; N, 7.57. Found: C, 42.31; H, 5.94; N, 8.82.

Synthesis of complex 4: PhLi (2.63 mL, 5 mmol, 1.9 M solution in di-*n*-butyl ether) was added to a stirring solution of N, N'- diisopropyl carbodiimide (0.63 g, 5 mmol) in diethyl ether (30 mL) at –78 °C. The reaction mixture was allowed to warm slowly to room temperature and stirred for 4 h at this temperature. This solution was transferred to a suspension of CaI_2 (1.47 g, 5 mmol) in diethyl ether (30 mL) at –78 °C. The reaction was warmed to room temperature and stirred for 3 days. The solution was filtered through celite and concentrated to one-third of its volume. Colourless crystals were obtained after 2 days at −35 °C in a freezer. Yield: 1.82 g (33.8 %). Mp: turns opaque at 120–125 °C, turns dark at 260-265 °C. ^{1}H NMR (500 MHz, DMSO-d_6, 25 °C) δ 0.88 (d, 18H, CH_3), 1.08 (m, 22H, CH_3 and diethyl ether protons merged), 3.09 (s, 2H, CH), 3.36 (m, 10H, diethyl ether), 3.96 (s, 2H, CH), 7.17 (dd, 4H, Ph), 7.37 (m, 6H, Ph) ppm; ^{13}C NMR (125.72 MHz, DMSO-d_6, 25 °C) δ 13.1, 15.1 (diethyl ether), 22.1 (CH_3), 48.7 (CHC$H3$), 64.9, 69.6 (diethyl ether), 127.2, 128.1, 136.5 (Ph), 155.5 (NCN) ppm.

6.2.2: Crystal structure details of complex 3 and 4

Crystal Data for complex 3: $C_{25}H_{43}CaIN_2O_3$, M=586.59, colorless block, 0.34 x 0.22 x 0.17 mm^3, monoclinic, space group *Pn*, a=9.7529(8)Å, b=10.6112(8)Å, c=14.3836(9)Å, β=93.676(4)°, V=1485.50(19) $Å^3$, Z=2, T=200(2) K, $2\theta_{max}$=50.00°, $D_{calc}(gcm^{-3})$=1.311, F(000)=608, μ (mm^{-1})=1.275, 9184 reflections collected, 4490 unique reflections (R_{int}=0.0250), 4091 observed ($I>2\sigma(I)$) reflections, multi-scan absorption correction, T_{min}=0.671, T_{max}=0.812, 293 refined parameters, S=1.149, R1=0.0502, wR2=0.1498 (all data R=0.0630, wR2=0.1715), maximum and minimum residual electron densities; $\Delta\rho_{max}$=1.20, $\Delta\rho_{min}$= −1.25 (e$Å^{-3}$).

Crystal data for complex 4: $C_{50}H_{103}Ca_4I_8Li_4N_4O_7$, $1.5(C_4H_{10}O)$, M=2181.78, colorless block, 0.15 x 0.12 x 0.10 mm^3, monoclinic, space group *C2/c*, a=44.890(9)Å, b=15.036(3)Å, c=29.267(5) Å, β=96.627(6)°, V=19623(6) $Å^3$, Z=8, T=100(2) K, $2\theta_{max}$=50.00°, $D_{calc}(gcm^{-3})$=1.477, F(000)=8488, μ mm^{-1})=2.775, 223701 reflections collected, 17622 unique reflections (R_{int}=0.1332), 9040 observed ($I>2\sigma(I)$) reflections, multi-scan absorption correction, T_{min}=0.681, T_{max}=0.769, 792 refined parameters, 153 restraints, S=1.045, R1=0.0849, wR2=0.1748 (all data R=0.1881, wR2=0.2277), maximum and minimum residual electron densities; $\Delta\rho_{max}$=1.60, $\Delta\rho_{min}$= −2.35 (e$Å^{-3}$).

6.2.3: General procedure for catalytic hydroboration of aldehydes

Aldehyde (0.25 mmol), pinacolborane (0.25 mmol), LCaI (0.5-2 mol%) [benzene (1 mL)] were charged in Schlenk tube inside glove box. The reaction mixture was allowed to run at room temperature. The progress of the reaction was monitored by ^{1}H NMR, which indicated the completion of the reaction by the disappearance of the aldehyde proton and appearance of a new CH_2 peak. Upon completion of reaction, the solvent was removed using high vacuum in Schlenk line and mesitylene (0.25 mmol) as internal standard, was added while making the NMR in $CDCl_3$.

6.2.4: Spectroscopic data for aldehyde hydroboration products

Compound 5a: product from hydroboration of benzaldehyde. ^{1}H NMR (CDCl$_3$, 200 MHz), δ 1.17 (s, 12H, Bpin-CH_3), 4.82 (s, 2H, pinBOCH_2), 7.24 (m, 5H, Ar-H); ^{13}C NMR (CDCl$_3$, 50.28 MHz), δ 24.6 (Bpin-CH_3), 66.7 (OCH_2Ph), 83.0 (Bpin-C), 126.6, 126.8, 127.0, 128.3, 137.7, 139.3 (Ar-C)
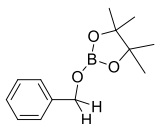
Compound 5b: product from hydroboration of 4–Methylbenzaldehyde. ^{1}H NMR (CDCl$_3$, 200 MHz), δ 1.17 (s, 12H, Bpin-CH_3), 2.25 (s, 3H, Ar–CH_3), 4.80 (s, 2H, pinBOCH_2), 7.07 (d, $^{3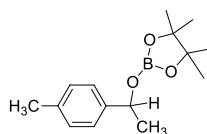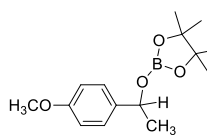}J_{HH}$=7.7 Hz, 2H, Ar–$H$), 7.14 (d, $^{3}J_{HH}$=8.2 Hz, 2H, Ar-H); ^{13}C NMR (CDCl$_3$, 50.28 MHz), 21.2 (PhCH_3), 24.6 (Bpin-CH_3), 66.6 (OCH_2Ph), 82.9 (Bpin-C), 126.9, 128.2, 129.0, 129.9, 137.0, 137.7 (Ar-C).
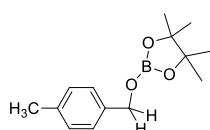
Compound 5c: product from hydroboration of 2–Bromobenzaldehyde. ^{1}H NMR (CDCl$_3$, 200 MHz), δ 1.19 (s, 12H, Bpin-CH_3), 4.90 (s, 2H, pinBOCH_2), 7.03 (d, $^{3}J_{HH}$=7.2 Hz, 1H, Ar-H), 7.27 (m, 1H, Ar-H), 7.40 (m, 1H, Ar-H), 7.44 (dd, $^{3}J_{HH}$=7.1 Hz, 1H, Ar-H); ^{13}C NMR (CDCl$_3$, 50.28 MHz), δ 24.6 (Bpin-CH_3), 66.3 (OCH_2Ph), 83.2 (Bpin-C), 121.4, 126.9, 127.4, 127.8, 128.6, 132.3 (Ar-C).
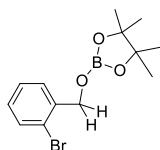
Compound 5d: product from hydroboration of 3–Bromobenzaldehyde. ^{1}H NMR (CDCl$_3$, 200 MHz), δ 1.17 (s, 12H, Bpin-CH_3), 4.80 (s, 2H, pinBOCH_2), 7.08 (d, $^{3}J_{HH}$=7.6 Hz, 1H, Ar-H), 7.14 (m, 1H, Ar-H), 7.26 (m, 1H, Ar-H), 7.43 (s, 1H, Ar-H); ^{13}C NMR (CDCl$_3$, 50.28 MHz), δ 24.6 (Bpin-CH_3), 65.9 (OCH_2Ph), 83.2 (Bpin-C), 122.5, 125.2, 126.9, 127.6, 128.4, 130.5 (Ar-C).
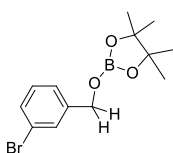
Compound 5e: product from hydroboration of 4–Bromobenzaldehyde. ^{1}H NMR (CDCl$_3$, 200 MHz), δ 1.17 (s, 12H, Bpin-CH_3), 4.78 (s, 2H, pinBOCH_2), 7.15 (d, $^{3}J_{HH}$=8.1 Hz, 2H, Ar-H), 7.34 (d, $^{3}J_{HH}$=8.5 Hz, 2H, Ar-H); ^{13}C NMR (CDCl$_3$, 50.28 MHz), δ 23.8 (Bpin-CH_3), 65.2 (OCH_2Ph), 82.3 (Bpin-C), 120.4, 126.1, 127.4, 128.6, 130.6, 136.9 (Ar-C).
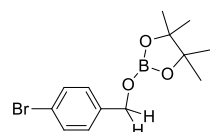
Compound 5f: product from hydroboration of 2–Methoxylbenzaldehyde. ^{1}H NMR (CDCl$_3$, 200 MHz), δ 1.18 (s, 12H, Bpin-CH_3), 3.70 (s, 3H, Ar-OCH_3), 4.90 (s, 2H, pinBOCH_2), 6.89 (m, 2H, Ar-H), 7.14 (m, 1H, Ar-H),7.34 (m, 1H, Ar-H); ^{13}C
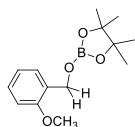
NMR (CDCl$_3$, 50.28 MHz), δ 24.5 (Bpin-CH_3), 55.0 (PhOCH_3), 62.2 (OCH_2Ph), 82.7 (Bpin-C), 120.2, 126.5, 127.2, 128.1, 137.5, 156.3 (Ar-C).

Compound 5g: product from hydroboration of 3–Methoxybenzaldehyde. ^{1}H NMR (CDCl$_3$, 200 MHz), δ 1.18 (s, 12H, Bpin-CH_3), 3.70 (s, 3H, PhOCH_3), 4.82 (s, 2H, pinBOCH_2), 6.84 (d, 2H, Ar-H, J=15.2 Hz), 7.11 (m, 2H, Ar-H); ^{13}C NMR (CDCl$_3$, 50.28 MHz), δ 25.0 (Bpin-CH_3), 65.8 (OCH_2Ph), 83.4 (Bpin-C), 126.9, 129.0, 129.6, 131.8, 137.4 (Ar-C),153.4 (PhOCH_3).
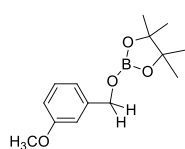
Compound 5h: product from hydroboration of 4–Hydroxybenzaldehyde. ^{1}H NMR (CDCl$_3$, 200 MHz), δ 1.18 (s, 12H, Bpin-CH_3), 4.75 (s, 2H, pinBOCH_2), 6.14 (b, 1H, Ph-OH), 6.77 (d,^3J $_{HH}$=8.4 Hz, 2H, Ar-H), 7.07 (d, ^3J $_{HH}$=8.5 Hz, 2H, Ar-H); ^{13}C NMR (CDCl$_3$, 50.28 MHz), δ 24.4 (Bpin-CH_3), 66.5 (OCH_2Ph), 83.0 (Bpin-C), 119.3, 121.4, 128.6, 130.9, 137.6, 155.3 (Ar-C).
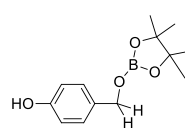
Compound 5i: product from hydroboration of 2-Hydroxybenzaldehyde. ^{1}H NMR (CDCl$_3$, 200 MHz), δ 1.18 (s, 12H, Bpin-CH_3), 4.88 (s, 2H, pinBOCH_2), 6.87 (d,^3J $_{HH}$=8.4 Hz, 2H, Ar-H), 6.34(b, 1H, Ph-OH), 7.07 (d, ^3J $_{HH}$=8.5 Hz, 2H, Ar-H); ^{13}C NMR (CDCl$_3$, 50.28 MHz), δ 25.0 (Bpin-CH_3), 72.5 (OCH_2Ph), 83.4 (Bpin-C), 121.4, 126.4, 128.8, 131.8, 138.2, 144.1 (Ar-C).
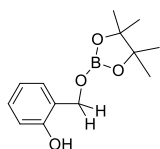
Compound 5j: product from hydroboration of 4-Nitrobenzaldehyde. ^{1}H NMR (CDCl$_3$, 200 MHz), δ 1.19 (s, 12H, Bpin-CH_3), 4.93 (s, 2H, pinBOCH_2), 7.43(d, ^3J $_{HH}$=8.6 Hz, 2H, Ar-H), 8.12(d,^3J $_{HH}$=8.9 Hz, 2H, Ar-H); ^{13}C NMR (CDCl$_3$, 50.28 MHz), δ 24.6 (Bpin-CH_3), 65.5 (OCH_2Ph), 83.4 (Bpin-C), 123.6, 125.4, 126.9, 128.3, 130.4, 137.7(Ar-C).
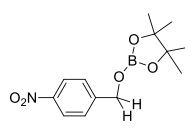
Compound 5k: product from hydroboration of 4-Cyanobenzaldehyde. ^{1}H NMR (CDCl$_3$, 200 MHz), δ 1.19 (s, 12H, Bpin-CH_3), 4.89 (s, 2H, pinBOCH_2), 7.37 (d, ^3J $_{HH}$ =8.0 Hz, 2H, Ar-H), 7.51 (d,^3J $_{HH}$=8.4 Hz, 2H, Ar-H); ^{13}C NMR (CDCl$_3$, 50.28 MHz), δ 21.7 (Bpin-CH_3), 66.2 (OCH_2Ph), 83.8 (Bpin-C), 111.6 (PhCN), 119.3, 124.6, 128.8, 132.6, 138.2, 145.1 (Ar-C).
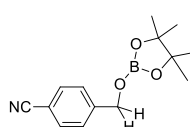
Compound 5l: product from hydroboration of 4-Fluorobenzaldehyde. ^{1}H NMR (CDCl$_3$, 200 MHz), δ 1.17 (s, 12H, Bpin-CH_3), 4.79 (s, 2H, pinBOCH_2), 6.92 (d,^3J $_{HH}$=8.9 Hz, 2H, Ar-H), 7.22 (d, ^3J $_{HH}$=7.8 Hz, 2H, Ar-H); ^{13}C NMR (CDCl$_3$, 50.28 MHz), δ 24.6 (Bpin-CH_3), 66.1 (OCH_2Ph), 83.1 (Bpin-C), 127.4, 126.9, 128.7, 132.1, 135.0, 137.7 (Ar-C).
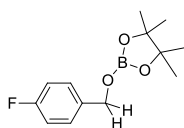
Compound 5m: product from hydroboration of Furfural. ^{1}H NMR (CDCl$_3$, 200 MHz), δ 1.18 (s, 12H, Bpin-CH_3), 4.74 (s, 2H, pinBOCH_2), 6.22(s, 1H, Ar-H), 6.72 (s, 2H, Ar-H); ^{13}C NMR (CDCl$_3$, 50.28 MHz), δ 23.5 (Bpin-CH_3), 58.1 (OCH_2Ph), 82.0 (Bpin-C), 125.8, 136.6, 141.4, 151.4 (Ar-C).
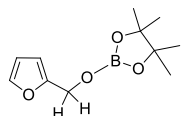
Compound 5n: product from hydroboration of 2,6-Dimethylbenzaldehyde. ^{1}H NMR (CDCl$_3$, 200 MHz), δ 1.17 (s, 12H, Bpin-CH_3), 2.34 (s, 6H, PhCH_3), 4.91 (s, 2H, pinBOCH_2), 6.93(m, 3H, Ar-H); ^{13}C NMR (CDCl$_3$, 50.28 MHz), δ 19.4, 21.1 (PhCH_3), 24.5 (Bpin-CH_3), 61.2 (OCH_2Ph), 82.7 (Bpin-C), 126.4, 127.9, 128.0, 134.9, 137.6, 137.7 (Ar-C).
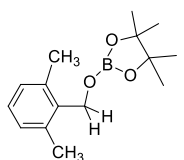
Compound 5o: product from hydroboration of trans-Cinnamaldehyde. ^{1}H NMR (CDCl$_3$, 200 MHz), δ 1.19 (s, 12H, Bpin-CH_3), 4.45 (d, 2H, ^3J=5.2 Hz, CH_2), 6.14-6.24 (m, 1H, CHCH), 6.50-6.58 (d, 1H, ^3J=15.7 Hz,ArCH), 7.22 (m, 5H, Ar-H); ^{13}C NMR (CDCl$_3$, 50.28 MHz), δ 21.1 (Bpin-CH_3), 65.1 (OCH_2Ph), 82.8 (Bpin-C), 126.3 (PhCHCH), 127.4, 128.4, 129.0, 130.5, 136.7, 137.5 (Ar-C).
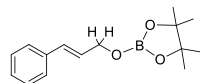
Compound 5p: product from hydroboration of Napthaldehyde. ^{1}H NMR (CDCl$_3$, 200 MHz), δ 1.19 (s, 12H, Bpin-CH_3), 5.32 (s, 2H, pinBOCH_2), 7.39 (m, 4H, Ar-H), 7.67 (m, 2H, Ar-H), 7.93 (m, 1H, Ar-H); ^{13}C NMR (CDCl$_3$, 50.28 MHz), δ 25.2 (Bpin-CH_3), 65.5 (OCH_2Ph), 83.5 (Bpin-C), 124.0, 125.4, 126.2, 126.6, 128.7, 129.1, 131.5, 134.1, 135.2, 138.2 (Ar-C).
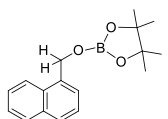
6.2.5: General procedure for catalytic hydroboration of ketones

Ketone (0.25 mmol), pinacolborane (0.25 mmol), LCaI (3 mol%) [benzene (1 mL)] were charged in Schlenk tube inside glove box. The reaction mixture was allowed to run at room temperature. The progress of the reaction was monitored by ^{1}H NMR, which indicated the

completion of the reaction by the appearance of a new CH peak. Upon completion of reaction, the solvent was removed using high vacuum in Schlenk line and mesitylene as internal standard, (0.25 mmol) was added while making the NMR in CDCl₃.

6.2.6: Spectroscopic data for aldehyde hydroboration products

Compound 6a: product from hydroboration of acetophenone. ^{1}H NMR (CDCl₃, 200 MHz), δ 1.13 (s, 6H, Bpin-CH_3), 1.16 (s, 6H, Ar-CH_3), 1.40 (d, $^3J_{HH}$=6.3 Hz, 3H, OCHCH_3), 5.18 (q, 1H, pinBOCH), 7.17 (m, 5H, Ar-H); ^{13}C NMR (CDCl₃, 50.28 MHz), δ 21.1 (Bpin-CH_3), 72.5 (OCH_2Ph), 82.6 (Bpin-C), 125.2, 127.0, 128.1, 128.3, 137.6, 144.4 (Ar-C).
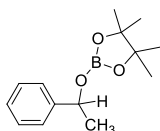
Compound 6b: product from hydroboration of 4-Methylacetophenone. ^{1}H NMR (CDCl₃, 200 MHz), δ 1.13 (s, 6H, Bpin-CH_3), 1.16 (s, 6H, Ar-CH_3), 1.38 (d, $^3J_{HH}$=6.3 Hz, 3H, OCHCH_3), 2.24 (s, 3H, PhCH_3), 5.16 (q, 1H, pinBOCH), 7.01 (d, $^3J_{HH}$=7.4 Hz, 2H, Ar-H), 7.16 (d, $^3J_{HH}$=8.6 Hz, 2H, Ar-H); ^{13}C NMR (CDCl₃, 50.28 MHz), δ 21.2 (PhCH_3), 24.5 (Bpin-CH_3), 25.9 (OCHCH_3), 72.4 (OCH_2Ph), 83.1 (Bpin-C), 125.2, 126.9, 128.3, 130.7, 137.7, 145.4 (Ar-C).

Compound 6c: product from hydroboration of 4-Methoxyacetophenone. ^{1}H NMR (CDCl₃, 200 MHz), δ 1.21 (s, 6H, Bpin-CH_3), 1.23 (s, 6H, Ar-CH_3), 1.46 (d, $^3J_{HH}$=6.4 Hz, 3H, OCHCH_3), 3.78 (s, 3H, PhOCH_3), 5.19 (q, 1H, pinBOCH), 6.87 (d, $^3J_{HH}$=8.1 Hz, 2H, Ar-H), 7.31(d, $^3J_{HH}$=8.9 Hz, 2H, Ar-H); ^{13}C NMR (CDCl₃, 50.28 MHz), δ 23.4 (Bpin-CH_3), 24.3 (OCHCH_3), 54.1 (PhOCH_3), 71.2 (OCH_2Ph), 81.6 (Bpin-C), 113.4, 125.8, 129.5, 135.7, 136.6, 157.7 (Ar-C).

Compound 6d: product from hydroboration of 4-Aminoacetophenone. ^{1}H NMR (CDCl₃, 200 MHz), δ 1.68 (s, 12H, Bpin-CH_3), 1.94 (d, $^3J_{HH}$=6.5 Hz, 3H, OCHCH_3), 4.09 (s, 2H, PhONH_2), 5.63 (q, 1H, pinBOCH), 7.11(d, $^3J_{HH}$=7.8 Hz, 2H, Ar-H), 7.61 (d, $^3J_{HH}$=8.7 Hz, 2H, Ar-H); ^{13}C NMR (CDCl₃, 50.28 MHz), 21.2 (OCHCH_3), 24.6 (Bpin-CH_3), 65.5 (OCH_2Ph), 83.4 (Bpin-C), 114.2, 123.6, 126.9, 128.3, 137.7, 146.6 (Ar-C).
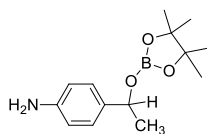
Compound 6e: product from hydroboration of 4-Nitrolacetophenone. ^{1}H NMR (CDCl$_3$, 200 MHz), δ 1.71 (s, 6H, Bpin-CH_3), 1.73 (s, 6H, Ar-CH_3), 2.02 (d, $^3J_{HH}$=6.4 Hz, 3H, OCHCH_3), 5.82 (q, 1H, pinBOCH), 7.96 (d, $^3J_{HH}$=7.7 Hz, 2H, Ar-H), 8.16 (d, $^3J_{HH}$=8.0 Hz, 2H, Ar-H); ^{13}C NMR (CDCl$_3$, 50.28 MHz), δ 21.2 (OCHCH$_3$), 24.5 (Bpin-CH$_3$), 71.7 (OCH$_2$Ph), 83.1 (Bpin-C), 122.3, 126.9, 129.3, 131.5, 133.8, 137.7 (Ar-C).
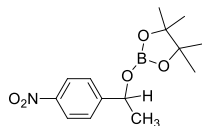
Compound 6f: product from hydroboration of 4-Bromoacetophenone. ^{1}H NMR (CDCl$_3$, 200 MHz), δ 1.12 (s, 6H, Bpin-CH_3), 1.15 (s, 6H, Ar-CH_3), 1.35 (d, $^3J_{HH}$=6.5 Hz , 3H, OCHCH_3), 5.12 (q, 1H, pinBOCH), 7.16 (d, $^3J_{HH}$=8.4 Hz, 2H, Ar-H), 7.26 (d, $^3J_{HH}$=8.6 Hz, 2H, Ar-H); ^{13}C NMR (CDCl$_3$, 50.28 MHz), δ 21.2 (OCHCH$_3$), 23.8 (Bpin-CH$_3$), 68.9 (OCH$_2$Ph), 71.2 (Bpin-C), 120.1, 126.5, 127.5, 130.5, 136.9, 142.8 (Ar-C).
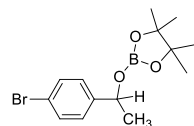
Compound 6g: product from hydroboration of Benzophenone. ^{1}H NMR (CDCl$_3$, 200 MHz), δ 1.11 (s, 12H, Bpin-CH_3), 6.12 (s, 1H, pinBOCH), 7.21 (m, 10H Ar-H); ^{13}C NMR (CDCl$_3$, 50.28 MHz), δ 20.4 (Bpin-CH$_3$), 82.2 (Bpin-C), 125.7, 126.1, 126.5, 127.5, 128.2, 132.3, 129.3, 136.9, 142.3, 143.1 (Ar-C).
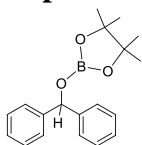
Compound 6h: product from hydroboration of 2-Chloroethylmethylketone. ^{1}H NMR (CDCl$_3$, 200 MHz), δ 1.18 (s, 12H, Bpin-CH_3), 1.40 (dd, $^3J_{HH}$=6.4 Hz, 3H, OCHCH_3), 4.19 (q, 1H, pinBOCH); ^{13}C NMR (CDCl$_3$, 50.28 MHz), δ 18.6 (CClCH$_3$), 20.0 (OCHCH$_3$), 21.7 (Bpin-CH$_3$), 61.2 (CClCH$_3$), 74.3 (BpinOCCH$_3$), 83.4 (Bpin-C).
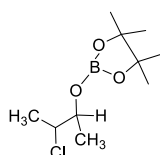
Compound 6i: product from hydroboration of 3-Hydroxyoropylmethylketone. ^{1}H NMR (CDCl$_3$, 200 MHz), δ 1.17 (s, 12H, Bpin-CH_3), 1.37 (m, 2H, HOCH$_2$CH_2), 1.39 (dd, $^3J_{HH}$=6.4 Hz, 3H, OCHCH_3), 3.85 (q, 1H, pinBOCH), 4.16 (m, 2H); ^{13}C NMR (CDCl$_3$, 50.28 MHz), δ 20.1 (OCHCH$_3$), 23.5 (Bpin-CH$_3$), 60.8 (OHCH$_2$), 66.9 (OHCH$_2$CH$_2$), 83.1 (Bpin-C).
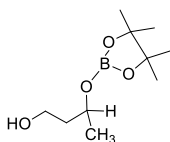
Compound 6j: product from hydroboration of Methyl isopropyl ketone. ^{1}H NMR (CDCl$_3$, 200 MHz), δ 0.79 (d, $^3J_{HH}$=2.79, 3H, EtH), 0.81(d, $^3J_{HH}$=2.8Hz, 3H, EtH), 1.04 (d, $^3J_{HH}$=6.09Hz, 3H, MeH), 1.16 (s,12 H, Bpin-CH_3), 1.56 (m, 1H, EtHCH), 3.87
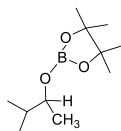
(q, 1H, pinBOC*H*); ^{13}C NMR (CDCl$_3$, 50.28 MHz), δ 18.0 (Et*C*), 21.1 (OCHC*H*$_3$), 24.4 (Bpin-*C*H$_3$), 34.3 (Et*C*HCHOBpin), 82.3 (Bpin-*C*).

6.3: Chapter 3 experimental details

6.3.1: General procedure for the cyanosilylation of aldehydes:

Aldehyde (0.25 mmol), TMSCN (0.25 mmol), LCaI (2 mol%)(**3**) [toluene (1 mL)] were charged in Schlenk tube inside glove box. The reaction mixture was allowed to run at room temperature. The progress of the reaction was monitored by ^{1}H NMR, which indicated the completion of the reaction by the disappearance of the aldehyde proton and appearance of a new CH peak. Upon completion of reaction, the solvent was removed using high vacuum in Schlenk line and mesitylene (0.25 mmol) as internal standard, was added while performing the NMR in CDCl$_3$.

6.3.2: Spectroscopic data for cyanosilylated product of aldehydes:

Compound 8a: ^{1}H NMR (200 MHz, CDCl$_3$, ppm): δ 0.13 (s, 9H, Si(C*H*$_3$)$_3$), 5.38 (s, 1H, C*H*OSi(CH$_3$)$_3$), 7.27–7.38 (m, 5H, Ph); ^{13}C NMR (50.28 MHz, CDCl$_3$, ppm): δ -0.3 (Si(*C*H$_3$)$_3$), 63.5 (*C*HOSi(CH$_3$)$_3$), 119.1 (*C*N), 126.2, 126.8, 128.8, 129.2, 136.2, 137.5 (*C*Ar).
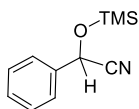
Compound 8b: ^{1}H NMR (200 MHz, CDCl$_3$, ppm): δ 0.16 (s, 9H, Si(C*H*$_3$)$_3$), 2.30 (s, 3H, PhC*H*$_3$), 5.38 (s, 1H, C*H*OSi(CH$_3$)$_3$), 7.16 (d, $^3J_{H,H}$=8.1 Hz, 2H, Ph), 7.27(d, $^3J_{H,H}$ =8.1 Hz, 2H, Ph); ^{13}C NMR (50.28 MHz, CDCl$_3$, ppm): δ -0.3 (Si(*C*H$_3$)$_3$), 21.1 (Ph*C*H$_3$), 63.4 (*C*HOSi(CH$_3$)$_3$), 119.2 (*C*N), 126.3, 126.8, 129.5, 133.3, 137.6, 139.2 (*C*Ar).
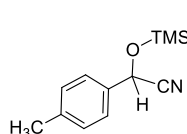
Compound 8c: ^{1}H NMR (200 MHz, CDCl$_3$, ppm): δ 0.19 (s, 9H, Si(C*H*$_3$)$_3$), 5.69 (s, 1H, C*H*OSi(CH$_3$)$_3$), 7.17 (t, $^3J_{H,H}$=7.5 Hz, 1H, Ph), 7.33 (t, $^3J_{H,H}$=7.6 Hz, 1H, Ph), 7.47 (d, $^3J_{H,H}$=7.6 Hz, 1H, Ph), 7.67 (d, $^3J_{H,H}$=7.7 Hz, 1H, Ph); ^{13}C NMR (50.28 MHz, CDCl$_3$, ppm): δ -0.3 (Si(*C*H$_3$)$_3$), 63.1 (*C*HOSi(CH$_3$)$_3$), 118.2 (*C*N), 121.6, 128.0, 128.5, 130.7, 132.9, 137.5 (*C*Ar).
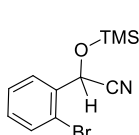
Compound 8d: ^{1}H NMR (200 MHz, CDCl$_3$, ppm): δ 0.17 (s, 9H, Si(C*H*$_3$)$_3$), 5.37 (s, 1H, C*H*OSi(CH$_3$)$_3$), 7.19 (t, $^3J_{H,H}$=7.8 Hz, 1H, Ph), 7.29 (d, $^3J_{H,H}$=7.9 Hz, 1H, Ph),
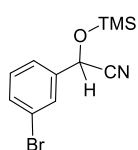
7.41(d, $^3J_{H,H}$=7.6 Hz, 1H, Ph), 7.54 (s, 1H, Ph), ^{13}C NMR (50.28 MHz, CDCl$_3$, ppm): δ -0.3 (Si(CH_3)$_3$), 62.7 (CHOSi(CH$_3$)), 118.5 (CN), 122.8, 124.7, 129.2, 130.4, 132.3, 137.5 (CAr).

Compound 8e: ^{1}H NMR (200 MHz, CDCl$_3$, ppm): δ 0.16 (s, 9H, Si(CH_3)$_3$), 5.37 (s, 1H, CHOSi(CH$_3$)$_3$), 7.31-7.35 (m, 4H, Ph); ^{13}C NMR (50.28 MHz, CDCl$_3$, ppm): δ -0.3 (Si(CH_3)$_3$), 62.8 (CHOSi(CH$_3$)$_3$), 118.7 (CN), 126.8, 127.6, 129.0, 134.7, 135.2, 137.5 (CAr).
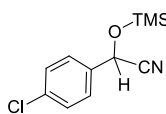
Compound 8f: ^{1}H NMR (200 MHz, CDCl$_3$, ppm): δ 0.13 (s, 9H, Si(CH_3)$_3$), 3.72 (s, 3H, PhOCH_3), 5.35 (s, 1H, CHOSi(CH$_3$)$_3$), 6.81-6.86 (d, $^3J_{H,H}$= 8.2 Hz, 2H, Ph), 7.22-7.33 (d, $^3J_{H,H}$=8.3 Hz, 2H, Ph); ^{13}C NMR (50.28 MHz, CDCl$_3$, ppm): δ -0.3 (Si(CH_3)$_3$), 55.1 (PhOCH_3), 63.2 (CHOSi(CH$_3$)$_3$), 119.2 (CN), 126.8, 127.8, 128.4, 131.8, 137.5, 160.2 (CAr).
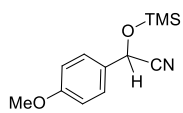
Compound 8g: ^{1}H NMR (200 MHz, CDCl$_3$, ppm): δ 0.22 (s, 9H, Si(CH_3)$_3$, 5.54 (s, 1H, CHOSi(CH$_3$)$_3$), 7.62 (d, $^3J_{H,H}$=8.8 Hz, 2H, Ph), 8.22 (d, $^3J_{H,H}$=8.4 Hz, 2H, Ph); ^{13}C NMR (50.28 MHz, CDCl$_3$, ppm): δ -0.4 (Si(CH_3)$_3$), 62.5 (CHOSi(CH$_3$)$_3$), 118.0 (CN), 124.0, 126.7, 127.0, 137.5, 142.8, 148.3 (CAr).
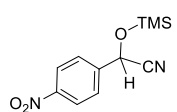
Compound 8h: ^{1}H NMR (200 MHz, CDCl$_3$, ppm): δ 0.18 (s, 9H, Si(CH_3)$_3$, 5.46 (s, 1H, CHOSi(CH$_3$)$_3$), 7.52 (d, $^3J_{H,H}$=7.5 Hz, 2H, Ph), 7.59 (d, $^3J_{H,H}$=7.6 Hz, 2H, Ph); ^{13}C NMR (50.28 MHz, CDCl$_3$, ppm): δ -0.4 (Si(CH_3)$_3$), 62.75 (CHOSi(CH$_3$)$_3$), 113.2 (PhCN), 118.0 (CN), 126.8, 127.1, 129.8, 133.6, 137.6, 141.0 (CAr).
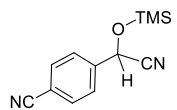
Compound 8i: ^{1}H NMR (200 MHz, CDCl$_3$, ppm): δ 0.15 (s, 9H, Si(CH_3)$_3$, 5.38 (s, 1H, CHOSi(CH$_3$)$_3$), 7.01 (m, 2H, Ph), 7.36 (d, 2H, Ph); ^{13}C NMR (50.28 MHz, CDCl$_3$, ppm): δ -0.2 (Si(CH_3)$_3$), 62.1 (CHOSi(CH$_3$)$_3$), 118.3 (CN), 123.4, 126.8, 128.6, 133.8, 134.9, 137.5(CAr).
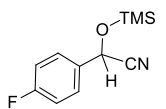
Compound 8j: ^{1}H NMR (200 MHz, CDCl$_3$, ppm): δ 0.18 (s, 9H, Si(CH_3)$_3$, 5.04 (d, $^3J_{H,H}$=6.2 Hz, 1H, CHOSi(CH$_3$)$_3$), 6.05 (dd, $^3J_{H,H}$=6.2 Hz, 1H, CHCHOSi(CH$_3$)$_3$), 6.72 (d, $^3J_{H,H}$=16.0 Hz, 1H, PhCHCH), 7.23-7.30 (m, 5H, Ph); ^{13}C NMR (50.28 MHz,

CDCl$_3$, ppm): δ -0.4 (Si(CH_3)$_3$), 62.9 (CHOSi(CH$_3$)$_3$), 115.6, 116.0 (PhCHCH), 118.9 (CN), 126.8, 128.1, 132.2, 137.5, 160.6, 165.5 (CAr).
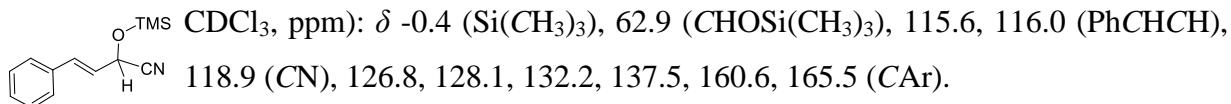
Compound 8k: ^{1}H NMR (200 MHz, CDCl$_3$, ppm): δ 0.11 (s, 9H, Si(CH_3)$_3$, 5.95 (s, 1H, CHOSi(CH$_3$)$_3$), 7.37-7.63 (m, 4H, Ph), 7.78 (d, $^3J_{H,H}$=7.5 Hz, 2H, Ph), 8.07 (d, $^3J_{H,H}$=8.0 Hz, 1H, Ph); ^{13}C NMR (50.28 MHz, CDCl$_3$, ppm): δ -0.2 (Si(CH_3)$_3$), 62.6 (CHOSi(CH$_3$)$_3$), 119.0 (CN), 123.1, 125.0, 125.3, 126.2, 126.8, 128.8, 130.3, 131.3, 133.9, 137.5 (CAr).
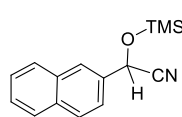
Compound 8l: ^{1}H NMR (200 MHz, CDCl$_3$, ppm): δ 0.21 (s, 9H, Si(CH_3)$_3$, 5.44 (s, 1H, CHOSi(CH$_3$)$_3$), 7.35 (m, 2H, Ph), 8.58 (m, 2H, Ph); ^{13}C NMR (50.28 MHz, CDCl$_3$, ppm): δ -0.4 (Si(CH_3)$_3$), 62.2 (CHOSi(CH$_3$)$_3$), 117.9 (CN), 120.5, 126.8, 137.6, 144.9, 150.2 (CAr).
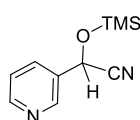
Compound 8m: ^{1}H NMR (200 MHz, CDCl$_3$, ppm): δ 0.28 (s, 9H, Si(CH_3)$_3$, 5.61 (s, 1H, CHOSi(CH$_3$)$_3$), 7.46 (m, 1H, CH), 6.61 (d, $^3J_{H,H}$=3.2 Hz, 1H, CH), 7.53 (m, 1H, CH); ^{13}C NMR (50.28 MHz, CDCl$_3$, ppm): δ -0.4 (Si(CH_3)$_3$), 57.4 (CHOSi(CH$_3$)$_3$), 109.6 (CH), 110.7 (CH), 117.0 (CN), 137.6, 143.8 (CH).
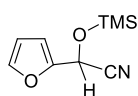
Compound 8n: ^{1}H NMR (200 MHz, CDCl$_3$, ppm): δ 0.24 (s, 9H, Si(CH_3)$_3$, 2.19 (s, 3H, NCOCH_3), 5.50 (s, 1H, CHOSi(CH$_3$)$_3$), 7.39 (d, $^3J_{H,H}$=8.4 Hz, 2H, Ph), 7.66 (d, , $^3J_{H,H}$=8.3 Hz, 2H, Ph); ^{13}C NMR (50.28 MHz, CDCl$_3$, ppm): δ -0.5 (Si(CH_3)$_3$), 24.0 (NHCOCH_3), 63.0 (CHOSi(CH$_3$)$_3$), 67.6 (NHCOCH$_3$), 119.0 (CN), 119.9, 126.5, 130.7, 131.4, 137.3, 138.7 (CAr).
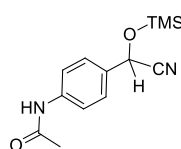
Compound 8o: ^{1}H NMR (200 MHz, CDCl$_3$, ppm): δ 0.28 (s, 9H, Si(CH_3)$_3$, 5.53 (s, 1H, CHOSi(CH$_3$)$_3$), 7.39 (m, 2H, Ph), 7.55 (d, 2H, Ph); ^{13}C NMR (50.28 MHz, CDCl$_3$, ppm): δ -0.3 (Si(CH_3)$_3$), 62.9 (CHOSi(CH$_3$)$_3$), 118.9 (CN), 122.0, 126.8, 127.4, 137.7, 137.5, 151.2 (CAr).
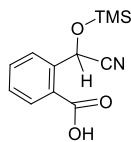
6.3.3: General procedure for the cyanosilylation of ketones

Ketone (0.25 mmol), TMSCN (0.25 mmol), LCaI (3 mol%)(**3**) [THF (1 ml)] were charged in Schlenk tube inside glove box. The reaction mixture was allowed to run at room temperature. The progress of the reaction was monitored by ^{1}H NMR, the methyl protons shifted upfield.

Upon completion of reaction, the solvent was removed using high vacuum and mesitylene (0.25 mmol) as internal standard, was added while performing the NMR in CDCl$_3$.
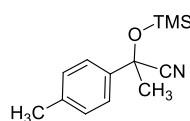
6.3.4: Spectroscopic data for cyanosilylated product of ketones

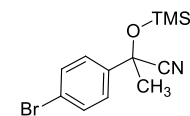**Compound 9a**: ^{1}H NMR (200 MHz, CDCl$_3$, ppm): δ 0.26 (s, 9H, Si(CH_3)$_3$), 1.94 (s, 3H, PhCCH_3), 7.42-7.66 (m, 5H, Ph); ^{13}C NMR (50.28 MHz, CDCl$_3$, ppm): δ 0.9 (Si(CH$_3$)$_3$), 33.4 (PhCCH$_3$), 67.9 (COSi(CH$_3$)$_3$), 121.5 (CN), 124.5, 126.8, 128.8, 133.0, 137.6, 141.9 (CAr).
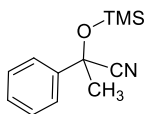
Compound 9b: ^{1}H NMR (200 MHz, CDCl$_3$, ppm): δ 0.23 (s, 9H, Si(CH_3)$_3$), 1.90 (s, 3H, PhCCH_3), 2.42 (s, 3H, PhCCH_3), 7.23-7.33 (d, $^3J_{H,H}$=6.4 Hz, 2H, Ph), 7.47-7.51 (d, $^3J_{H,H}$=8.0 Hz, 1H, Ph), 7.91 (d, $^3J_{H,H}$=8.5 Hz, 1H, Ph); ^{13}C NMR (50.28 MHz, CDCl$_3$, ppm): δ 0.9 (Si(CH$_3$)$_3$), 26.4 (PhCH$_3$), 33.4 (PhCCH$_3$), 71.4 (COSi(CH$_3$)$_3$), 121.6 (CN), 124.5, 126.8, 128.4, 129.1, 137.6, 143.9 (CAr).

Compound 9c: ^{1}H NMR (200 MHz, CDCl$_3$, ppm): δ 0.24 (s, 9H, Si(CH_3)$_3$), 1.86 (s, 3H, PhCCH_3), 7.43-7.59 (m, 4H, Ph); ^{13}C NMR (50.28 MHz, CDCl$_3$, ppm): δ 0.9 (Si(CH$_3$)$_3$), 33.4 (PhCCH$_3$), 69.7 (COSi(CH$_3$)$_3$), 121.1 (CN), 122.6, 126.3, 129.7, 131.7, 137.6, 141.2 (CAr).

Compound 9d: ^{1}H NMR (200 MHz, CDCl$_3$, ppm): δ 0.28 (s, 9H, Si(CH_3)$_3$), 1.92 (s, 3H, PhCCH_3), 7.63 (t, $^3J_{H,H}$=7.9 Hz, 1H, Ph), 7.90 (d, $^3J_{H,H}$=8.0 Hz, 1H, Ph), 8.23 (d, $^3J_{H,H}$=7.9 Hz, 1H, Ph), 8.43 (d, $^3J_{H,H}$=7.8 Hz, 1H, Ph); ^{13}C NMR (50.28 MHz, CDCl$_3$, ppm): δ 0.9 (Si(CH$_3$)$_3$), 33.2 (PhCCH$_3$), 67.9 (COSi(CH$_3$)$_3$), 119.7 (CN), 123.5, 129.8, 130.5, 137.5, 144.4, 148.3 (CAr).
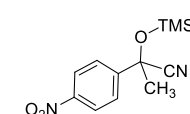
Compound 9e: ^{1}H NMR (200 MHz, CDCl$_3$, ppm): δ 0.21 (s, 9H, Si(CH_3)$_3$), 1.82 (s, 3H, PhCCH_3), 3.85 (s, 1H, PhOCH_3), 6.92 (d, $^3J_{H,H}$=8.8 Hz, 2H, Ph), 7.49 (d, $^3J_{H,H}$=9.2 Hz, 2H, Ph); ^{13}C NMR (50.28 MHz, CDCl$_3$, ppm): δ 0.9 (Si(CH$_3$)$_3$), 25.5 (PhOCH$_3$), 33.3 (PhCCH$_3$), 71.1 (COSi(CH$_3$)$_3$), 121.7 (CN), 125.9, 126.4, 129.9, 130.5, 130.2, 133.9 (CAr).
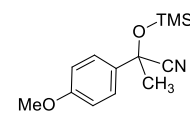
Compound 9f: ^{1}H NMR (200 MHz, CDCl$_3$, ppm): δ 0.05 (s, 9H, Si(CH_3)$_3$), 1.77 (m, 2H, PhCCH_2CH$_3$), 1.87 (m, 3H, PhCCH$_2$CH_3), 7.27-7.45 (m, 5H, Ph); ^{13}C NMR
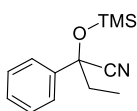
(50.28 MHz, CDCl$_3$, ppm): δ 0.8 (Si(CH_3)$_3$), 25.5 (PhCCH_2CH_3), 33.2 (PhCCH_2CH_3), 68.1 (COSi(CH$_3$)$_3$), 120.7 (CN), 125.0, 126.4, 128.4, 129.9, 132.2, 140.8 (CAr).

Compound 9g: ^{1}H NMR (200 MHz, CDCl$_3$, ppm): δ 0.10 (s, 9H, Si(CH_3)$_3$), 7.26-7.33 (m, 5H, Ph), 7.45-7.54 (m, 4H, Ph), 7.74-778 (m, 1H, Ph), 8.43 (d, $^3J_{H,H}$ =7.8 Hz, 1H, Ph); ^{13}C NMR (50.28 MHz, CDCl$_3$, ppm): δ 0.9 (Si(CH_3)$_3$), 67.8 (COSi(CH$_3$)$_3$), 120.6 (CN), 125.7, 126.7, 128.1, 128.4, 128.5, 129.9, 132.3, 137.4, 137.5, 141.8 (CAr).
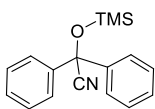
6.3.5: Characterization and isolation of intermediate

1 mmol of catalyst (LCaI; **3**) and 1 mmol of TMSCN were charged in Schlenk tube with 1ml of THF as reaction solvent. After 30 min., 0.5 ml of reaction mixture was submitted for NMR spectroscopy. In ^{1}H NMR, the development of new TMS peak at δ 0.06 ppm was observed along with free TMSCN peak at 0.23 ppm. ^{13}C NMR spectrum also changed with new peaks appearing at δ 1.59 and 127.43 ppm along with free TMSCN peak at −1.95 and 127.62 ppm. In ^{29}Si NMR, new peak developed at δ 7.39 ppm with free TMSCN peak at −11.63 ppm. The reaction mixture was further kept under vacuum for 1h and again submitted for NMR spectroscopy. The free TMSCN peak disappeared from ^{1}H, ^{13}C and ^{29}Si NMR and clean intermediate NMR spectra were observed.

6.3.6: Details of DFT calculations

All the calculations in this study have been performed with density functional theory (DFT), with the aid of the Turbomole 7.1 suite of programs, using the PBE functional. The QZVP basis set has been employed. The resolution of identity (RI), along with the multipole accelerated resolution of identity (marij) approximations have been employed for an accurate and efficient treatment of the electronic Coulomb term in the DFT calculations. Dispersion corrections (disp3) and solvent corrections have been incorporated with optimization calculations using the COSMO model, with chloroform (ε=4.8) as the solvent. The values reported are ΔG values, with zero point energy corrections, internal energy and entropic contributions included through frequency calculations on the optimized minima, with the temperature taken to be 298.15 K. Harmonic

frequency calculations were performed for all stationary points to confirm them as a local minima or transition state structures.

6.4: Chapter 4 experimental details

6.4.1: Synthesis and experimental details of complex 10 and 11

Synthesis of complex 10:

THF (30 mL) was added to a mixture of ligand (1.05 g, 3 mmol) and KN(SiMe$_3$)$_2$ (0.60 g, 3 mmol). The reaction mixture was stirred for 1 hour, after that it was transferred to another flask containing MgI$_2$ (0.42 g, 1.5 mmol) in 10 mL of THF and the resulting mixture was stirred overnight. The volatile was removed under vacuum and highly soluble homoleptic complexes were extracted with hexane. Crystallization was done in concentrated solution of hexane at –4 °C to give reddish yellow crystals of **10** (79%). ^{1}H NMR (200 MHz, CDCl$_3$, 25 °C): δ 8.69 (d, $^3J_{HH}$=5.1 Hz, 2H, Py-*H*), 7.83 (td, $^3J_{HH}$=7.8 Hz and $^4J_{HH}$=1.6 Hz, 2H, Py-*H*), 7.35-7.51 (m, 6H, Py-*H*), 7.19-7.31 (m, 6H, Ar-*H*), 4.96 (s, 2H, MeC(N)C*H*), 4.77 (s, 4H, NC*H$_2$*), 3.07 (sep, *J*=6.86 Hz, 4H, ArC*H*Me$_2$), 2.17 (s, 6H, *Me*C), 1.87 (s, 6H, *Me*C), 1.38 (d, $^3J_{HH}$=7.1 Hz, 12H, ArCH*Me$_2$*), 1.26 (d, $^3J_{HH}$=7.0 Hz, 12H, ArCH*Me$_2$*); ^{13}C NMR (100.6 MHz, CDCl$_3$, 25 °C): δ 165.4, 160.0, 155.2 (imine-*C* and Py-*C*), 149.2, 146.4, 137.9, 136.8, 128.3, 122.7, 121.9, 120.4 (Ar-*C* and Py-*C*), 94.4 (MeC(N)*C*H), 48.7 (N*C*H$_2$), 28.0 (Ar*C*HMe$_2$), 23.7 (ArCH*Me$_2$*), 22.9 (ArCH*Me$_2$*), 21.7 (*Me*C), 19.2 (*Me*C). Anal. Calcd for C$_{46}$H$_{66}$N$_6$Mg (727.36): C, 75.96; H, 9.15. Found: C, 74.97; H, 8.52; ESI-HRMS: calcd. for C$_{46}$H$_{67}$N$_6$Mg [M+H]$^+$= 727.5272; found: 727.4588.

Synthesis of complex 11:

Method a) THF (30 mL) was added to a mixture of ligand (1.05 g, 3 mmol) and KN(SiMe$_3$)$_2$ (0.60 g, 3 mmol). The reaction mixture was stirred for 1 hour, after that it was transferred to another flask containing CaI$_2$ (0.44 g, 1.5 mmol) in 10 mL of THF and the resulting mixture was stirred overnight. The volatile was removed under vacuum and highly soluble homoleptic complexes were extracted with hexane. Crystallization was done in concentrated solution of hexane at −4 °C to give yellow crystals of **11** (65%).

Method b) THF (30 mL) was added to a mixture of ligand (1.05 g, 3 mmol) and Ca[N(SiMe$_3$)$_2$]$_2$ (0.54 g, 1.5 mmol). The resulting brown color solution was stirred overnight. It was filtered through celite and the volatile was removed under vacuum. Single crystals suitable for XRD

were grown from the concentrated solution of hexane at -4 °C which afforded yellow crystals of **11** (74%). ^{1}H NMR (200 MHz, CDCl$_3$, 25 °C): δ 8.52 (d, $^3J_{HH}$=4.7 Hz, 2H, Py-*H*), 7.64 (td, $^3J_{HH}$=7.7 Hz and $^4J_{HH}$=2.1 Hz, 2H, Py-*H*), 7.27-7.32 (m, 6H, Py-*H*), 7.02-7.09 (m, 6H, Ar-*H*), 4.78 (s, 2H, MeC(N)C*H*), 4.59 (s, 4H, NC*H$_2$*), 2.92 (sep, *J*=6.74 Hz, 4H, ArC*H*Me$_2$), 1.99 (s, 6H, *Me*C), 1.68 (s, 6H, *Me*C), 1.20 (d, $^3J_{HH}$=7.1 Hz, 12H, ArCH*Me$_2$*), 1.07 (d, $^3J_{HH}$=7.0 Hz, 12H, ArCH*Me$_2$*). Anal. Calcd for C$_{46}$H$_{66}$N$_6$Ca (743.13): C, 74.35; H, 8.95; Found: C, 74.48; H, 8.87; ESI-HRMS: calcd. for C$_{46}$H$_{67}$N$_6$Ca [M+H]$^+$=743.5048; found: 743.4993

6.4.2: Crystal structure details of complex 10 and 11

Crystal data of 10: CCDC 1836442. C$_{46}$H$_{60}$MgN$_6$, 1.5(C$_6$H$_{10}$), M=850.56, pale pink plate, 0.31 x 0.22 x 0.06 mm^3, triclinic, space group *P-1*, *a*=15.3738(7) Å, 15.4978(7) Å, *c*=22.9087(11)Å, α=76.035(2)°, β=75.845(2)°, δ=71.315(2)°, *V*=4934.0(4)Å^3, *Z*=4, *T*=100(2) K, 2θ_{max}=50.00°, D_{calc} (g cm^{-3})=1.145, F(*000*)=1860, μ (mm^{-1})=0.078, 99063 reflections collected, 17328 unique reflections (R_{int}=0.0397), 15532 observed (*I* > 2σ (*I*)) reflections, multi-scan absorption correction, T_{min}=0.976, T_{max}=0.995, 1091 refined parameters, S=1.024, R1=0.0652, wR2= 0.1768 (all data R=0.0699, wR2=0.1801), maximum and minimum residual electron densities; $\Delta\rho_{max}$=1.124, $\Delta\rho_{min}$= –0.581 (eÅ^{-3}).

Crystal data of 11: CCDC 1836447. M=808.21, colorless block, 0.22 x 0.16 x 0.06 mm^3, monoclinic, space group *C2/c*, *a*=13.8404(5) Å, *b*=24.8889(7) Å, *c*=13.2292(4) Å, β=98.6200(10), *V*=4505.6(2) Å^3, *Z*=4, *T*=100(2) K, 2θ_{max}=50.00°, D_{calc}(g cm^{-3})=1.191, F(*000*)=1756, μ (mm^{-1})=0.181, 38181 reflections collected, 4398 unique reflections (R_{int}=0.0220), 4311 observed (*I* > 2σ (*I*)) reflections, multi-scan absorption correction, T_{min}=0.961, T_{max}=0.989, 247 refined parameters, 153 restraints, S=1.095, R1=0.0337, wR2=0.0860 (all data R =0.0341, wR2=0.0863), maximum and minimum residual electron densities; $\Delta\rho_{max}$=0.254, $\Delta\rho_{min}$= –0.189 (eÅ^{-3}).
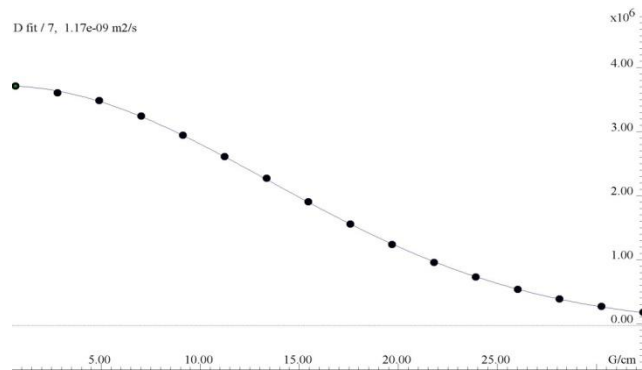
6.4.3: DOSY NMR of complex 11

DOSY (diffusion ordered spectroscopy) plot. Shows log (diffusion coefficient) on vertical axis. The two THF signals show higher diffusion coefficients, indicating THF molecules are moving much faster than the solute.
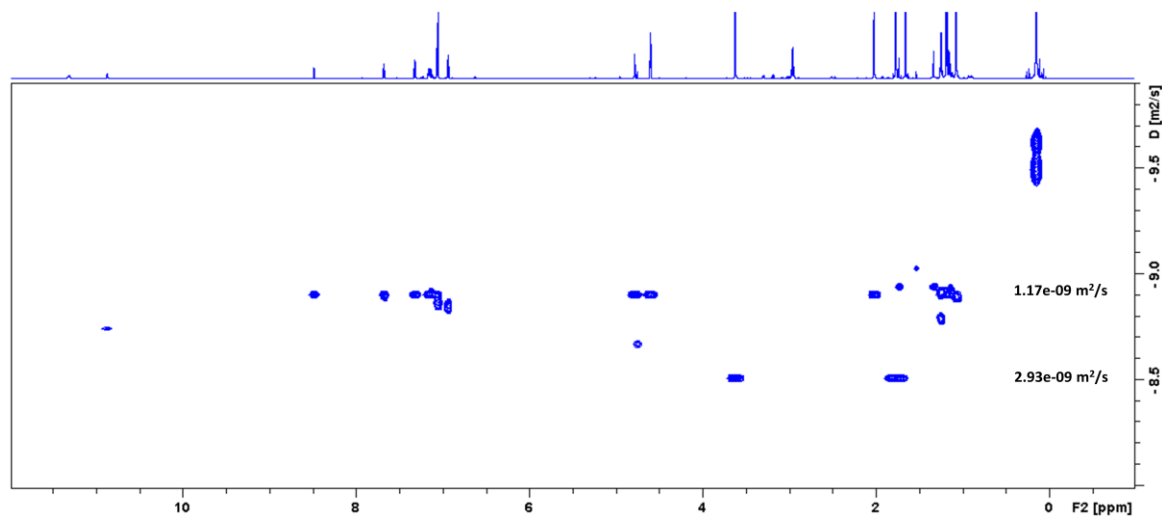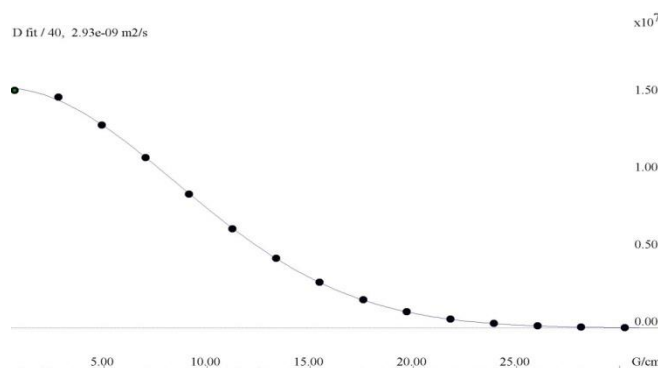

Representative fits (signal attenuation vs gradient strength, Gauss/cm)
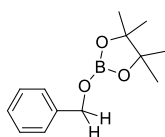
1Signal at 7.667ppm
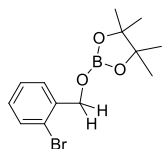

THF signal

~ 3.6ppm

6.4.4: Spectroscopic data for hydroborated product of aldehydes

Compound 12a: product from hydroboration of benzaldehyde. ^{1}H NMR (CDCl$_3$, 200 MHz), δ 1.18 (s, 12H, Bpin-CH_3), 4.85 (s, 2H, pinBOCH_2), 7.11-7.27 (m, 5H, Ar-H); ^{13}C NMR (CDCl$_3$, 50.28 MHz), δ 24.5 (Bpin-CH$_3$), 66.6 (OCH$_2$Ph), 82.8 (Bpin-C), 126.6, 126.8, 127.3, 128.2, 137.6, 139.1 (Ar-C)

Compound 12b: product from hydroboration of 2-Bromobenzaldehyde. ^{1}H NMR (CDCl$_3$, 200 MHz), δ 1.18 (s, 12H, Bpin-CH_3), 4.78 (s, 2H, pinBOCH_2), 7.11-7.15 (m, 2H, Ar-H), 7.34-7.38 (m, 2H, Ar-H); ^{13}C NMR (CDCl$_3$, 50.28 MHz), δ 24.5 (Bpin-CH$_3$), 65.8 (OCH$_2$Ph), 83.0 (Bpin-C), 121.1, 128.3, 131.3, 132.3, 137.6, 138.1 (Ar-C).

Compound 12c: product from hydroboration of 4-Bromobenzaldehyde. ^{1}H NMR (CDCl$_3$, 200 MHz), δ 1.17 (s, 12H, Bpin-CH_3), 4.78 (s, 2H, pinBOCH_2), 7.15 (d, $^3J_{HH}$=8.1 Hz, 2H, Ar-H), 7.34 (d, $^3J_{HH}$=8.5Hz, 2H, Ar-H); ^{13}C NMR (CDCl$_3$, 50.28 MHz), δ 24.5 (Bpin-CH$_3$), 65.8 (OCH$_2$Ph), 83.0 (Bpin-C), 121.1, 126.8, 128.3, 137.6, 138.1, 136.9 (Ar-C).
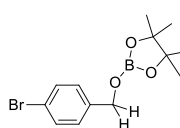
Compound 12d: product from hydroboration of 4-Nitrobenzaldehyde. ^{1}H NMR (CDCl$_3$, 200 MHz), δ 1.20 (s, 12H, Bpin-CH_3), 4.94 (s, 2H, pinBOCH_2), 7.39 (d, $^3J_{HH}$=9.2 Hz, 2H, Ar-H), 8.13 (d, $^3J_{HH}$=8.8 Hz, 2H, Ar-H); ^{13}C NMR (CDCl$_3$, 50.28 MHz), δ 24.5 (Bpin-CH$_3$), 65.4 (OCH$_2$Ph), 83.3 (Bpin-C), 123.5, 126.8, 126.2, 137.6, 146.5, 147.1 (Ar-C).
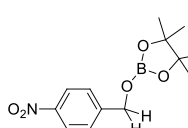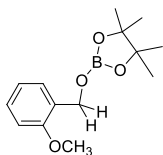
Compound 12e: product from hydroboration of 4-Cyanobenzaldehyde. ^{1}H NMR (CDCl$_3$, 200 MHz), δ 1.19 (s, 12H, Bpin-CH_3), 4.89 (s, 2H, pinBOCH_2), 7.37 (d, $^3J_{HH}$=7.7 Hz, 2H, Ar-H), 7.51 (d, 3J_{HH}=8.3 Hz, 2H, Ar-H); ^{13}C NMR (CDCl$_3$, 50.28 MHz), δ 24.4 (Bpin-CH$_3$), 65.6 (OCH$_2$Ph), 83.2 (Bpin-C), 111.0 (PhCN), 118.7, 126.8, 128.2, 132.0, 137.5, 144.4 (Ar-C). The product was further acid hydrolyzed to its corresponding alcohol; yield: 76%. ^{1}H NMR (CDCl$_3$, 200 MHz): δ 2.04 (s, 1H, OH), 4.77 (s, 2H, CH_2), 7.50-7.46 (d, $^3J_{HH}$=8.59 Hz, 2H, ArH), 7.63-7.67 (d, $^3J_{H\text{-}H}$ =8.34 Hz, 2H, ArH) ppm; ^{13}C NMR (CDCl$_3$, 50.28
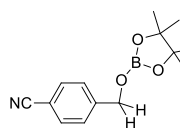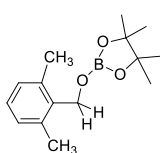
MHz): δ 64.2 (CH$_2$), 118.8 (CN), 111.3, 126.9, 128.1, 129.4, 132.2, 143.2 (Ar-C) ppm.

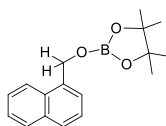**Compound 12f:** product from hydroboration of 2-Methoxylbenzaldehyde. ^{1}H NMR (CDCl$_3$, 200 MHz), δ 1.17 (s, 12H, Bpin-CH_3), 3.69 (s, 3H, Ar-OCH_3), 4.90 (s, 2H, pinBOCH_2), 6.81-7.34 (m, 5H, Ar-H) ; ^{13}C NMR (CDCl$_3$, 50.28 MHz), δ 24.5 (Bpin-CH$_3$), 55.0 (PhOCH$_3$), 62.2 (OCH$_2$Ph), 82.7 (Bpin-C), 109.7, 120.2, 126.8, 128.1, 137.6, 156.4 (Ar-C).

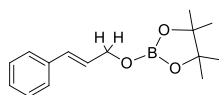**Compound 12g:** product from hydroboration of 2,6-Dimethylbenzaldehyde. ^{1}H NMR (CDCl$_3$, 200 MHz), δ 1.17 (s, 12H, Bpin-CH_3), 2.33 (s, 6H, PhCH_3), 4.91 (s, 2H, pinBOCH_2), 6.93-7.11(m, 3H, Ar-H); ^{13}C NMR (CDCl$_3$, 50.28 MHz), δ 19.4, (PhCH$_3$), 24.5 (Bpin-CH$_3$), 61.3 (OCH$_2$Ph), 82.7 (Bpin-C), 127.9, 128.0, 129.6, 134.8, 137.6, 137.7 (Ar-C).

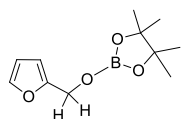**Compound 12h:** product from hydroboration of Napthaldehyde. ^{1}H NMR (CDCl$_3$, 200 MHz), δ 1.19 (s, 12H, Bpin-CH_3), 5.33 (s, 2H, pinBOCH_2), 7.31-7.55 (m, 4H, Ar-H), 7.67-7.79 (m, 2H, Ar-H), 7.94-7.98 (m, 1H, Ar-H); ^{13}C NMR (CDCl$_3$, 50.28 MHz), δ 24.5 (Bpin-CH$_3$), 64.9 (OCH$_2$Ph), 82.9 (Bpin-C), 123.3, 124.7, 125.2, 125.2, 125.5, 128.4, 130.8, 133.5, 134.5, 137.6 (Ar-C).

Compound 12i: product from hydroboration of trans-Cinnamaldehyde. ^{1}H NMR (CDCl$_3$, 200 MHz), δ 1.19 (s, 12H, Bpin-CH_3), 4.47 (d, 2H, ^{3}J=5.2 Hz, CH_2), 6.16-6.26 (m, 1H, CHCH), 6.51-6.59 (d, 1H, ^{3}J=15.7 Hz, ArCH), 7.13-7.45 (m, 5H, Ar-H); ^{13}C NMR (CDCl$_3$, 50.28 MHz), δ 24.5 (Bpin-CH$_3$), 65.2 (OCH$_2$Ph), 82.8 (Bpin-C), 126.3, 126.7 (PhCHCH), 128.4, 129.0, 130.5, 131.1, 136.8, 137.6 (Ar-C).
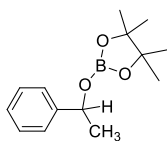
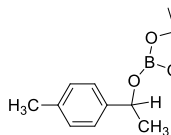**Compound 12j:** product from hydroboration of Furfural. ^{1}H NMR (CDCl$_3$, 200 MHz), δ 1.17 (s, 12H, Bpin-CH_3), 4.74 (s, 2H, pinBOCH_2), 6.21(s, 1H, Ar-H), 7.26 (s, 2H, Ar-H); ^{13}C NMR (CDCl$_3$, 50.28 MHz), δ 24.4 (Bpin-CH$_3$), 59.1 (OCH$_2$Ph), 82.9 (Bpin-C), 108.2, 110.1, 137.6, 142.3 (Ar-C).

**6.4.5: Spectroscopic data for hydroborated product of ketones**

Compound 13a: product from hydroboration of acetophenone. ^{1}H NMR (CDCl$_3$, 200 MHz), δ 1.13-1.16 (d, ^3J $_{HH}$=5.7Hz 12H, Bpin-CH_3), 1.40-1.43 (d, ^3J $_{HH}$=5.4 Hz, 3H, OCHCH_3), 5.19 (q, J=6.21 Hz, 1H, pinBOCH), 7.11-7.27 (m, 5H, Ar-H); ^{13}C NMR (CDCl$_3$, 50.28 MHz), δ 24.4 (Bpin-CH$_3$), 25.3 (BpinOCCH$_3$), 72.5 (OCH$_2$Ph), 82.6 (Bpin-C), 125.2, 128.1, 128.2, 133.0, 137.6, 144.5 (Ar-C).
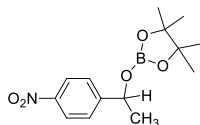
Compound 13b: product from hydroboration of 4-Methylacetophenone. ^{1}H NMR (CDCl$_3$, 200 MHz), δ 1.13 (s, 6 H, Bpin-CH_3), 1.16 (s, 6H, Ar-CH_3), 1.39-1.42 (d, ^3J $_{HH}$=6.3 Hz, 3H, OCHCH_3), 2.24 (s, 3H, PhCH_3), 5.16 (q, J= 6.36 Hz, 1H, pinBOCH), 7.02 (d, 3J $_{HH}$=7.4 Hz, 2H, Ar-H), 7.16 (d, ^3J $_{HH}$=8.6 Hz, 2H, Ar-H); ^{13}C NMR (CDCl$_3$, 50.28 MHz), δ 21.1 (PhCH$_3$), 24.4 (Bpin-CH$_3$), 25.3 (OCHCH$_3$), 72.3 (OCH$_2$Ph), 82.5 (Bpin-C), 125.2, 128.2, 128.7, 136.5, 137.5, 141.5 (Ar-C).
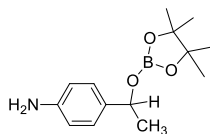
Compound 13c: product from hydroboration of 4-Bromoacetophenone. ^{1}H NMR (CDCl$_3$, 200 MHz), δ 1.13 (s, 6 H, Bpin-CH_3), 1.15 (s, 6H, Ar-CH_3), 1.36 (d, 3J $_{HH}$=6.5 Hz ,3H, OCHCH_3), 5.09 (q, J=6.42 Hz, 1H, pinBOCH), 7.13-7.16 (d, 3J_{HH}=8.4 Hz, 2H, Ar-H), 7.33-7.37 (d, $^3J_{HH}$=9.1 Hz, 2H, Ar-H); ^{13}C NMR (CDCl$_3$, 50.28 MHz), δ 24.4 (Bpin-CH$_3$), 25.2 (OCHCH$_3$), 71.9 (OCH$_2$Ph), 82.8 (Bpin-C), 120.8, 127.1, 128.2, 131.2, 137.4, 143.5 (Ar-C). The product was further acid hydrolyzed to its corresponding alcohol; yield: 68 %. ^{1}H NMR (200 MHz, CDCl$_3$): δ 1.46 (d, $^3J_{HH}$=4.1 Hz, 3H, CH_3), 1.78 (s, 1H, OH), 4.86 (q, J=6.3 Hz, 1H, OCH), 7.29-7.32 (m, 4H, Ar–H) ppm; ^{13}C NMR (CDCl$_3$, 50.28 MHz) δ 25.3 (CHCH$_3$), 69.9 (OCH), 126.8, 128.6, 128.5, 133.2, 144.4 (Ar–C).
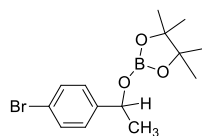
Compound 13d: product from hydroboration of 4-Nitroacetophenone. ^{1}H NMR (CDCl$_3$, 200 MHz), δ 1.15 (s, 6H, Bpin-CH_3), 1.18 (s, 6H, Ar-CH_3), 1.43-1.46 (d, ^3J $_{HH}$=6.4 Hz, 3H, OCHCH_3), 5.26 (q, J=6.72 Hz, 1H, pinBOCH), 7.40 (m, 1H, Ar-H), 7.60 (m, 1H, Ar-H), 8.01 (m, 1H, Ar-H), 8.16 (m, 1H, Ar-H); ^{13}C NMR (CDCl$_3$, 50.28 MHz), δ 24.4 (Bpin-CH$_3$), 25.1 (OCHCH$_3$), 71.6 (OCH$_2$Ph), 83.0 (Bpin-C), 120.5, 122.1, 131.4, 137.6, 146.5, 148.2 (Ar-C).
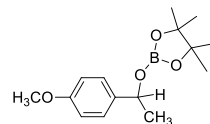
Compound 13e: product from hydroboration of 4-Aminoacetophenone. ^{1}H NMR (CDCl$_3$, 200 MHz), δ 1.15 (s, 12H, Bpin-CH_3), 1.37-1.39 (d, $^3J_{HH}$=6.5 Hz, 3H, OCHCH_3), 3.25 (s, 2H, PhNH_2), 5.08 (q, J=6.24 Hz, 1H, pinBOCH), 6.51 (d, $^3J_{HH}$=7.8 Hz, 2H, Ar-H), 7.05 (d, $^3J_{HH}$=8.7 Hz, 2H, Ar-H); ^{13}C NMR (CDCl$_3$, 50.28 MHz), δ 24.4 (Bpin-CH_3), 25.0 (OCHCH_3), 72.3 (OCH_2Ph), 82.4 (Bpin-C), 114.7, 128.2, 130.6, 134.5, 137.5, 145.4 (Ar-C).

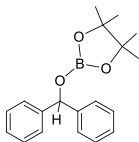**Compound 13f:** product from hydroboration of 4-Methoxyacetophenone. ^{1}H NMR (CDCl$_3$, 200 MHz), δ 1.13 (s, 12H, Bpin-CH_3), 1.41 (d, $^3J_{HH}$=6.4 Hz, 3H, OCHCH_3), 3.69 (s, 3H, PhOCH_3), 5.14 (q, J=6.25 Hz, 1H, pinBOCH), 6.78 (d, $^3J_{HH}$=8.1 Hz, 2H, Ar-H), 7.19(d, $^3J_{HH}$=8.9 Hz, 2H, Ar-H); ^{13}C NMR (CDCl$_3$, 50.28 MHz), δ 24.4 (Bpin-CH_3), 25.2 (OCHCH_3), 55.1 (PhOCH_3), 72.1 (OCH_2Ph), 82.5 (Bpin-C), 113.4, 126.5, 128.2, 136.7, 137.5, 158.6 (Ar-C).

Compound 13g: product from hydroboration of Benzophenone. ^{1}H NMR (CDCl$_3$, 200 MHz), δ 1.09 (s, 12H, Bpin-CH_3), 6.09 (s, 1H, pinBOCH), 7.10-7.31 (m, 10H, Ar-H); ^{13}C NMR (CDCl$_3$, 50.28 MHz), δ 24.4 (Bpin-CH_3), 82.9 (Bpin-C), 126.4, 126.8, 127.2, 128.1, 128.2, 128.3, 129.9, 132.3, 137.6, 143.0 (Ar-C).

Compound 13h: product from hydroboration of 2-Chloroethylmethylketone. ^{1}H NMR (CDCl$_3$, 200 MHz), δ 1.17 (s, 12H, Bpin-CH_3), 1.39 (dd, $^3J_{HH}$=6.4 Hz, 3H, OCHCH_3), 3.87 (q, J=6.21 Hz, 1H, pinBOCH), 4.19 (q, 1H, CH$_3$CHCl); ^{13}C NMR (CDCl$_3$, 50.28 MHz), δ 19.1 (CClCH_3), 19.9 (OCHCH_3), 24.5 (Bpin-CH_3), 60.9 (CClCH$_3$), 74.1 (BpinOCCH$_3$), 82.8 (Bpin-C).
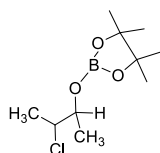
6.4.6: Details of DFT calculations

All the calculations in this study have been performed with density functional theory (DFT), with the aid of the Turbomole 7.1 suite of programs, using the PBE functional. The TZVP basis set has been employed. The resolution of identity (RI), along with the multipole accelerated resolution of identity (marij) approximations have been employed for an accurate and efficient treatment of the electronic Coulomb term in the DFT calculations. Solvent corrections were incorporated with optimization calculations using the COSMO model, with benzene (ε=2.27) as the solvent. The harmonic frequency calculations were performed for all stationary points to

confirm them as a local minima or transition state structures. In addition, intrinsic reaction coordinate (IRC) calculations were done with all the transition state structures in order to further confirm that they represented the correct transition states, yielding the correct reactant and product structures for each case. The values reported are ΔG values, with zero-point energy corrections, internal energy and entropic contributions included through frequency calculations on the optimized minima, with the temperature taken to be 298.15 K. The translational entropy term in the calculated structures was corrected through a free volume correction introduced by Mammen *et al.* This volume correction is to account for the unreasonable enhancement in translational entropy that is generally observed when employing computational softwares. Then, in order to find the efficiency of the catalytic cycle in our mechanism, we have calculated the relative efficiency with the AUTOF program by employing the "Energetic Span Model" (ESM), on all the free energy profiles discussed in the manuscript. The turnover frequency (TOF) calculations take into account the principal rate-determining transition state, potentially rate-influencing transition states and intermediates during the catalysis process. The TOF is calculated by the following equation:

$$\text{TOF} = \frac{K_B T}{h} e^{-\delta E/RT}$$

$\delta E = T_{TDTS} - T_{TDI}$ If TDTS appears after TDI

$\delta E = T_{TDTS} - T_{TDI} - \Delta G_r$ If TDTS appears before TDI

This model has been employed to calculate the TOFs for the free energy profiles obtained for the reactions discussed in the manuscript. This model can also be employed for stoichiometric reactions, where the TOF would correspond to the efficiency of the reaction.

6.5: Experimental details of chapter 5

6.5.1: Synthesis and experimental details of complex 14 and 15

Synthesis of [PhC(N*t*Bu)₂Si{N(SiMe₃)₂}→ZnI₂]·THF(14). Toluene (20 mL) was added to a mixture of [PhC(N*t*Bu)₂SiN(SiMe₃)₂] (0.419 g, 1 mmol) and ZnI₂ (0.319 g, 1 mmol) at ambient temperature. The solution was turned from yellow to colourless with the formation of a white precipitate. The resulting suspension was stirred for 12 hours. The supernatant solvent was removed by using cannula filtration and the precipitate obtained was dried and washed with 10

mL of *n*-hexane. After drying in vacuum, a white powder was obtained which was further dissolved in 10 mL THF and 5 mL dioxane. Super saturation of the solution and storing at –35 °C in a freezer resulted the colorless single crystals of **14**·0.5$C_4H_8O_2$ suitable for X-ray analysis. Yield: 0.495 g (67.0 %). M.p.: 133 °C. ^{1}H NMR (400 MHz, $CDCl_3$, 25 °C): δ 0.43 (s, 9H, Si*Me*$_3$), 0.55 (s, 9H, Si*Me*$_3$), 1.35 (s, 18H, *t*Bu), 2.01 (m, 4H, C_4H_8O), 4.12 (m, 4H, C_4H_8O), 7.48–7.56 (m, 4H, *Ph*), 7.98–8.01 (m, 1H, *Ph*) ppm; ^{13}C NMR (100.61 MHz, $CDCl_3$, 25 °C): δ 4.6 (Si*Me*$_3$), 5.9 (Si*Me*$_3$), 25.5 (C_4H_8O), 31.6 (C*Me*$_3$), 55.8 (*C*Me$_3$), 68.9 (C_4H_8O), 127.4, 128.5, 129.7, 131.2, 132.8, 133.5 (*Ph*), 171.7 (N*C*N) ppm; ^{29}Si NMR (79.49 MHz, $CDCl_3$, 25 °C): δ 8.6 (*Si*Me$_3$), 6.6 (*Si*Me$_3$), –9.5 (*Si*N(SiMe$_3$)$_2$); ^{29}Si Solid State NMR (79.43 MHz, 25°C): δ 11.5 (*Si*Me$_3$), 8.2 (*Si*Me$_3$), –13.9 (*Si*N(SiMe$_3$)$_2$); HRMS *m/z* ($C_{21}H_{41}N_3ISi_3Zn$): 610.0916 [M–(I+THF)]$^+$. For elemental analysis, **14** was heated which led to the removal of THF molecule and formation of **15**. So, the values obtained are same as those of **15** (*vide infra*).

Synthesis of [{PhC(N*t*Bu)$_2$}(N(SiMe$_3$)$_2$)SiZnI(μ-I)]$_2$(15): Toluene (20 mL) was added to a mixture of [PhC(N*t*Bu)$_2$SiN(SiMe$_3$)$_2$] (0.419 g, 1 mmol) and ZnI_2 (0.319 g, 1 mmol) at ambient temperature. The solution became colourless with immediate formation of a white precipitate. The resulting suspension was stirred for 12 hours. The supernatant solution was removed by using cannula filtration and the precipitate obtained was dried and washed with 10 mL of *n*-hexane. After drying in vacuum, a white powder obtained which was further dissolved acetonitrile (5 mL), supersaturated, and kept at room temperature to obtain the single crystals suitable for X-ray analysis. Yield: 0.54 g (73.1 %). M.p.: 147 °C. ^{1}H NMR (400 MHz, $CDCl_3$, 25 °C): δ 0.39 (s, 18H, Si*Me*$_3$), 0.53 (s, 18H, Si*Me*$_3$), 1.33 (s, 36H, *t*Bu), 7.40-7.56 (m, 8H, *Ph*), 7.80-7.85 (m, 2H, *Ph*) ppm; ^{13}C NMR (100.61 MHz, $CDCl_3$, 25 °C): δ 4.9 (Si*Me*$_3$), 6.3 (Si*Me*$_3$), 31.8 (C*Me*$_3$), 55.5 (*C*Me$_3$), 127.4, 128.2, 128.3, 129.7, 129.9, 131.2 (*Ph*), 171.1 (N*C*N) ppm; ^{29}Si NMR (79.49 MHz, $CDCl_3$, 25 °C): δ 10.1 (*Si*Me$_3$), 8.1 (*Si*Me$_3$), −6.4 (*Si*N(SiMe$_3$)$_2$); ^{29}Si Solid State NMR (79.43 MHz, 25°C): δ 11.5 (*Si*Me$_3$), 8.3 (*Si*Me$_3$), –13.3 (*Si*N(SiMe$_3$)$_2$); Anal. Calcd: C, 34.13; H, 5.59; N, 5.69. Found: C, 33.91; H, 5.34; N, 6.21.

6.5.2: Crystal structure details of complex 14 and 15

Crystal data for 14: $C_{25}H_{49}I_2N_3OSi_3Zn$,0.5($C_4H_8O_2$), M=855.16, colorless block, 0.250 x 0.210 x 0.190mm^3, triclinic, space group *P*1, *a*=9.825(2)Å, *b*=9.851(2)Å, *c*=19.935(5) Å, α= 88.975(4)°, β=86.600(4)°, γ=70.447(4)°, *V*=1814.9(8) Å^3, *Z*=2, *T*=100(2) K, $2\theta_{max}$=53.98°,

D_{calc}(g cm^{-3})=1.565, $F(000)$=860, μ (mm^{-1})=2.503, 30496 reflections collected, 7897 unique reflections (R_{int}=0.1626), 4203 observed ($I > 2\sigma$ (I)) reflections, multi-scan absorption correction, T_{min}=0.573, T_{max}=0.648, 355 refined parameters, S=1.006, $R1$=0.0625, $wR2$=0.0974(all data R = 0.1613, $wR2$=0.1278), maximum and minimum residual electron densities; $\Delta\rho_{max}$=0.821, $\Delta\rho_{min}$= −0.939(eÅ^{-3}).

Crystal data for 15: $C_{42}H_{82}I_4N_6Si_6Zn_2$, M=1478.01, colourless block, 0.305 x 0.247 x 0.085 mm^3, monoclinic, space group $P2_1/n$, a=11.0979(4)Å, b=15.3333(6)Å, c=17.7409(7)Å, β=91.1100(10)°, V=3018.4(2) Å^3, Z=2, T=100(2) K, $2\theta_{max}$=50.00°, D_{calc} (g cm^{-3})=1.626, $F(000)$ =1464, μ (mm^{-1})=2.992, 58512 reflections collected, 9165 unique reflections (R_{int}=0.0165), 8966 observed ($I > 2\sigma$ (I)) reflections, multi-scan absorption correction, T_{min}=0.461, T_{max}=0.775, 283 refined parameters, S=1.106, $R1$=0.0136, $wR2$=0.0325 (all data R=0.0140, $wR2$=0.0325), maximum and minimum residual electron densities; $\Delta\rho_{max}$=0.433, $\Delta\rho_{min}$= −0.671 (eÅ^{-3}).

6.5.3: Synthesis and experimental details of complex 16 and 17

Synthesis of [{PhC(NtBu)$_2$}(N(SiMe$_3$)$_2$)GeZnI(μ-I)]$_2$(16): THF (20 mL) was added to a mixture of [PhC(NtBu)$_2$GeN(SiMe$_3$)$_2$] (0.462 g, 1 mmol) and ZnI$_2$ (0.319 g, 1 mmol) at ambient conditions. The reaction mixture was stirred overnight. After the completion of reaction, all the solvent was removed under reduced pressure to get white precipitate compound. It was further washed with 10 mL of hexane and dried. Single crystals suitable for X-ray analysis were grown in the mixture of THF and toluene at −35 °C. ^{1}H NMR (400 MHz, CDCl$_3$, 25 °C): δ 0.41 (s, 18H, SiMe_3), 0.50 (s, 18H, SiMe_3), 1.28 (s, 36H, tBu), 7.43–7.58 (m, 8H, Ph), 8.41–8.50 (m, 2H, Ph) ppm; ^{13}C NMR (100.61 MHz, CDCl$_3$, 25 °C): δ 5.0 (SiMe_3), 5.9 (SiMe_3), 31.9 (CMe_3), 54.9 (CMe$_3$), 120.3, 127.5, 127.9, 129.8, 132.1, 148.2, 148.9 (Ph), 165.8 (NCN) ppm.

Synthesis of [{PhC(NtBu)$_2$}(N(SiMe$_3$)$_2$)GeZnBr(μ-Br)]$_2$(17): Similar procedure as of **16** was performed by taking ZnBr$_2$ instead of ZnI$_2$. Single crystals suitable for X-ray analysis were grown in the THF at −35 °C. ^{1}H NMR (400 MHz, CDCl$_3$, 25 °C): δ 0.40 (s, 18H, SiMe_3), 0.50 (s, 18H, SiMe_3), 1.27 (s, 36H, tBu), 7.42–7.56 (m, 8H, Ph), 8.02–8.27 (m, 2H, Ph) ppm; ^{13}C NMR (100.61 MHz, CDCl$_3$, 25 °C): δ 5.1 (SiMe_3), 6.4 (SiMe_3), 32.1 (CMe_3), 54.9 (CMe$_3$), 126.6, 127.4, 128.2, 129.6, 130.2, 132.3 (Ph), 165.6 (NCN) ppm.

6.5.4: Crystal structure details of complex 16 and 17

Crystal data for 16: $C_{42}H_{82}Ge_2I_4N_6Si_4Zn_2$,$2(C_7H_8)$, M=1751.28, colorless block, 0.310 x 0.240 x 0.190 mm^3, monoclinic, space group $P2_1/n$, a=11.5550(3)Å, b=13.1465(3)Å, c=23.9510(6)Å, β= 93.4210(10)°, V=3631.86(16)Å^3, Z=2, T=100(2) K, $2\theta_{max}$=50.00°, D_{calc} (g cm^{-3})=1.601, $F(000)$ =1736, μ (mm^{-1})=3.275, 53395 reflections collected, 6399 unique reflections (R_{int}=0.0272), 5795 observed ($I > 2\sigma (I)$) reflections, multi-scan absorption correction, T_{min}=0.405, T_{max}=0.537, 348 refined parameters, S=1.066, $R1$=0.0433, $wR2$=0.1228 (all data R=0.0478, $wR2$=0.1228), maximum and minimum residual electron densities; $\Delta\rho_{max}$=3.331, $\Delta\rho_{min}$= −2.884(eÅ^{-3}).

Crystal data for 17: $C_{42}H_{82}Br_4Ge_2N_6Si_4Zn_2$, M=1379.05, colorless sphere, 0.32 x 0.22 x 0.14 mm^3, triclinic, space group $P\text{-}1$, a=10.2897(9)Å, b=10.6808(10)Å, c=15.1154(13)Å, α= 81.949(4)°, β=80.125(3)°, γ=63.830(3), V=1464.9(2)Å^3, Z=1, T=100(2) K, $2\theta_{max}$=50.00°, D_{calc} (g cm^{-3})=1.563, $F(000)$= 696, μ(mm^{-1})=4.667, 28348 reflections collected, 4868 unique reflections (R_{int}=0.0364), 4868 observed ($I > 2\sigma (I)$) reflections, multi-scan absorption correction, T_{min}=0.303, T_{max}=0.520, 284 refined parameters, S=1.101, $R1$=0.0273, $wR2$=0.0603 (all data R=0.0389, $wR2$=0.0603), maximum and minimum residual electron densities; $\Delta\rho_{max}$=0.683, $\Delta\rho_{min}$= −0.535 (eÅ^{-3}).

About the author

Mr. Sandeep, son of Virender Singh and Krishna Devi, was born in Guriani village of Rewari district, Haryana, India, in 1992. He completed his B.Sc. Chemistry from Hindu College, University of Delhi. He obtained his master degree from IIT Roorkee. After qualifying CSIR-National Eligibility Test (NET-JRF) examination, he moved to Catalysis Division, CSIR-National Chemical Laboratory, Pune, India to pursue his Ph.D. degree under the guidance of Dr. Sakya Singha Sen. His research interests include the synthesis and reactivity studies of alkaline earth metal complexes.

Education and Research Experience:

Ph.D.: From July 2014 to till date working under the supervision of Dr. Sakya Singha Sen at CSIR- National Chemical Laboratory. I will be completing my doctoral work by May 2019.

M.Sc.: (2012-2014) Chemistry, IIT Roorkee, India

B.Sc.: (2009-2012) Chemistry, Hindu College, University of Delhi

List of Scientific Contributions:

Publications

1. Benz-amidinato Stabilized a Monomeric Calcium Iodide and a Lithium Calciate(II) Cluster featuring Group 1 and Group 2 Elements; **S. Yadav**, V. S. V. S. N. Swamy, R. G. Gonnade, S. S. Sen*, ChemistrySelect*, **2016**, *1*, 1066–1071.

2. Compounds having Low-Valent p-Block Elements for Small Molecule Activation and Catalysis; **S. Yadav**, S. Saha, S. S. Sen, *ChemCatChem.*, **2016**, *8*, 486–501.

3. Facile Access to a Ge(II) Dication Stabilized by Isocyanides; V. S. V. S. N. Swamy, **S. Yadav**, S. Pal, T. Das, K. Vanka, S. S. Sen, *Chem. Commun.*, **2016**, *52*, 7890–7892.

4. Benz-amidinato Calcium Iodide Catalyzed Aldehyde and Ketone Hydroboration with Unprecedented Functional Group Tolerance; **S. Yadav**, S. Pahar, S. S. Sen, *Chem. Commun.*, **2017**, *53*, 4562–4564.

5. Unprecedented Solvent Induced Inter-conversion Between Monomeric and Dimeric Silylene-Zinc Iodide Adducts; **S. Yadav**, E. Sangtani, D. Dhawan, R. G. Gonnade, D. Ghosh, S. S. Sen, *Dalton Trans.*, **2017**, *46*, 11418–11424.

6. Beyond Hydrofunctionalization: A Well-Defined Calcium Compound Catalyzed Mild and Efficient Carbonyl Cyanosilylation; **S. Yadav**, R. Dixit, K. Vanka, S. S. Sen*, Chem. Eur. J*., **2018**, *24*, 1269–1273.

7. Alkaline Earth Metal Compounds of Methylpyridinato β-Diketiminate Ligands and their Catalytic Application in Hydroboration of Aldehydes and Ketones; **S. Yadav**, R. Dixit, M. K. Bisai, K. Vanka, S. S. Sen, *Organometallics*., **2018**, *37*, 4576–4584.

8. Structural Diversity in Ketiminato Calcium and Magnesium Complexes; **S. Yadav**, R. Kumar, K. Gour, S. S. Sen, Communicated

Symposia Attended

National conferences: 1 (Participation)

International conferences: 1 (Participation)

                              2 (Poster presentation)